For Reference

NOT TO BE TAKEN FROM THIS ROOM

62F-52

For Reference

NOT TO BE TAKEN FROM THIS ROOM

Ex LIBRIS
UNIVERSITATIS
ALBERTAENSIS

UNIVERSITY OF ALBERTA
QUAECUMQUE VERA

University of Alberta
Printing Department

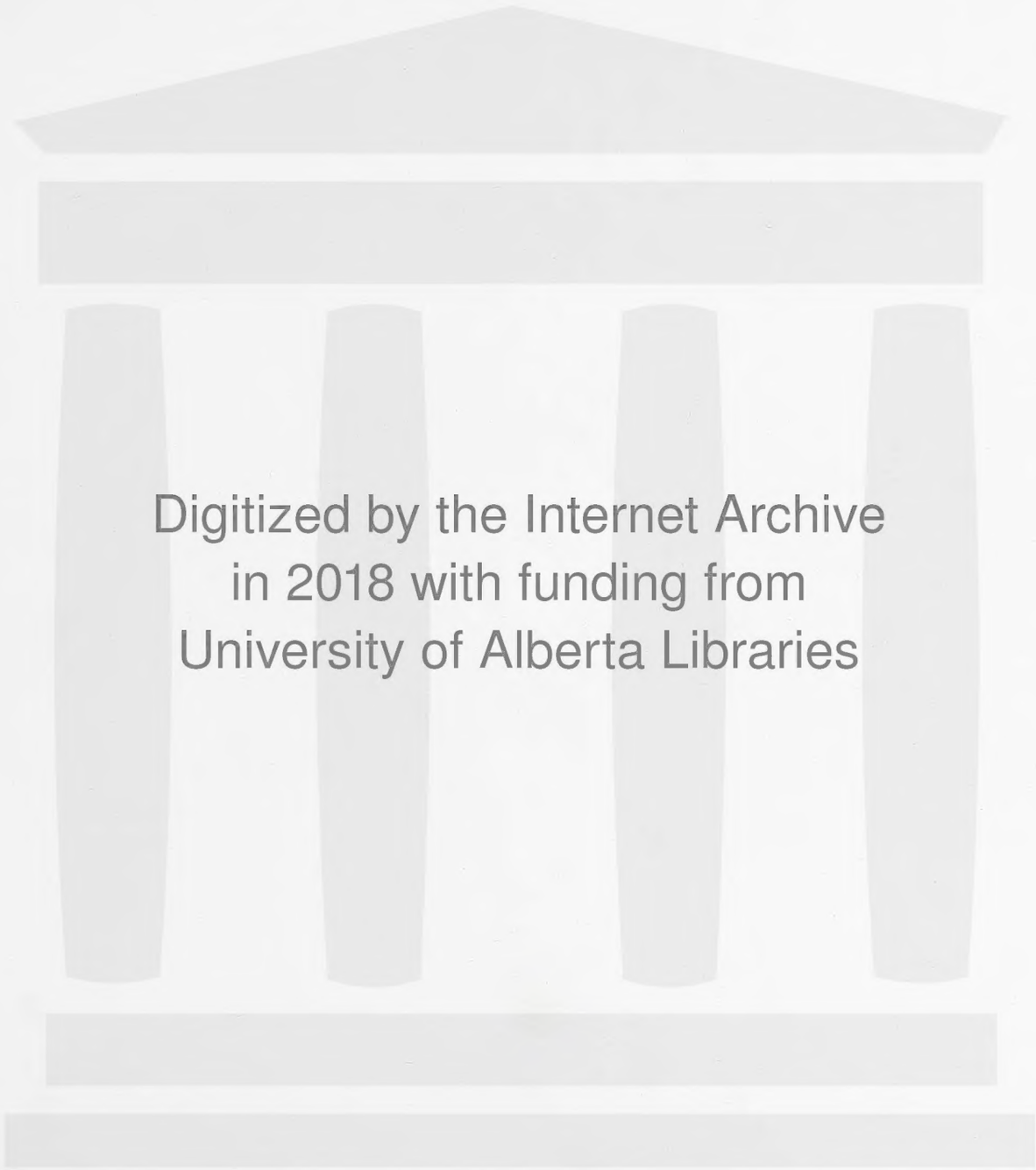

Digitized by the Internet Archive
in 2018 with funding from
University of Alberta Libraries

https://archive.org/details/rheologyofsuspen00aema

Thesis
1962(F)
#52.

THE UNIVERSITY OF ALBERTA

THE RHEOLOGY OF SUSPENSIONS OF SPHERES

EFFECT OF SIZE DISTRIBUTION

A THESIS

SUBMITTED TO THE FACULTY OF GRADUATE STUDIES

IN PARTIAL FULFILMENT OF THE REQUIREMENTS FOR THE DEGREE OF

MASTER OF SCIENCE IN CHEMICAL ENGINEERING

DEPARTMENT OF CHEMICAL AND PETROLEUM ENGINEERING

by

A.E. MATHER, B.Sc.

EDMONTON, ALBERTA

OCTOBER, 1962

ABSTRACT

The effect of the size distribution of the disperse phase upon the rheological behavior of suspensions of spheres was studied with a rotational viscometer. The suspensions were found to behave as Newtonian fluids over the range of concentration studied (0 to 50 volume percent). For the three unimodal suspensions studied (average particle diameter 47, 86.5 and 390 microns), no effect of particle size upon the viscosity was found. A bimodal distribution of particle sizes was found to have a significant effect upon the viscosity of the suspensions, the viscosity being lower than that of a unimodal suspension at the same concentration. It was found that the minimum viscosity for any volume concentration occurs when 70% of the total solids are large particles and 30% are small particles. Increasing the diameter ratio of large to small particles also decreases the viscosity at any volume concentration. These facts are explained in terms of the packing of the smaller spheres into the interstices between the larger spheres. The results of this work agree well with those of Sweeny (46).

ABSTRACT

ACKNOWLEDGEMENTS

The author wishes to express his appreciation of the criticism and assistance given by Dr. G.W. Govier who supervised this investigation.

The many contributions of my wife towards this thesis are gratefully acknowledged.

To F. Zwartzes for rebuilding the viscometer gear train and to J. Sandercock and R. Brown for assistance with the photography, the author expresses his sincere thanks.

The author appreciates the financial aid of the National Research Council of Canada and the Department of Chemical and Petroleum Engineering of the University of Alberta received in the course of this work.

TABLE OF CONTENTS

		Page
	List of Figures	1
I.	INTRODUCTION	4
II.	THEORY AND LITERATURE REVIEW	6
	1. Rheological Background	6
	2. Theory of Concentric Cylinder Viscometer	14
	3. Literature Review	23
III.	EXPERIMENTAL EQUIPMENT AND METHOD	33
	1. Viscometer	33
	2. Suspensions	37
	3. Auxiliary Equipment	42
	4. Experimental Method	43
	5. Mechanical Difficulties	46
IV.	EXPERIMENTAL RESULTS AND DISCUSSION	54
	1. Unimodal Suspensions	55
	2. Bimodal Suspensions	65
V.	CONCLUSIONS AND RECOMMENDATIONS	90
	Table of Nomenclature	93
	References	96
	Appendices	100
	A Calibration of the Viscometer	100
	B Criteria for Laminar Flow in the Annulus of the Viscometer	105

Appendices (cont.) Page

C Calibration of Thermometer 107

D Sieve Analyses of Styrene-Divinylbenzene Powders 109

E Experimental Data 112

F Calculated Data 137

G Derivation of Equation for Concentric Cylinder Viscometer 143

H Power Series Correlation of the Data 144

LIST OF FIGURES

		Page
1.	Flow Curves on Arithmetic Coordinates	7
2.	Flow Curves on Logarithmic Coordinates	8
3.	Photograph of the Viscometer	34
4.	Size Distribution of the Spherical Powders	38
5.	Photomicrographs of the 40/60 Mesh and the 100/200 Mesh Powders	39
6.	Photomicrograph of the 200/400 Mesh Powder	40
7.	Relative Viscosity versus Concentration for Unimodal Suspensions	56
8.	Test of Einstein's Equation for Unimodal Suspensions	58
9.	Plot of $(\eta_r - 1)/c$ versus Concentration	60
10.	Test of Fitted Quadratic Equation for Unimodal Suspensions	61
11.	Test of Fitted Equation for Unimodal Suspensions	64
12.	Relative Viscosity versus Concentration for Bimodal Mixtures of A and B	66
13.	Test of Fitted Equation for Bimodal Suspensions of 25% A - 75% B	67
14.	Test of Fitted Equation for Bimodal Suspensions of 50% A - 50% B and 75% A - 25% B	68
15.	Relative Viscosity versus Concentration for Bimodal Mixtures of A and C	69

Page

16. Test of Fitted Equation for Bimodal Suspensions of 25% A - 75% C 71

17. Test of Fitted Equation for Bimodal Suspensions of 50% A - 50% C and 75% A - 25% C 71

18. Relative Viscosity versus Concentration for Suspensions of 50% B - 50% C and 33 1/3% A - 33 1/3% B - 33 1/3% C 72

19. Test of Fitted Equation for Bimodal Suspensions of 50% B - 50% C 74

20. Test of Fitted Equation for Trimodal Suspensions of 33 1/3% A - 33 1/3% B - 33 1/3% C 75

21. Coefficient of c^2 versus Diameter Ratio 76

22. Coefficient of c^3 versus Diameter Ratio 77

23. Ratio of the Bimodal Relative Viscosity to the Unimodal Relative Viscosity versus Percent Larger Particles for Bimodal Mixtures of B and C 78

24. Ratio of the Bimodal Relative Viscosity to the Unimodal Relative Viscosity versus Percent Larger Particles for Bimodal Mixtures of A and B 79

25. Ratio of the Bimodal Relative Viscosity to the Unimodal Relative Viscosity versus Percent Larger Particles for Bimodal Mixtures of A and C 80

26. Ratio of the Bimodal Relative Viscosity to the Unimodal Relative Viscosity versus Percent Larger Particles for Bimodal Mixtures at 40 Volume Percent Total Solids 82

Page

27. Ratio of the Bimodal Relative Viscosity to the Unimodal Relative Viscosity versus Diameter Ratio for Suspensions Containing 25% Larger Particles 83

28. Ratio of the Bimodal Relative Viscosity to the Unimodal Relative Viscosity versus Diameter Ratio for Suspensions Containing 50% Larger Particles 84

29. Ratio of the Bimodal Relative Viscosity to the Unimodal Relative Viscosity versus Diameter Ratio for Suspensions Containing 75% Larger Particles 85

30. Stability Correlations of Taylor and Schlichting 106

31. Calibration of Mercury-in-Glass Thermometer No. 249 108

32. Power Series Correlation for Unimodal Suspensions 145

33. Power Series Correlation for Bimodal Suspensions of A and B 147

34. Power Series Correlation for Bimodal Suspensions of A and B 149

35. Power Series Correlation for Bimodal Suspensions of A and C 151

36. Power Series Correlation for Bimodal Suspensions of A and C 153

37. Power Series Correlation for Bimodal Suspensions of B and C 155

38. Power Series Correlation for Trimodal Suspensions of A, B and C 157

I. INTRODUCTION

This work is an experimental investigation of the effect of the size distribution of the solid phase upon the rheological behavior of suspensions of spherical particles. The ultimate aim of work such as this is the thorough understanding of the process of flow of particulate solids in liquids.

The flow behavior of solid-liquid mixtures is important in a number of industrial processes, especially those involved in the transport of raw materials such as cement, sand, gravel, coal and various ores. The sucessful application of suspension transport depends to a large extent on the ability to predict the power consumption involved in the process. This in turn is directly dependent upon the rheological behavior of the solid-liquid mixture. It would be desirable to be able to relate the physical properties of the system - the particle size, shape, size distribution and concentration of the disperse phase, to the rheological behavior of the suspension. At present, it is not possible to do this because of the scarcity of both theoretical and experimental work on the effect of the various physical properties upon the rheological behavior of the suspension.

A survey of the literature showed that even suspensions of spheres, the most idealized system possible, could not be fully characterized by the physical parameters. The effect of the size

distribution of the disperse phase had not been studied extensively, although there was some indication that a wide size distribution contributed to a lower consistency than a narrow size distribution at the same concentration of solid phase. At the time that this work was begun, there were only a few cases of study of the effect of size distribution upon the rheological properties of suspensions of spheres and these were at low concentrations. For this reason, it was decided to undertake an experimental investigation of the effect of the size distribution of the spheres upon the rheological behavior of the resulting suspension.

The rheological properties of the suspensions used in this investigation were measured by means of a concentric cylinder viscometer. This type of viscometer was chosen because of its advantages over other instruments in the measurement of rheological properties of suspensions. These include the nearly constant shear rate throughout the sample, the ease of operation and the ability to detect and study thixotropic breakdown in a fluid.

This study to determine the effect of the size distribution upon the rheological behavior of suspensions of spheres is presented under the subjects of rheological and viscometric theory, a literature review of the most important work on suspensions of spheres, in particular that concerning the effect of size distribution, the experimental equipment and method used in this investigation, experimental results and a discussion and some conclusions warranted as a result of this work.

II. THEORY AND LITERATURE REVIEW

1. Rheological Background

Fluid Classification

Fluids are classified as Newtonian or non-Newtonian depending upon their behavior, at constant temperature and pressure, under imposed shearing stresses which give rise to laminar motion. A Newtonian fluid is one which obeys Newton's (36) law,

$$\tau = -\eta \left(\frac{dv}{dx} \right) \tag{1}$$

where η is the coefficient of viscosity, often simply termed viscosity, poise (gm/sec-cm)

τ is the unit shearing stress, dynes/cm^2

$\frac{dv}{dx}$ is the shear rate, sec^{-1}

A graphical representation of the flow curve of a Newtonian fluid is shown in Figures 1 and 2 on arithmetic and logarithmic coordinates. The flow curve of a Newtonian fluid is completely characterized by the single physical property of viscosity.

By exclusion, fluids which do not obey Newton's law are called non-Newtonian fluids. Non-Newtonian fluids may be further subdivided into three broad categories:

FIGURE 1

FLOW CURVES
on
ARITHMETIC COORDINATES

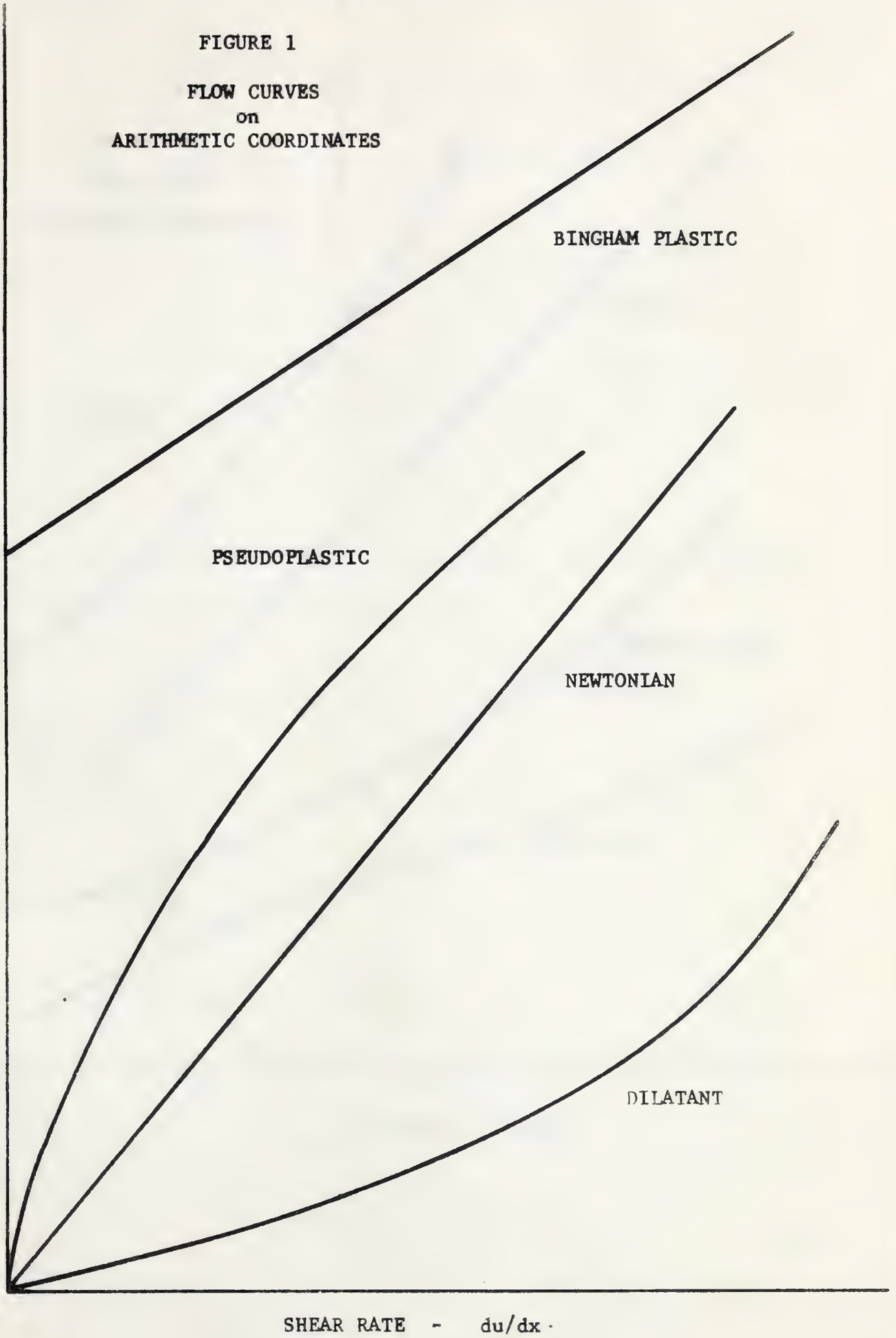

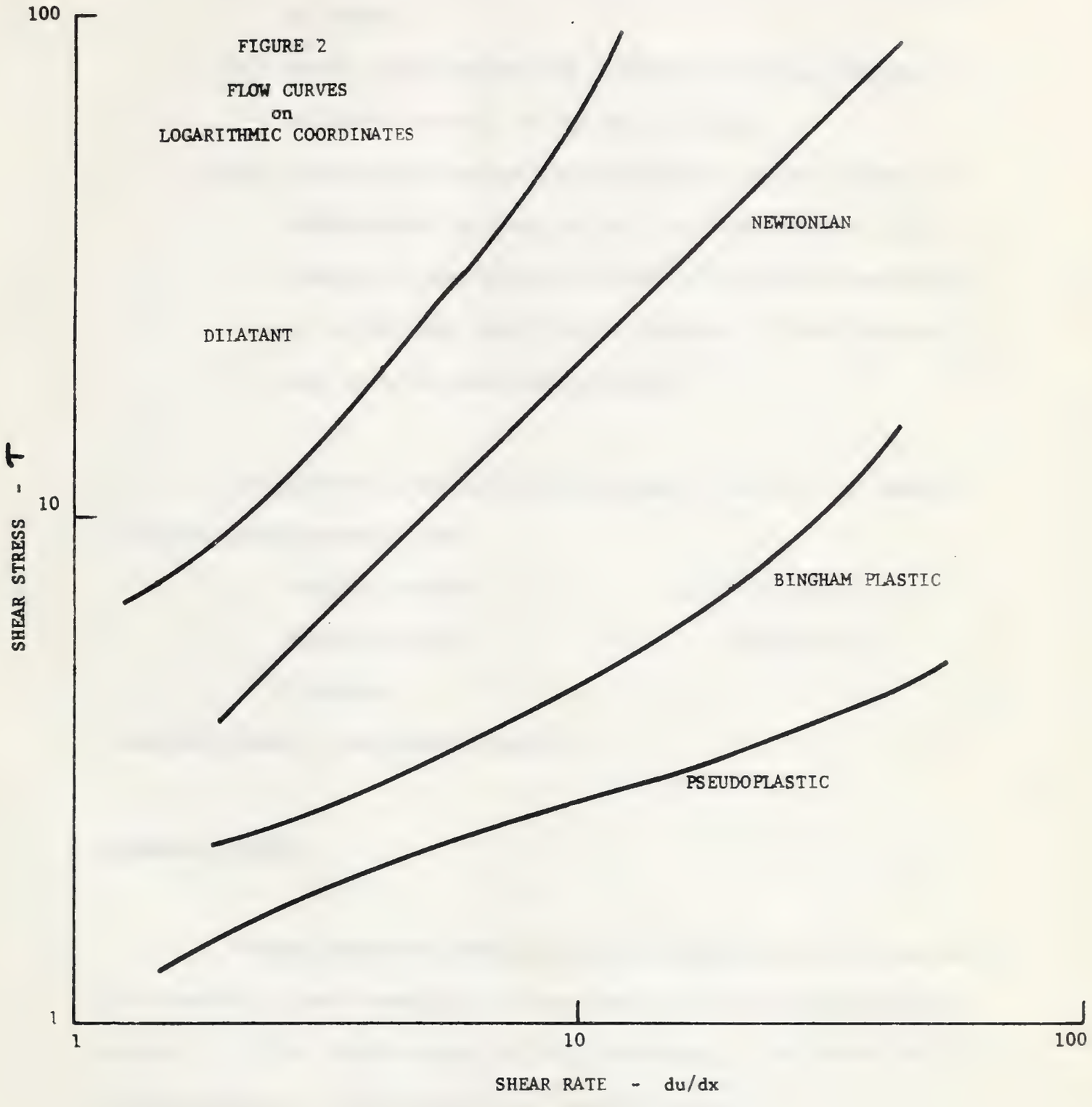

FIGURE 2

FLOW CURVES
on
LOGARITHMIC COORDINATES

i) Fluids with properties independent of time or duration of shear

ii) Fluids with properties dependent upon the duration of shear as well as the shear stress.

iii) Fluids with properties dependent upon the extent of deformation (strain) as well as shear stress. This last case involves fluids which have characteristics of solids and show elastic recovery. This category will not be considered further.

Non-Newtonian fluids in categories i) and ii) are subdivided into five general types:

i) Bingham plastic
Pseudoplastic
Dilatant

ii) Thixotropic
Rheopectic

These will now be considered in turn.

Bingham plastic

Fluids exhibiting Bingham plastic behavior do not flow until the shearing stress exceeds a minimum value. This minimum shearing stress, τ_y, the yield stress, is the intercept on the shear stress axis in Figure 1. The equation of the flow curve is:

$$\tau - \tau_y = \mu_R \left(\frac{du}{dx} \right) \qquad (2)$$

where μ_R is the coefficient of rigidity and is the slope of the flow curve. On logarithmic coordinates, Figure 2, the flow curve becomes asymtotic to τ_y at low shear rates and approaches a slope of unity at high shear rates.

Bingham plastic behavior has been ascribed to the presence of a three-dimensional structure within the fluid while at rest, which collapses completely when the yield stress is exceeded. Actually, the Bingham plastic model represents a very idealized behavior and it is doubtful that any true Bingham fluids exist.

Pseudoplastic

From the flow curves of Figure 1, it is seen that the ratio of the unit shearing stress and the rate of shear for a non-Newtonian fluid depends upon the rate of shear. This ratio is different at different rates of shear and hence the consistency varies. To refer to these different consistencies as viscosities is incorrect; however, they may be referred to as apparent viscosities which have meaning only when the rate of shear is given.

Many fluids, known as pseudoplastics, exhibit a type of flow in which the rate of flow increases faster than the shearing stress. Thus the apparent viscosity decreases as the rate of shear increases.

Pseudoplastic fluids exhibit no yield value and the flow curve becomes almost linear at very high rates of shear.

Many explanations have been proposed to account for this behavior. One explanation is that highly asymmetric molecules or particles are randomly dispersed and entangled when the fluid is at rest. Under shear they tend to align themselves in the direction of the shearing motion. A second possible explanation of pseudoplasticity may be the progressive shearing off of liquid carried by particles as envelopes of solvation, thus decreasing their effective size with increasing rate of shear.

The logarithmic plot of shear stress versus rate of shear for these materials frequently approaches a straight line with a slope between zero and unity. For this reason, an empirical relation known as the power law is used to characterize fluids of this type. It is of the form:

$$\tau = K\left(\frac{du}{dx}\right)^n \qquad (3)$$

This relation was originally proposed by Ostwald (37) and has been critically discussed by Reiner (39).

Dilatant

Dilatant fluids are those for which the apparent viscosity increases with increasing rate of shear. Originally, the term dilatant was applied to those systems which increased in volume, or dilated under shear. This type of behavior was found in concentrated suspensions by Reynolds (40). When the suspension is at rest the voidage is a minimum and the liquid is sufficient only to fill the voids. On shearing, the dense packing of the system is broken and the material "dilates", increasing the voidage. There is now insufficient liquid to lubricate the flow of particles past each other and the applied stresses have to be much greater. This causes the apparent viscosity to increase rapidly with increasing rates of shear and is termed volumetric dilatancy.

Freundlich and Röder, (17) in their work on starch-water and quartz-water suspensions, found that the apparent viscosity increased with increased shear rate. This was called dilatant behavior and the term dilatancy has been used to describe both volumetric dilatancy and rheological dilatancy. The latter can occur at concentrations much below that required for volumetric dilatancy.

Some dilatant systems can be characterized rheologically by means of the "power law", Equation (3), except that in this case the exponent is greater than unity.

Thixotropic

The classification, thixotropic, is used to denote those fluids whose consistency decreases with time under shear and builds up again when at rest. Thixotropy was first defined as an isothermal, reversible sol-gel-sol transformation. This definition has been broadened to include fluids that exhibit an isothermal reversible transformation from a higher to a lower consistency gel. A physical model for thixotropic fluids consists of coiled chains of long molecules, entangled in the fluid at rest. Upon shear, the chains begin to align themselves in the direction of the shear. At the same time breaking and disentanglement of some of the chains may occur. These processes are not instantaneous and the shear stress, at constant shear rate, is observed to decrease with time.

Rheopectic

Rheopectic fluids exhibit the opposite behavior to thixotropic, that is, at constant rate of shear, the consistency increases with time. Freundlich and Juliusberger (18) first used the term to describe the "solidification" of vanadium oxide suspensions under low rates of shear. It has been postulated that rheopexy is simply the same as dilatancy except that a finite time interval is required. Rheopexy has been noted in various sols and in some bentonitic clay suspensions (57).

2. Theory of the Concentric Cylinder Viscometer

The concentric cylinder or Couette viscometer is well suited for the study of the rheological properties of fluids. Its simple geometry allows the direct relation of the observed variables with the shearing stress and rate of shear. The shear rate is nearly constant throughout the sample and the instrument is simple to operate. This type of viscometer is also one of the few that can be used for a quantitative study of thixotropic breakdown because the shearing stress can be measured as a function of time at constant shear rate and temperature. Another reason for the suitability of Couette viscometers for measurement of the rheological properties of suspensions is that no wall effect is noted. Workers studying the rheology of suspensions of spheres in capillary viscometers have found that the viscosity of Newtonian suspensions is markedly dependent upon the capillary diameter (51), (24), (53). However, Eveson, Whitmore and Ward (14) found no effect of the gap width in a Couette viscometer upon the measured viscosity. For this reason, coaxial cylinder viscometers are to be preferred to capillary tube viscometers for the measurement of the rheological behavior of suspensions.

The Couette viscometer consists of two concentric cylinders arranged so that the liquid sample is placed between them. One cylinder, usually the outer, is rotated at a constant speed and the torque transmitted by the liquid to the inner cylinder is measured

by means of the deflection of a torsion wire. The apparatus is usually placed in a thermostat to insure a constant temperature of the sample.

It is possible to use the alternate system of the inner cylinder rotating and the outer cylinder fixed. Taylor (48) has shown that the outer cylinder rotating is considerably more stable than the inner cylinder rotating, in that laminar flow occurs up to much higher speeds.

The experimental measurements consist of the angular velocity, Ω, of the outer cylinder and the torque, M, exerted on the inner cylinder. From the measurement of these relations it is possible to determine the flow curve of the liquid. The following assumptions are made regarding the motion of the liquid:

i) the liquid is incompressible,

ii) the motion of the liquid is laminar,

iii) the laminae are circles on the horizontal planes perpendicular to the axis of rotation,

iv) the motion is constant with time, (there is no acceleration)

v) there is no slip at the walls, i.e. the velocity of the fluid at the surface of the cylinders is zero, and,

vi) the cylinders are assumed to be infinite in length.

With these assumptions, it is possible to obtain the following equation (see Appendix G) which relates Ω and shearing stress for any arbitrary time-independent fluid.

$$\Omega = \int_{\tau_o}^{\tau_i} \frac{f(\tau)\,d\tau}{2\tau} \tag{4}$$

where the rheological behavior of the fluid is expressed as

$$f(\tau) = \frac{du}{dr} \tag{5}$$

and shearing stress is related to torque by

$$\tau(r) = \frac{M}{2\pi r^2 h} \tag{6}$$

where r = radial distance (some value between the radius of the inner cylinder and that of the outer cylinder)

h = length of cylinder immersed in the sample.

Equation (4) can be integrated if a $f(\tau)$ is assumed for a fluid. For a Newtonian fluid, $f(\tau) = \tau/\eta$ and

$$\Omega = \int_{\tau_o}^{\tau_i} \frac{\tau\,d\tau}{2\eta\tau} = \frac{\tau_i - \tau_o}{2\eta} \tag{7}$$

Expressing τ in terms of M:

$$\Omega = \frac{M}{4\pi h\eta}\left[\frac{1}{R_i^2} - \frac{1}{R_o^2}\right] \tag{8}$$

where R_i = radius of the inner cylinder

R_o = radius of the outer cylinder

This equation is the well-known Margules equation.

When dealing with non-Newtonian fluids, it is desirable to be able to construct the flow curve (shearing stress - rate of shear diagram) without the assumption of any particular behavior for the fluid. This is easily done for the shearing stress since Equation (6) is valid for any fluid. At the surface of the bob, therefore, the shearing stress for any fluid is:

$$\tau_{R_i} = \frac{M}{2\pi R_i^2 h} \tag{9}$$

To obtain the rate of shear at the surface of the bob for any fluid is more difficult. Pawlowski (38) and Krieger and Elrod (28) have solved this problem. The equations are independent of the rheological nature of the fluid. The Krieger and Elrod equation consists of an infinite series which may be truncated to three terms if the ratio $s = R_o/R_i$ is less than 1.2.

$$\left(\frac{du}{dr}\right)_{R_i} = \frac{4\pi N}{1 - 1/s^2}\left\{ 1 + k_1(1/n'' - 1) + k_2\left[(1/n'' - 1)^2 + \frac{d(1/n'' - 1)}{d \log M}\right]\right\} \tag{10}$$

where k_1 and k_2 are instrument constants

$$k_1 = \frac{s^2 - 1}{2s^2}\left(1 + 2/3 \, (\ln s) \right) \tag{11}$$

$$k_2 = \frac{(s^2 - 1) \ln s}{6s^2} \qquad (12)$$

n" is the slope of a logarithmic plot of torque M versus rotational speed N at the value of N in question. Use of Equations (9) and (10) allows the construction of a true shear stress - rate of shear diagram from which the rheological class of the fluid can be determined.

End Effects

The equation for the rotational viscometer, Equation (9) is based on the assumption that the cylinders are of infinite length, i.e. that the viscous drag on the top and bottom of the inner cylinder is negligible compared with the drag on the cylindrical surfaces. This factor can be taken into account in one of the following ways:

i) use of a very long inner cylinder of small radius with a small clearance between the inner and outer cylinders to make the end correction negligible,

ii) calibration of the instrument with liquids of known viscosity, absorbing the end effect in the instrument constant,

iii) reduction of the relative motion of the liquid above and below the ends of the inner cylinder by mechanical means, and,

iv) measurement of the effect experimentally in order to include it in the calculations of the shearing stress.

Method i) imposes many difficulties in the design of a suitable apparatus. However, Shangraw et al (44) used this method with a ratio of length of inner cylinder to annular gap of 243 to 1.

Method ii) has been widely used and was used in this investigation. However, it was found that the end effect varies with viscosity.

Method iii) includes the use of guard cylinders, which were introduced by Couette (4) and have been used by many investigators including Hatschek (23). Above and below the suspended cylinder, guard rings, (i.e. cylinders of the same diameter), were rigidly fixed so as to be co-axial with it and to allow the minimum clearance between the free and fixed edges. Each of the guards is about 2/5 of the length of the inner cylinder so that the viscous drag exerted by the base of the outer cylinder was not transmitted to the inner one. The liquid under examination filled up the interior of the suspended and guard cylinders. To prevent the liquid inside the inner cylinder from rotating, the opposite ends of the guard rings were filled with perforated plates. The required length of the guard cylinder varies with the annular gap and the velocity of rotation. In the apparatus of Couette, the guard cylinders had a length of 14 times the annular gap.

Method iv) has been widely used and is usually described in terms of an equivalent length of cylindrical bob. The plot of deflection versus bob length immersed, when extrapolated back is a straight line not passing through the origin, but intersecting the abscissa at a negative value equal to the effective end contribution. In further calculations, the measured depth of immersion may be adjusted by adding the equivalent length of the bob.

Theoretically, end effect corrections of this type are suitable only for Newtonian fluids, since the consistency of a non-Newtonian fluid varies with the rate of shear and would vary across the base of the bob. However, in a well-designed apparatus, the end effect is small and the contribution to the total torque is small. Thus a relatively large error in the end effect correction itself is permissible.

Stability of the Flow in the Viscometer Annulus

In all the equations presented previously for the measurement of the rheological properties in a concentric cylinder viscometer it has been assumed that the flow is laminar. However, at high velocities, the flow may not be laminar and a suitable criterion must be used for the stability of the flow. A good treatment of the problem of stability of flow in the annulus of concentric cylinder viscometers is that of Chandrasekhar (2).

Probably the best known and most widely used correlation is that of G.I. Taylor who considered this problem from both the theoretical and experimental viewpoint. In 1923 Taylor (48) solved the equations of motion for the system of concentric cylinders containing a viscous fluid in the annulus. This allowed him to predict the onset of instability (turbulence) theoretically and his experimental work was an excellent confirmation of the theoretical work. Later Taylor (49) performed more experiments on different types of fluids and again the results were in excellent agreement with the theory.

Taylor's theoretical work has been checked a number of times and found to be correct. Recent solutions of the theoretical problem include those of Meksyn (34), Chandrasekhar (3) and Di Prima (6).

Experimental confirmation of Taylor's theory by other workers include the experiments of Lewis (29), Terada and Hattori (47) and Wendt (55). The most recent and probably the most accurate experiments are those of Donnelly (7) and Donnelly and Fultz (8). They check Taylor's theoretical predictions very closely. Taylor's working correlation is in the form of a log-log plot of Ut/ν versus t/R_o where

U = linear velocity of the outer cylinder

t = gap between the cylinders

ν = kinematic viscosity of the fluid contained in the annulus

R_o = radius of the outer cylinder

From a knowledge of the geometry of the system it is possible to calculate t/R_o and obtain Ut/ν from the correlation. From the value, the speed for instability to occur can be calculated.

Another correlation, that of Schlichting (43) can be used to predict the onset of instability in a concentric cylinder viscometer. This correlation is a log-log plot of UR_o/ν versus t/R_o.

In Appendix B, the results of calculations for the viscometer used in this work are given. It is seen that the agreement between the correlations of Schlichting and Taylor is very good. In this work, the velocity for instability in the annulus was always greater than 20 times the maximum speed of the instrument.

3. Literature Review

A large amount of work has been done on the rheological behavior of suspensions of spheres. However, there is not complete agreement on the quantitative effect of the various physical parameters. Good reviews of the rheology of suspensions have recently been published by Frisch and Simha (19) and Roscoe (41). In this section, a brief treatment of the most important studies is given with particular reference to the effect of particle size distribution upon the rheology of suspensions of spheres.

Einstein (10), in a theoretical paper, solved the linearized Navier-Stokes equations for the case of a dilute suspension of spheres. The assumptions involved include the restrictions that the particles are rigid spheres their size being large compared to the size of the solvent molecules and yet small in comparison to the size of the apparatus in which the viscosity is measured. Another important restriction of Einstein's treatment is that the concentration of suspended spheres is infinitely dilute, so that the particles exert no forces on each other. With these assumptions, the expression obtained for the relative viscosity has the form:

$$\eta_r = \frac{\eta_s}{\eta} = 1 + 2.5c \qquad (c \rightarrow 0) \qquad (13)$$

Thus this case is a limiting result and states that the slope of the η_r - c curve has a value of 2.5 where it cuts the η_r axis.

The Einstein equation was extended to higher concentrations in a theoretical work by Guth and Simha (21) who solved the Navier-Stokes equations by the method of successive reflections. The calculation was later revised slightly by Gold (22) and the result is:

$$\eta_r = 1 + 2.5c + 14.1c^2 + \ldots \quad (14)$$

Eirich and Goldschmid (12) found that Equation (14) held up to 6 volume percent for suspensions of glass spheres in mercuric nitrate - nitric acid solution.

Other experiments by Eirich, Bunzl and Margaretha (11) were made with suspensions of glass spheres in mercuric nitrate - nitric acid solutions, mushroom spores in olive oil - tetrachloroethane mixtures, and yeast particles in water. The suspensions were Newtonian and the viscosity was measured in three types of viscometers - Couette, rising sphere and capillary viscometers. It was found that the Einstein equation was satisfactory up to about 5 volume percent and the following empirical equation represented the experimental results:

$$\eta_r = 1 + 2.5c + 8c^2 + 40c^3. \quad (15)$$

In 1948, Vand (50) (51) studied the problem of the viscosity of suspensions of spheres both theoretically and experimentally. In his calculation of the viscosity of a suspension, he allows for the effect of collisions between spheres as well as the hydrodynamic interaction. He obtains as a result:

$$\eta_r = 1 + 2.5c + 7.35c^2 + \ . \ . \ . \qquad (16)$$

Experimentally, Vand measured the viscosity of suspensions of glass spheres in a solution of ZnI_2 - water - glycerol and the results satisfy the empirical equation:

$$\eta_r = 1 + 2.5c + 7.17c^2 + 16.2c^3 + \ . \ . \ . \qquad (17)$$

in excellent agreement with his theoretical equation.

Manley and Mason (31) found that there was an error in Vand's calculation of the collision frequency of the spheres and when corrected, Vand's theoretical equation becomes,

$$\eta_r = 1 + 2.5c + 10.05c^2 + \ . \ . \ . \qquad (18)$$

Later experiments by Manley and Mason (32) using suspensions of glass spheres in ZnI_2 - glycerol gave as a result,

$$\eta_r = 1 + 2.5c + 12.7c^2 + \ . \ . \ . \qquad (19)$$

In a different approach to the problem, Mooney (35) considered the space crowding effect of the suspended spheres. This is the only theory to postulate an effect of size distribution upon the viscosity of the suspensions. For a suspension of groups of spheres, each group of different diameter, an equation of the form:

$$\ln \eta_r = 2.5 \sum_{i=1}^{m} \frac{c_i}{1 - \sum_{j=1}^{m} \lambda_{ji} c_j} \qquad (20)$$

is presented where λ_{ji} is the crowding factor. For a suspension containing only one size particle the equation reduces to :

$$\ln \eta_r = \frac{2.5\, c}{1 - kc} \qquad (21)$$

where k is the self-crowding factor λ_{ii}. Mooney's approach is partly empirical in that the crowding factors must be experimentally determined, as they can only be predicted approximately.

Effect of Size Distribution

Ward and Whitmore (52) performed experiments with suspensions of spherical polymethylmethacrylate particles in lead nitrate - glycerol - water. The suspensions used were of varying size ratios (ratio of largest to smallest particle diameter) and the viscosities were measured in a rising sphere apparatus. It was found that the relative viscosity depended upon the size ratio of the suspension, decreasing with increasing size ratio.

Eveson (13), using a Couette viscometer, studied similar suspensions to those of Whitmore and also used suspensions consisting of two widely different sizes. It was found that the unimodal suspensions were Newtonian fluids over the range investigated (0 - 20 volume percent), while the bimodal suspensions were pseudoplastic at concentrations higher than 7.5 volume percent. No adequate explanation could be given for this behavior. However, it was found that the relative apparent viscosity was a minimum when about 50 percent by volume large particles composed the suspension.

Another paper by Eveson (15) considered the influence of size distribution upon the viscosity of suspensions of spheres. Three size fractions of average diameter 378, 200 and 47 microns were used. The viscosity of suspensions of mixtures containing:

50% 378 micron	-	50% 47 micron
25% 378 micron	-	75% 47 micron
75% 378 micron	-	25% 47 micron
50% 200 micron	-	50% 47 micron
25% 200 micron	-	75% 47 micron

33 1/3% 378 micron - 33 1/3% 200 micron - 33 1/3% 47 micron

was measured over a concentration range of 0 to 22.5 volume percent. It was found that for suspensions with a discontinuous size-distribution curve, the relative viscosity at a given solids concentration was never higher and was usually lower than the relative viscosity of the components of the mixture at the same concentration. This effect became pronounced at volume concentrations greater than 17.5 volume percent.

Later, Eveson (16) investigated the effect of size ratio of the dispersed phase upon the relative viscosity of suspensions of spheres. There was disagreement on the effect of size ratio, Ward and Whitmore (52) having found a significant decrease in relative viscosity with increasing size ratio, while Eveson (13) and Higginbotham, Oliver and Ward (24) found little if any, effect of size ratio upon the relative viscosity. Eveson prepared eight samples, all having about the same average diameter, but with size ratios varying from 1.60 : 1 to 24 : 1. He found that there was no effect of size ratio upon the relative viscosity. Eveson concluded that the effect of size ratio is unimportant and that a suspension possessing a discontinuous size distribution curve would be more likely to have a lower viscosity than a unimodal suspension.

Some workers with synthetic rubber latices have studied the effect of size distribution upon the rheological properties of the latex. Synthetic rubber latex consists of small, almost spherical particles in a solution composed mainly of water. Fatty acids are used in the polymerization process and these are considered to be adsorbed on the surface of the latex particles. This adsorbed layer may be responsible for the pseudoplastic behavior of latices at higher concentration, this adsorbed layer being progressively sheared off as the shear rate increases. Maron and Madow (33) studied mixtures of two synthetic rubber latices, one with an average particle diameter of 980 Å, the other with an average particle diameter of 1920 Å. It was found

that the latices were Newtonian at concentrations below 25 volume percent and pseudoplastic at higher concentrations up to 55 volume percent. Also the consistency was a minimum at any volume concentration when the large latex was 75 - 80 volume percent of the total.

Johnson and Kelsey (26) (27) carried out a practical study of the effect of size distribution upon the rheology of synthetic rubber latices. Since a Brookfield viscometer was used and the results for the pseudoplastic latices interpreted as if they were Newtonian fluids, their results can give only a qualitative picture of the effect of size distribution. They used three latices of average particle diameter 950, 1710 and 3250 $\mathring{A}$ and found that when the large particles comprise about 75 volume percent of the total and when the difference between the small and large diameters is large, the greatest reduction in "viscosity" was noted.

Sweeny and Geckler (45) studied the rheology of suspensions of glass spheres in ZnI_2 - glycerol - water. They found the suspensions to be pseudoplastic and characterized the rheological behavior by the terms viscosity at low rate of shear η_o and viscosity at infinite rate of shear η_∞. As part of this study they investigated the effect of size distribution on the rheology of the following suspensions at 55 volume percent.

i) 100% 262 microns

ii) 75% 262 microns - 25% 164 microns

iii) 75% 262 microns - 25% 97 microns

iv) 75% 262 microns - 25% 36 microns

v) 75% 262 microns - 25% 13 microns

It was found that the relative viscosity at zero rate of shear and at infinite rate of shear decreased from suspension i) to suspension v) in the above table indicating the influence of the diameter ratio upon the consistency of bimodal suspensions.

In an unpublished paper, Sweeny (46) recently extended the previous work to include results of suspensions of glass spheres. Measurements were made at 40 and 55 volume percent only and four diameter ratios were considered as in the previous paper. However, measurements were made at 25, 50 and 75% of the larger spheres at each of the four diameter ratios. It was found that the minimum "viscosity" occurred when about 70 volume percent of the total solids consisted of large spheres. The diameter ratio also had a significant effect upon the observed viscosity, the maximum reduction in viscosity occurring with mixtures of the largest and smallest spheres. Mooney's equation (Equation (20)) was found to represent the data well, but there is an error in the calculations which invalidates this conclusion.

From the published literature the following conclusions can be drawn:

i) There is no general agreement among the equations of various workers relating the dependence of viscosity upon concentration.

ii) Suspensions of true spheres in polar media usually behave as Newtonian fluids. Thixotropic and pseudoplastic behavior has been noted. In some cases, these anomalies can be explained in terms of surface effects (adsorption), or flocculation of the spheres. Within the experimental error, no dilatancy has been found in suspensions of spheres.

iii) The particle diameter of the spheres in a unimodal suspension has no effect upon the viscosity over a wide range of diameters (10 to 1000 microns).

iv) When the solid phase has a continuous distribution of diameters, there is little effect of size upon the rheological behavior of the suspension over a large range of size ratios (the ratio of the size of the largest sphere in the suspension to that of the smallest).

v) When the solid phase has a discontinuous size distribution, the consistency of the suspension is lower than that of the unimodal components at the same volume concentration. This effect is pronounced at volume concentrations exceeding 20 volume percent and is greatly influenced by the diameter ratio of the two components in

a bimodal suspension, the suspension having the highest diameter ratio also having the lowest consistency.

vi) The effect of size distribution has been carefully studied up to concentrations of 20 volume percent. Above this data are available only at 40 and 55 volume percent. The need is evident for work at intermediate concentrations to tie together the effect of size distribution upon the rheology of suspensions of spheres.

III. EXPERIMENTAL EQUIPMENT AND METHOD

1. Viscometer

A concentric cylinder viscometer was used to determine the rheological properties of the suspensions in this investigation. A "Fann V-G Meter" (Model 35) manufactured by the Fann Instrument Corporation, Houston, Texas previously used by Lindley (30) and Alcorn (1) in their work on the rheology of suspensions was also used in this work. Figure 3 shows the basic features of the instrument. When the sample cup is raised, fluid enters the annular space between the two co-axial cylinders. The rotating cylinder or cup is driven through a system of gears by a 115 volt - 50 cycle dual speed synchronous motor. The torque exerted by the viscous drag on the inner cylinder or bob is balanced by a double-wound helical torsion spring. One end of the spring is coupled to the upper end of the bob shaft; the other end is secured by a mounting clamp. The angular deflection of the bob is read from the scale on the upper surface of the indicating dial which is mounted on the bob shaft. The scale is marked at 1-degree intervals through 270 degrees and is numbered at 10-degree intervals. An optical reticule is provided for accurate reading of the scale.

FIGURE 3

PHOTOGRAPH OF THE VISCOMETER

In the standard model, cup speeds of 3, 6, 100, 200, 300 and 600 rpm are obtained smoothly and rapidly without stopping rotation by means of a three position gear shift in conjunction with the two position switch controlling the motor speed.

The instrument used in this work was modified in three ways. Firstly, the stainless steel cup used on the standard model was replaced by a copper cup with an annular jacket. Ethylene glycol solution from a large (10 Imp. Gal.) constant temperature bath was circulated through the sample cup jacket by means of an immersion pump. The temperature in the sample cup was held at $20 \pm 0.1^{\circ}C$ by means of a Thermotrol (Hallikainen Instruments, Berkeley, California) controlling the temperature of the bath. Secondly, additional shear rates were obtained by the interposition of a 9 : 1 reduction gear between the synchronous motor and the body of the instrument. This modification permitted greater coverage in the region from 6 to 100 rpm. Thirdly, two additional cups of larger diameter than the standard cup were machined from brass. This permitted the use of large particles in the suspensions without binding or wall effects.

In addition to the standard helical torsion spring, two weaker springs were purchased from the manufacturer. These springs were 1/2 and 1/5 as strong as the standard spring, and allowed measurements to be made on fluids of low viscosity.

The various cup-bob combinations were calibrated with Newtonian standard oils. The viscosities of these oils had been determined at 70°F in Master Cannon-Fenske capillary viscometers. Four oils were used, of viscosity 19.1, 56.7, 93.6 and 147.9 centipoise. The results of these calibrations are presented in Appendix A.

2. Suspensions

The suspensions used in this work consisted of spherical particles of styrene-divinylbenzene resin in an equal density solution of glycerol, isopropanol and water. The styrene-divinylbenzene copolymer resin (8% divinylbenzene) was obtained from Dow Chemical Company, Midland, Michigan and three nominal sizes were used. They were 40/60, 100/200 and 200/400 mesh (U.S. Standard Sieve Series). Duplicate sieve analyses employing both dry sieving and wet sieving with isopropanol were performed using stainless steel U.S. Standard Sieves. The results of these analyses are given in Appendix D and they are plotted in Figure 4 to show the size distribution of the original materials. The density of the beads was determined by the standard pycnometer method and the average density was found to be 1.0487 gm/ml.

Samples of three powders were photographed through a microscope (71X) to give an indication of the size distribution and shape of the particles. These photomicrographs are shown in Figures 5 and 6. It can be seen that the particles are all spheres and that the size distribution for any powder is not large.

Suspending solution No. 1 had the following approximate composition:

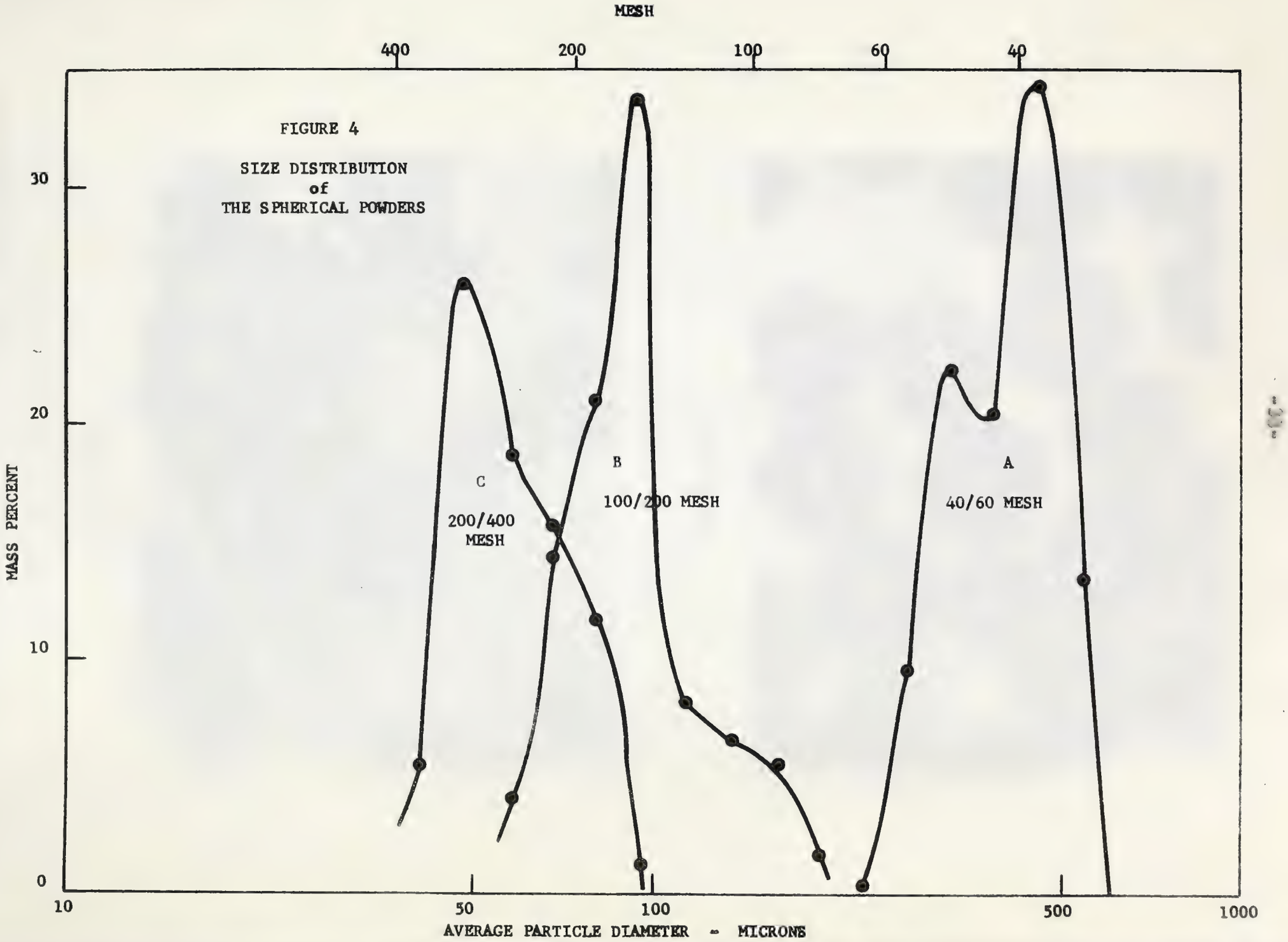
MESH
400
200
100
60
40
FIGURE 4
SIZE DISTRIBUTION
of
THE SPHERICAL POWDERS
30
20
10
0
MASS PERCENT
C
200/400
MESH
B
100/200 MESH
A
40/60 MESH
10
50
100
500
1000
AVERAGE PARTICLE DIAMETER - MICRONS

40/60 MESH

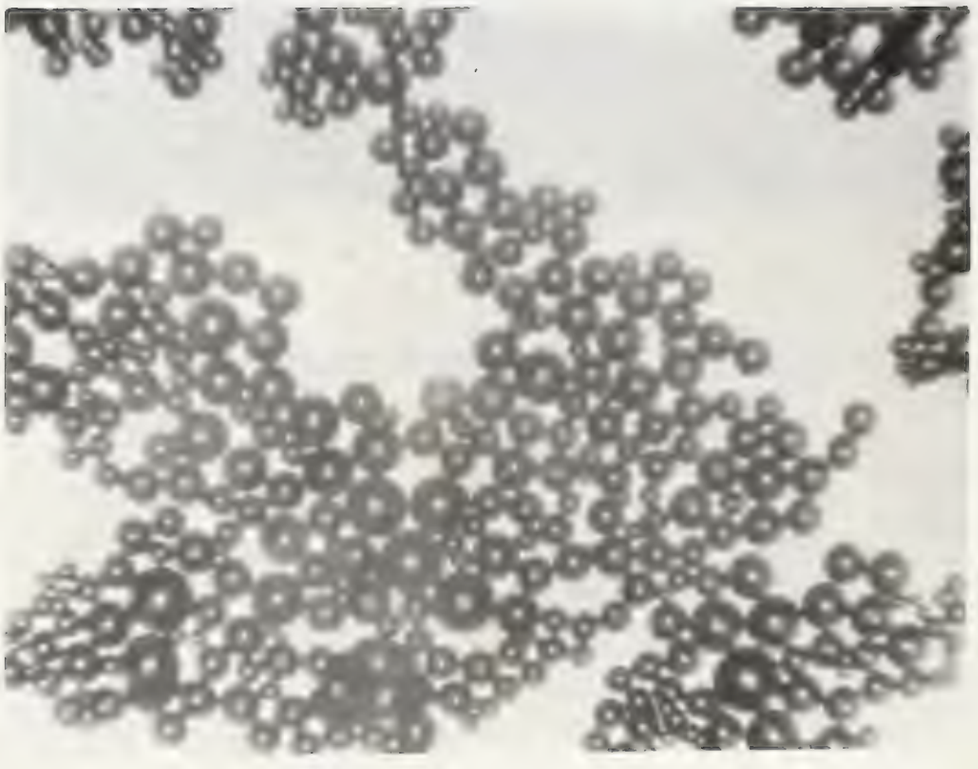

100/200 MESH

FIGURE 5

PHOTOMICROGRAPHS OF THE 40/60 MESH AND THE 100/200 MESH POWDERS (71X)

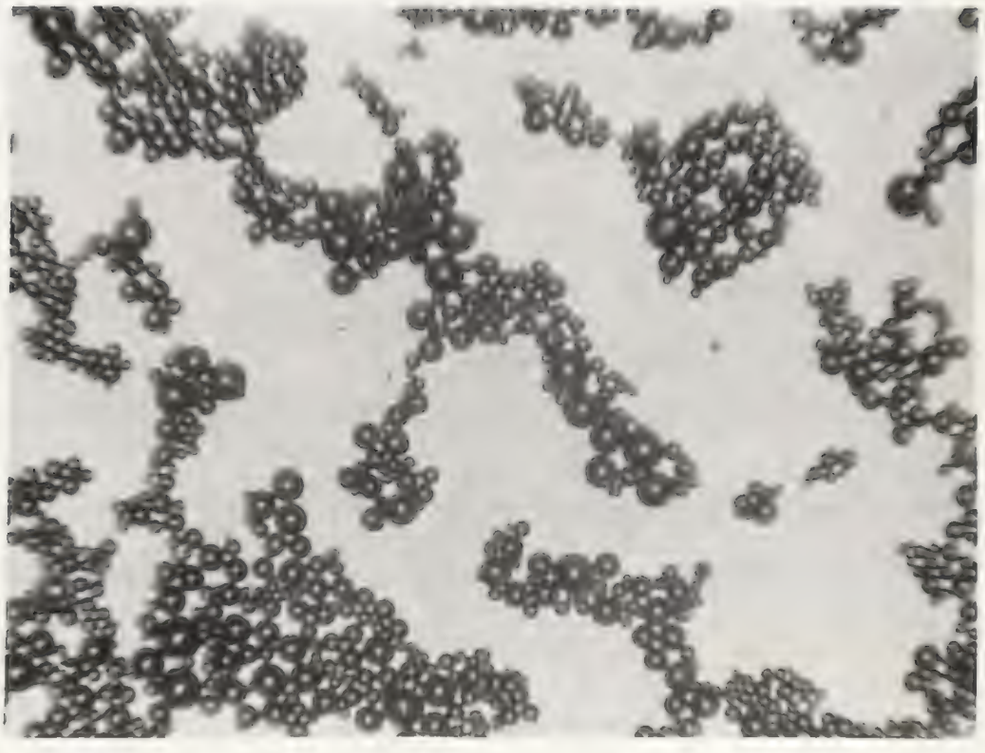

FIGURE 6

PHOTOMICROGRAPH OF THE 200/400 MESH POWDER (71X)

	Weight Percent
Glycerol	40
Isopropanol	25
Distilled water	35
	100

The density and viscosity of the solution were determined at 20.0°C. The standard pycnometer method was used in the density determination and the viscosity was measured in a Master Cannon-Fenske capillary viscometer.

Density - 1.0491 gm/ml at 20.0°C

Viscosity - 12.14 centipoise at 20.0°C

Near the completion of this investigation suspending solution No. 1 was exhausted and a second solution was prepared. It had the following composition and properties:

	Weight Percent
Glycerol	45
Isopropanol	30
Distilled water	25
	100

Density - 1.0494 gm/ml at 20.0°C

Viscosity - 17.29 centipoise at 20.0°C

3. Auxiliary Equipment

Temperatures were measured by a sixteen inch mercury-in-glass thermometer (Scale: - 1^{o} to 51^{o} C). The thermometer was calibrated against a standard platinum resistance thermometer. The calibration data and curve are given in Appendix C. All temperature readings were made with a thermometer reading lens which allowed the thermometer to be read to 0.02^{o}C.

Other equipment used included an analytical balance accurate to 0.001 grams with a maximum load of 500 grams and a graduated cylinder marked at 1 milliliter intervals. These two pieces of equipment were used to determine the volume concentration of the suspensions.

4. Experimental Method

Two procedures were followed in measuring the rheological properties of the suspensions. In the first, a known volume of suspending solution was poured into the sample cup and allowed to attain the bath temperature. When the temperature, measured with the standard thermometer, was $20.0^{\circ}C \pm 0.1^{\circ}C$, the sample cup was raised so that the fluid covered the top of the tape on the viscometer cup. The viscometer was switched on the lowest speed at which a reading could be obtained. After the stable reading had been noted, the viscometer was switched to the next highest speed. This was continued until the highest speed was reached and the reverse procedure was followed, obtaining the readings at successively lower speeds.

Next, solids from a weighed beaker were poured into the sample cup and the beaker reweighed. The sample cup was placed on top of a magnetic stirrer and stirred by means of a Teflon-covered magnet for about 2 minutes. The temperature of the suspension was read and the dial deflections versus speed obtained as before. In order to avoid cumulative errors in weighing, the spheres were added from a full beaker and the beaker weighed when full and after each addition of solids.

This procedure was followed until the torque was too great to be measured with the weakest spring (No. 3). Then the No. 2 spring

was inserted and the readings continued. Eventually, above 55 volume percent, the suspension became so viscous that readings with the strongest spring could be obtained only at very slow speeds and the readings became so erratic that at this point the test was terminated.

Although this procedure would seem to be satisfactory, a problem arose in the calculation of the volume concentration. Over the course of a run (4 to 6 hours) the viscometer cup was out of the sample cup for long periods of time. Evaporation of solution occurred and portions of the suspensions were lost when the thermometer was removed after a temperature reading. Also since the sample cup was of fixed volume and enough solution was added initially to allow a reading to be obtained, after some solid had been added, the sample cup was full. In the process of removing suspension between tests errors may have occurred in the volume withdrawn. These problems were brought out by samples taken during a run. It was found that the measured concentration was higher than that calculated from the initial volume of solution plus the solids added minus the amount of suspension removed. This was also checked by experiments made at an accurate volume concentration, by mixing together the amount of solid and liquid necessary for a particular desired concentration. On the basis of these two checks, the calculated concentrations were corrected at the higher volume fractions; however, the correction was not a constant and increased as the concentration increased. For this reason a second procedure was adopted for later runs.

In this method, an amount of solution required to produce a suspension of the desired solids concentration and a total volume of 240-250 ml was poured into the sample cup. The amount of solids necessary to give the desired solids concentration was weighed out by means of the analytical balance and the suspension mixed together in the sample cup with the magnetic stirrer. The temperature of the suspension was measured with the standard thermometer; then the sample cup was raised and the dial deflections read as the speed was increased to maximum and decreased to zero. The sample cup was allowed to remain around the viscometer cup and bob for 5 minutes. Then the dial deflection-speed sequence was run as before. The sample cup was lowered, the sample discarded and the viscometer cup and bob and the sample cup cleaned with water in preparation for a new test. In this way, the solids concentration was known accurately and the major portion of the error is in the viscometric measurement. However, this method requires much more solid and solution than the first procedure.

5. Mechanical Difficulties

Bearing Friction

In preliminary calibration experiments, it was found that dial deflection versus speed data for Newtonian standard oils did not fall on a straight line with a slope of unity when plotted on log-log paper. There was a definite curvature at low speeds, the data being higher than the line with a slope of unity. It was found that this was a result of friction in the bearings separating the bob shaft from the rotating sleeve that drives the cup. It was suggested that the bearings were old or worn; however, replacement with new bearings gave the following results. If the viscometer dial was set to zero when the cup was not in motion, a deflection of 1 to 2 degrees was observed when the viscometer cup was removed and the instrument turned on. This deflection accounts for the higher readings at low values of speed. For example, at low speeds with a deflection of say 10 degrees, 1 to 2 degrees is an appreciable fraction of the total, while at high speeds with a deflection of say 220 degrees, this amount is almost insignificant. It was found that the error due to bearing friction could be partially eliminated by setting the dial deflection to zero while the viscometer was running in air without the cup attached. This was done at a speed of 300 rpm and it was found that at very low speeds the dial deflection at no load was slightly negative, while at 600 rpm, the deflection was about 0.5 degrees.

This fact limited the precision of the dial readings for the instrument to $\pm$ 0.5 degrees.

Temperature Variations

Although the bath temperature control was very good, problems were encountered whenever the ambient temperature differed from the bath temperature by more than about 0.5°C. Before a test, the viscometer is at the room temperature. When the sample cup is raised, covering the viscometer cup and bob, any difference between the ambient temperature and the sample cup temperature results in a temperature gradient along the viscometer annulus. The viscosity of the suspending solution changed about 6% per degree centigrade change in temperature, so only a slight difference between the room temperature and the bath temperature had a significant effect upon the measured rheological properties. For this reason, in all tests, the room temperature was adjusted to 20.0 $\pm$ 0.5° C before any tests were performed. It would seem that a constant temperature room or cabinet is necessary for ease in taking measurements.

Another problem in temperature control is the heat buildup upon prolonged shearing. It was found that after shearing a Newtonian standard oil for 2 to 3 minutes, at 300 rpm, a slow decrease in dial deflection with time was noted. This was probably due to inefficient conduction of the heat produced in shearing. In this viscometer heat

produced in the annulus must first be conducted through the viscometer cup to the bulk sample of suspension. Thus another temperature gradient exists, after shear, between the wall of the sample cup and the annulus of the viscometer. This inefficiency in removal of heat produced in shearing meant that accurate viscometric measurements could not be made continuously for more than about 2 minutes.

Cylinder Alignment

It was noticed that the viscometer cups or outer cylinders did not turn concentric with the viscometer bob, but precessed as much as 3.5 thousandths of an inch. It is to be expected that this misalignment would increase the dial deflection since the minimum dissipation of energy would occur when the cup and bob are concentric. It was considered, however, that errors due to this cause were insignificant compared with those due to temperature control and other mechanical difficulties.

Oscillation of Viscometer Bob

In preliminary tests to determine the suitability of suspending solutions, tests were made with solutions of viscosity 3.2 and 6.5 centipoise. However, it was found that the dial readings oscillated widely with the 6.5 centipoise solution for about 1 minute. With the 3.2 centipoise solution no stable reading was obtained. For

this reason, the 12.14 centipoise solution used in this work represents a practical minimum with which accurate viscometric measurements are possible. Weltmann (54) has stated that in order to obtain dial deflections rapidly, the system should be slightly overdamped. In the case of the Fann viscometer, the heavy metal bob ensured that the system is underdamped unless fluids of viscosity 50 centipoise or more are studied. For accurate work on fluids, the viscosity of which is as low as water, a light plastic bob with low inertia would be required.

Sample Level in Viscometer Annulus

In preliminary calibration runs with a Newtonian standard oil, it was found that dial readings at 600 rpm were consistently lower than those required for a straight line of dial deflection versus speed. An insight into this phenomenon was obtained when it was found that if the sample cup were not raised to the scribe mark on the viscometer cup, a linear response was obtained including the 600 rpm speed. The article by Savins and Roper (42) explained this matter fully. These workers used a Fann VG Meter and found the deflection at 600 rpm to be 1.5% low compared to the straight line drawn through zero and the 300 rpm reading. Whereupon, they constructed a transparent plastic viscometer cup and a transparent sample cup in order to observe the flow pattern in the annulus. When a small amount of dye was introduced near the base of the bob, it was observed to flow upwards in the annulus and out the ports in the upper portion of the

viscometer cup. Also the position of the liquid level in the annulus was found to depend upon the cup speed. These workers found that,

> " at the 300 rpm setting the liquid level dropped appreciably below the rest level but very little of the upper portion of the bob was exposed above the liquid. The drop in level at the 600 rpm setting was so pronounced that in most cases the conical upper surface of the bob was completely exposed above the sample. However, by sealing the sleeve ports with tape, the circulation was eliminated with the result that the liquid level did not drop below the upper tip of the conical portion of the bob at either rotor speed."

Since this was reponsible for the apparent low readings at 600 rpm, the sleeve ports were sealed with electrical tape for all subsequent calibration and experimental work. With this technique the 600 rpm data lay on a straight line through the origin and the lower speed data points.

Apparent Thixotropy in Sphere Suspensions

In preliminary experiments with polystyrene spheres (Dominion Anilines and Chemicals, Toronto), thixotropic behavior was noted at concentrations as low as 20 volume percent. That this was thixotropy and not a temperature effect was evident from the rapidity with which the dial deflection decreased in the first minute of shear. After this period the dial deflection decreased slowly making it difficult to separate the effects of temperature increase and thixotropy.

Since it was not desired to study the thixotropic breakdown of a suspension and also because it is difficult to envision a suspension of spheres as a thixotropic fluid, attempts were made to disperse the spheres with chemical dispersants. However, a large number of dispersants of various classes of compounds failed to have any effect.

At this time, the styrene-divinylbenzene copolymer spheres were received and in experiments with these particles, thixotropic behavior was noted at concentrations greater than about 30 volume percent. Thus both types of spheres appeared to be similar in their suspension properties.

The reason for the thixotropic behavior is thought to be flocculation of the spheres. In the process of shear, these aggregates are broken down, decreasing the consistency with time as shearing progresses. Since flocculation was considered to be the cause of the problem, the forces involved which create the aggregates were considered.

Three possible types of forces can cause flocculation. These are chemical forces, electrical forces and physical forces. Firstly, the thixotropy did not seem to be a result of chemical forces, in that dispersants of various chemical types had no effect. Electrical (electrostatic attraction) forces also did not seem to be the answer because the solution is polar and charge induced on the particles

should slowly drain off, especially since the suspension was placed in a copper cup which was grounded. Another reason why electrical charges were not considered to be the cause of the thixotropy is that addition of ionic compounds such as NaCl and $Pb(NO_3)_2$ had no effect. The addition of compounds such as these increases the conductivity of the solution and would tend to dissipate electrical charges very quickly. Physical forces, in particular surface tension, appear to be the most plausible explanation of the thixotropic behavior. The particles are originally in air and when placed in the suspending solution, they would presumably retain some air on the surface. This air bubble could hold two or three particles together by the suface tension between the solution and the air bubble. Since these forces are weak, shearing breaks up these doublets and triplets. However, the air bubble would not necessarily rise as it is very small and the head of solution over it may effectively prevent its escape. Some evidence in support of this explanation may be found in the determination of the density of the plastic particles. In this determination, the particles were placed in a density bottle and a heavy oil poured over them. Vacuum was applied to the bottle to remove all traces of air. It was found that small bubbles of air continued to rise from the solid for as long as four hours on the vacuum pump. From this it can be seen that small traces of air might never come to the surface of the suspension. Unfortunately, attempts to apply a vacuum to the suspension caused the solution to boil, because of the large amount of water and isopropanol which it

contained. The experience of Vand (51) also supports this explanation. He used a Couette viscometer and stirred the suspension of glass spheres by bubbling air through it. It was found that at concentrations above 40 volume percent the dial deflection immediately after air stirring was much greater than normal, and decreased with time exponentially to its normal value.

Since the true effect of the spheres in the liquid is noted when the aggregates are completely broken, mechanical shear outside the viscometer was attempted. The sample cup was placed on a magnetic stirrer and a Teflon-covered magnet placed inside the cup. It was found that shearing by this method gave no further change in the rheological properties after 2 minutes and the suspension remained in a broken down state for up to 30 minutes after shearing ceased. The procedure adopted for viscometric measurements involved 2 minutes of shear with the magnetic stirrer immediately before a test was made. Tests were conducted on a particular suspension for up to 20 minutes after shearing by this method. By this standard procedure, a sample upon which reproducible measurements could be made was prepared.

IV. EXPERIMENTAL RESULTS AND DISCUSSION

Viscometric measurements were made on the following suspensions over a concentration range of 0 to 50 volume percent:

i) 40/60 mesh - Material A

ii) 100/200 mesh - Material B

iii) 200/400 mesh - Material C

iv) 50% A - 50% B

v) 25% A - 75% B

vi) 75% A - 25% B

vii) 50% A - 50% C

viii) 25% A - 75% C

ix) 75% A - 25% C

x) 50% B - 50% C

xi) 33 1/3% A - 33 1/3% B - 33 1/3% C

It was found that the suspensions behaved as Newtonian fluids over the entire range of concentration studied. The basic experimental data are given in Appendix E, and the calculated results are given in Appendix F.

1. Unimodal Suspensions

The relative viscosity-concentration data for the three unimodal suspensions are plotted in Figure 7. It can be seen that there is a significant difference between suspensions composed of material B as received and those composed of materials A or C. This difference did not appear to be a dependence of viscosity upon particle size as material B is intermediate in size. Nor did it appear to be a result of size distribution, since all three original powders had essentially the same narrow distribution of particle sizes. Only one physical difference between the powders was noted. Samples A and C were free-flowing, that is, the angle of repose in air was very small. On the contrary, sample B was not free-flowing. Material on a spatula would not fall off even when the spatula was held vertically. The reason for this difference in dry flow properties was thought to be due to solvent which caused adherence of the particles. This solvent was presumed to be the material in which the particles were polymerized, and was not completely removed when the particles were dried. For this reason the particles were washed with isopropanol to remove the solvent. About 2 pounds of material B was mixed with isopropanol to form a dilute slurry. A portion of this slurry was poured on a 400 mesh sieve and the isopropanol allowed to drain off. Fresh isopropanol was then poured over the sieve to remove any trace of solvent remaining. The sieve was set to dry in an oven at 40°C. When dry the powder was found to be free-flowing. This procedure was continued until all the slurry had been washed in isopropanol and dried. Figure 7 shows

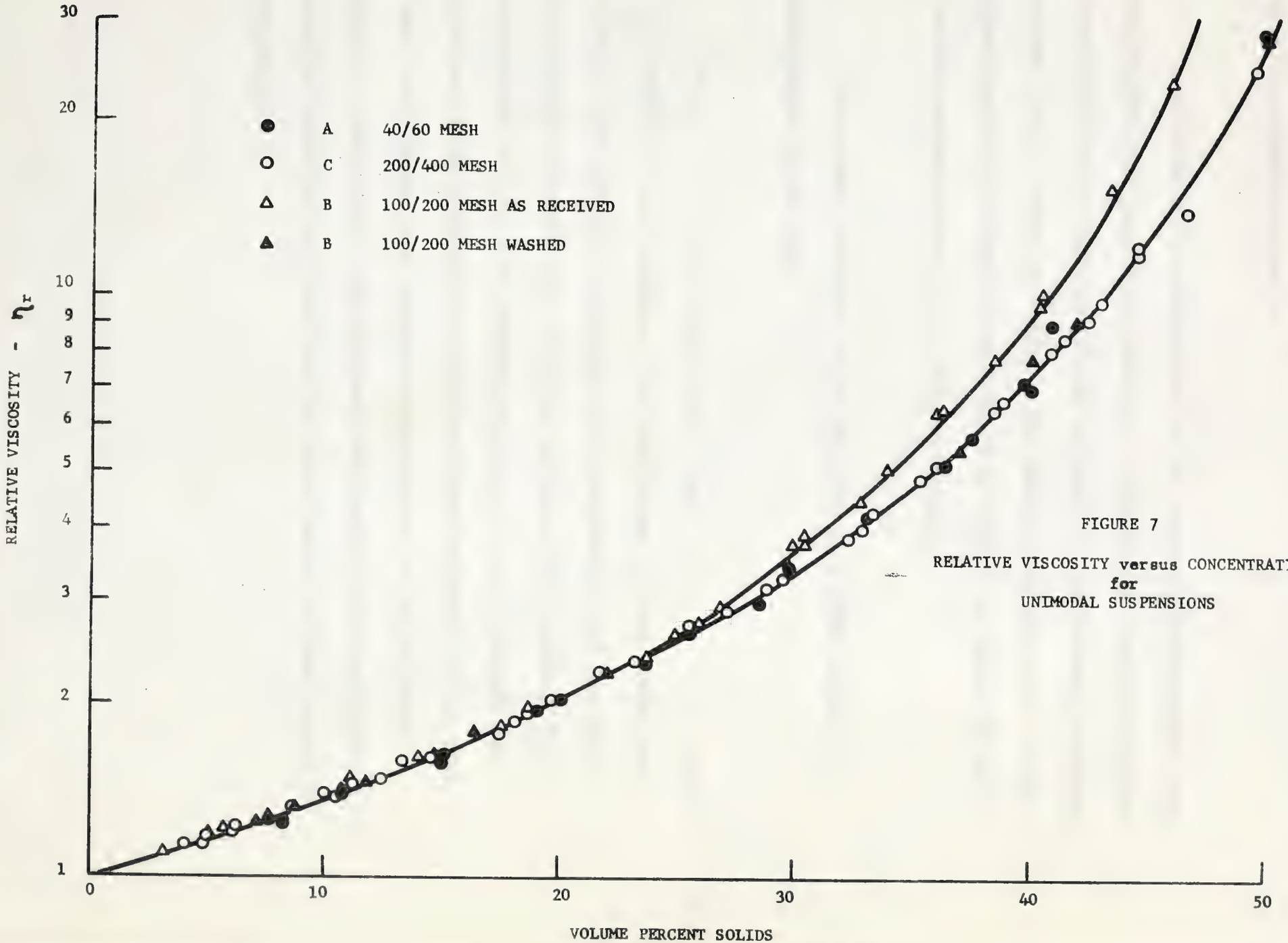

FIGURE 7

RELATIVE VISCOSITY versus CONCENTRATION
for
UNIMODAL SUSPENSIONS

that the washed material exhibits a viscosity-concentration relationship similar to materials A and C.

An interesting observation is the range of concentration over which the Einstein equation is valid. A plot of the observed relative viscosity divided by that calculated by means of the Einstein equation, Equation (13), is shown in Figure 8 for unimodal suspensions. It can be seen that the Einstein equation would be correct to within 1% only at volume concentrations up to 2 volume percent.

An attempt was made to fit the data to a power series in concentration of the form

$$\eta_r = 1 + 2.5c + ac^2 + bc^3 + ec^4 \quad . \quad . \qquad (22)$$

by the method of least squares. The coefficient 2.5 was chosen for the second term because theoretical and experimental work has shown this constant to be correct. Also the curvature of a graph of η_r - concentration is such that accurate estimates of this constant can only be made from measurements at volume concentrations of less than 5% and this requires very accurate determination of the relative viscosity. Since only a few data were obtained in this concentration range, the value 2.5 was taken for the first term of a power series in concentration.

FIGURE 8

TEST OF EINSTEIN'S EQUATION
for
UNIMODAL SUSPENSIONS

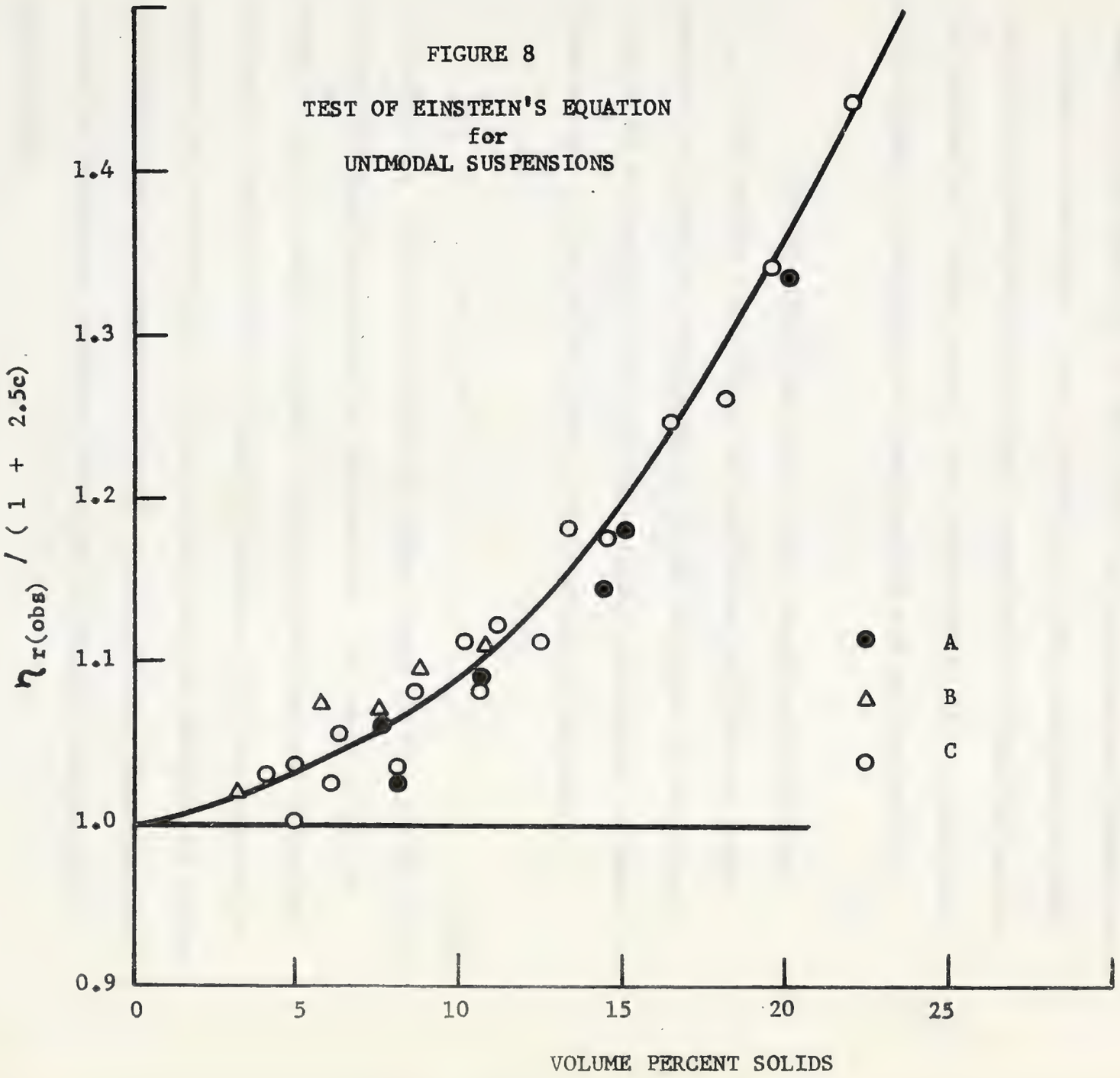

Since the relative viscosity increases continuously and monotonically with concentration, $d^2\eta_r/dc^2 > 0$, and all coefficients in Equation (22) must be positive. However, using the method of least squares to fit the data, it was found that negative coefficients were obtained in some cases. Also, coefficients that were negative when say a third power series was tried, became positive when the series was changed to a fourth power. For these reasons it was concluded that fitting by the method of least squares was not satisfactory.

A second method was tried. This consisted of plotting $(\eta_r - 1)/c$ versus c to obtain the coefficient of c as the intercept at $c = 0$ and the coefficient of c^2 as the slope of the linear portion of the graph. This plot for unimodal suspensions is shown in Figure 9 and it can be seen that a power series of the form

$$\eta_r = 1 + 2.5c + 10c^2 + \ldots \qquad (23)$$

is indicated. It was found that the higher terms of this series could not be determined accurately by this method. The range of fit of Equation (23) is shown in Figure 10 in which the observed viscosity divided by that calculated by means of Equation (23) is plotted as a function of concentration. It can be seen that the equation is correct to within 5% at concentrations up to 14 volume percent. Equation (23) checks the theoretical equation of Manley and Mason, Equation (18), very closely.

FIGURE 9

$\frac{\eta_r - 1}{c}$ versus c

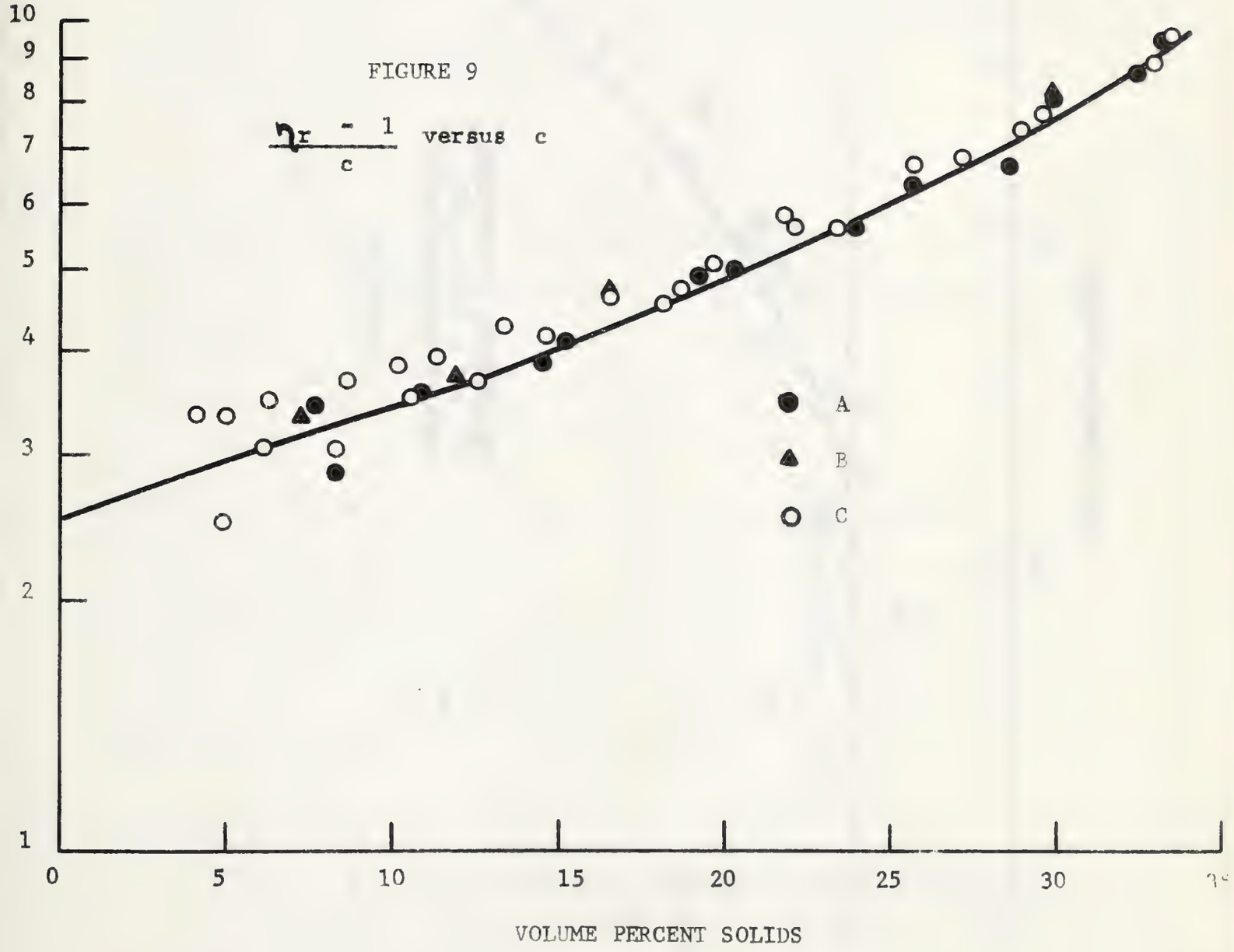

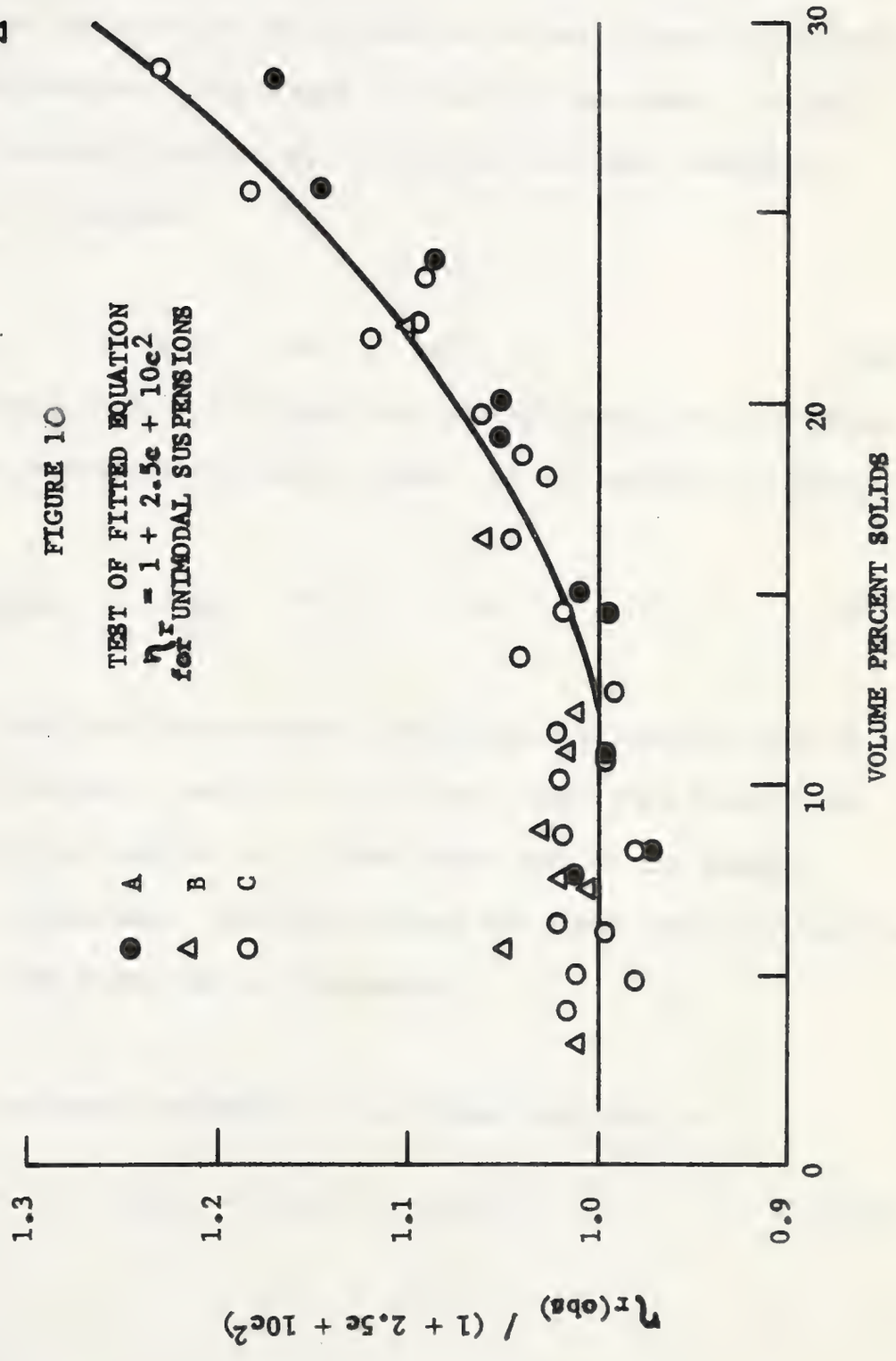
FIGURE 10
TEST OF FITTED EQUATION
$\eta_r = 1 + 2.5c + 10c^2$
for UNIMODAL SUSPENSIONS
A
B
C
$\eta_{r(obs)} / (1 + 2.5c + 10c^2)$
1.3
1.2
1.1
1.0
0.9
0
10
20
30
VOLUME PERCENT SOLIDS

It can be seen that there is little difference among the results for unimodal and the various bimodal suspensions at concentrations below 20 volume percent. Thus all the results may be fitted by Equation (23) at low concentrations. For this reason, a method of correlation was sought which would show the effect of size distribution at high concentrations. The method of Vand (51) was used. In this method, the relative fluidity, ϕ_r, is fitted to a power series in concentration of the form

$$\phi_r = 1 - 2.5c + ac^2 + bc^3 \qquad (24)$$

Because the curve of $\phi_r - c$ is much more nearly linear than the curve of $\eta_r - c$, only three terms need be used. If the equation is recast in the form

$$\frac{1 - \phi_r}{c^2} - \frac{2.5}{c} = -a - bc \qquad (25)$$

a plot of the left hand side versus c should give a straight line of slope $-b$ and intercept $-a$ at $c = 0$. It was found that this method worked well and was used for all of the other data on the bimodal and trimodal suspensions. The calculations and plots used to obtain the coefficients a and b are given in Appendix H.

For unimodal suspensions, the fitted equation is

$$\phi_r = 1 - 2.5c - 0.3c^2 + 2.9c^3. \qquad (26)$$

In Figure 11, a test of the fitted equation is given by plotting η_r (observed) X ϕ_r (calculated from Equation (26)) versus concentration. It can be seen that most of the points are within $\pm$ 5% of unity. This method of correlation is satisfactory for ϕ_r because of the relative linearity of the ϕ_r - c plot; the series can then be truncated at 3 terms. However, if this three term series is converted to a series of η_r - c by long division, the resulting series is only very slowly convergent and cannot be truncated. For this reason, all of the fitted equations were left in the ϕ_r form.

FIGURE 11

TEST OF FITTED EQUATION
for
UNIMODAL SUSPENSIONS

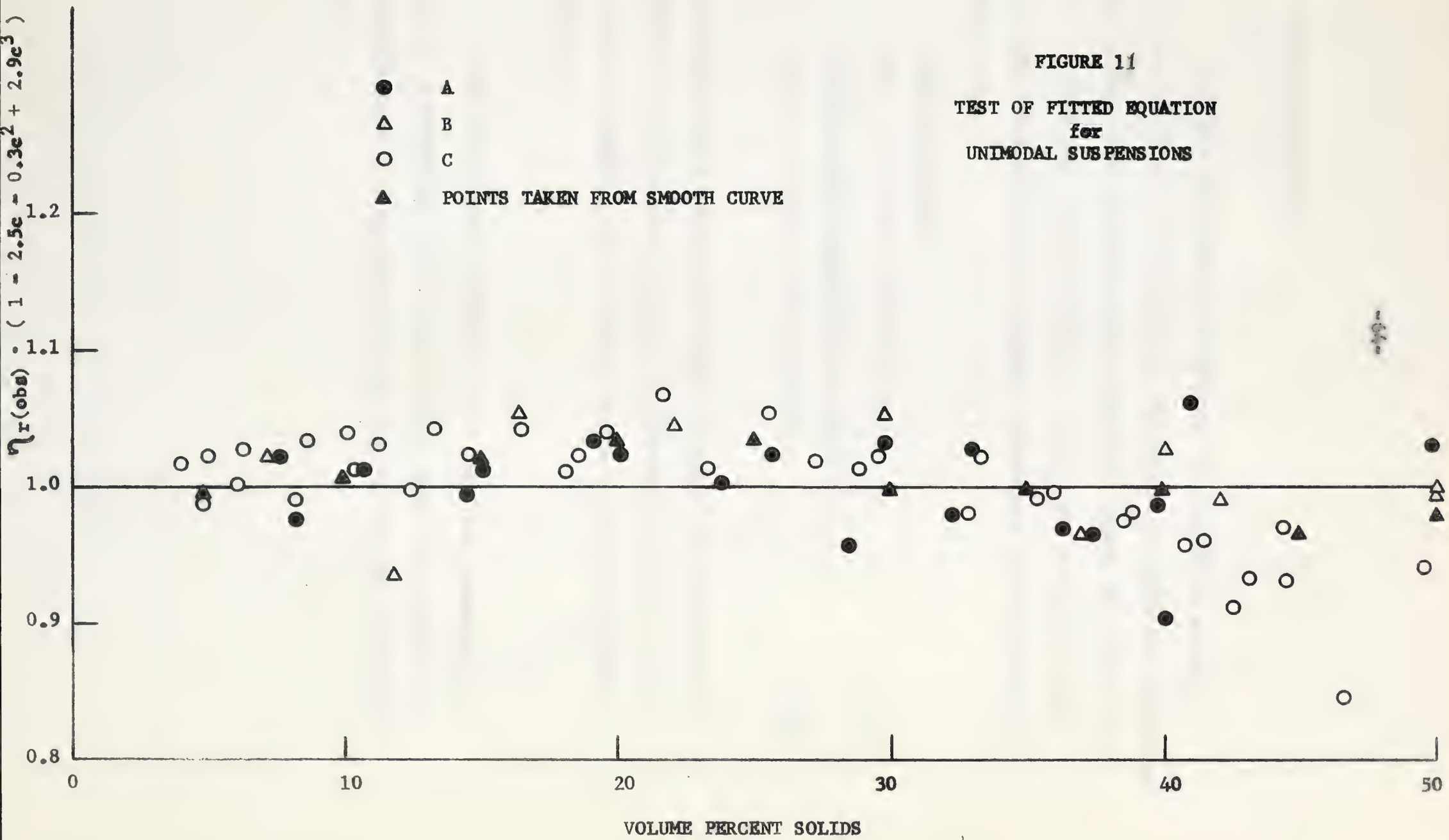

2. Bimodal Suspensions

The data for bimodal suspensions of A and B are given in Figure 12. The line for the unimodal suspensions is given for reference. It can be seen that there is little difference between the results for 50% A - 50% B and those for 75% A - 25% B. The data were fitted by the same procedure used for unimodal suspensions and the resulting equations are:

25% A - 75% B

$$\phi_r = 1 - 2.5c + 0.2c^2 + 1.96c^3 \qquad (27)$$

50% A - 50% B and 75% A - 25% B

$$\phi_r = 1 - 2.5c + 0.8c^2 + 0.92c^3 \qquad (28)$$

These equations were tested by the same procedure used for unimodal suspensions and the results are given in Figures 13 and 14. Most of the points are within $\pm$ 3% of unity in Figure 13 and $\pm$ 5% of unity in Figure 14.

Data for bimodal suspensions of A and C are presented in Figure 15. A comparison with Figure 12 shows that the viscosity at any concentration is slightly lower than that for bimodal mixtures of A and B.

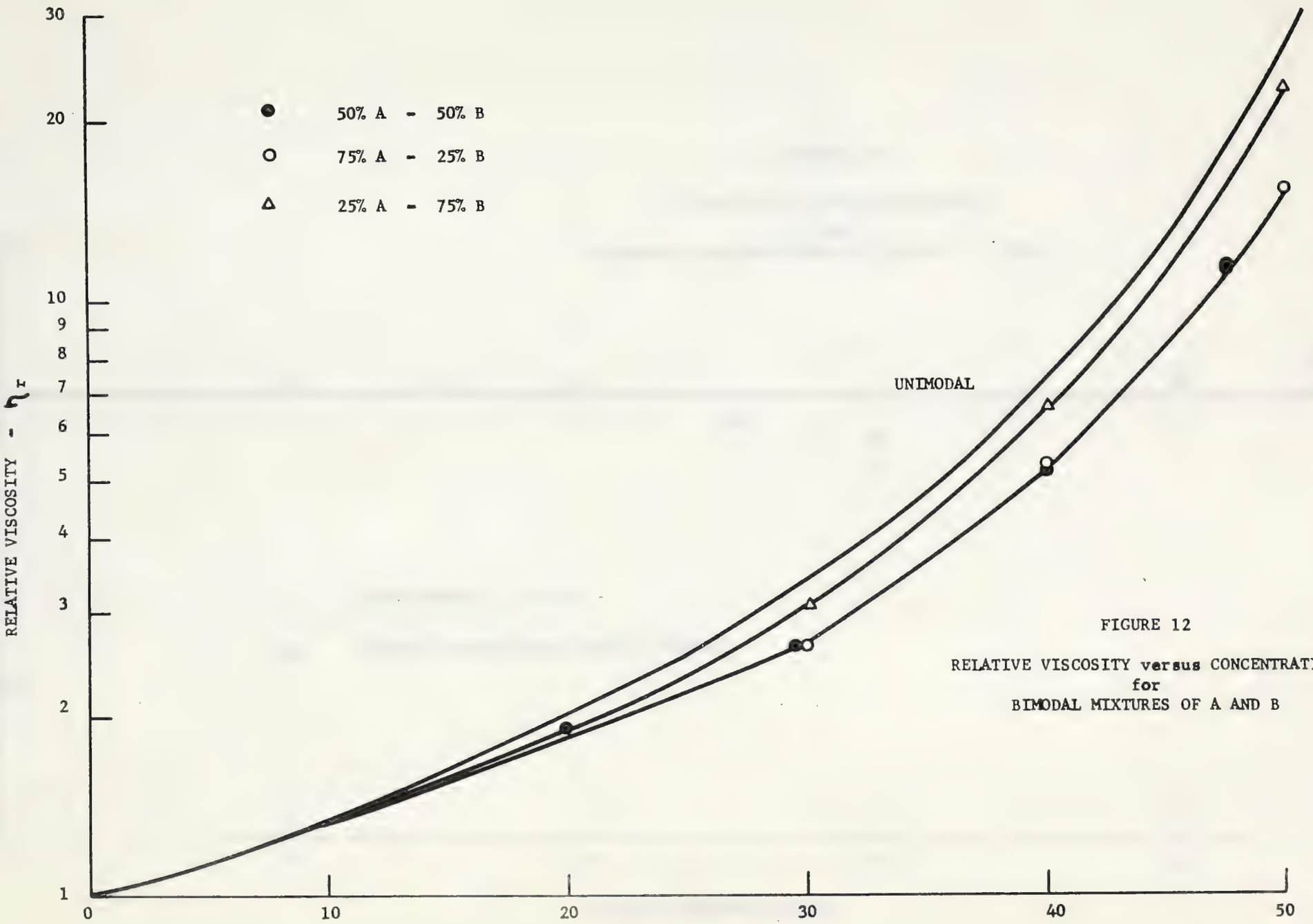

FIGURE 12

RELATIVE VISCOSITY versus CONCENTRATION
for
BIMODAL MIXTURES OF A AND B

FIGURE 13

TEST OF FITTED EQUATION
for
BIMODAL SUSPENSIONS OF 25% A - 75% B

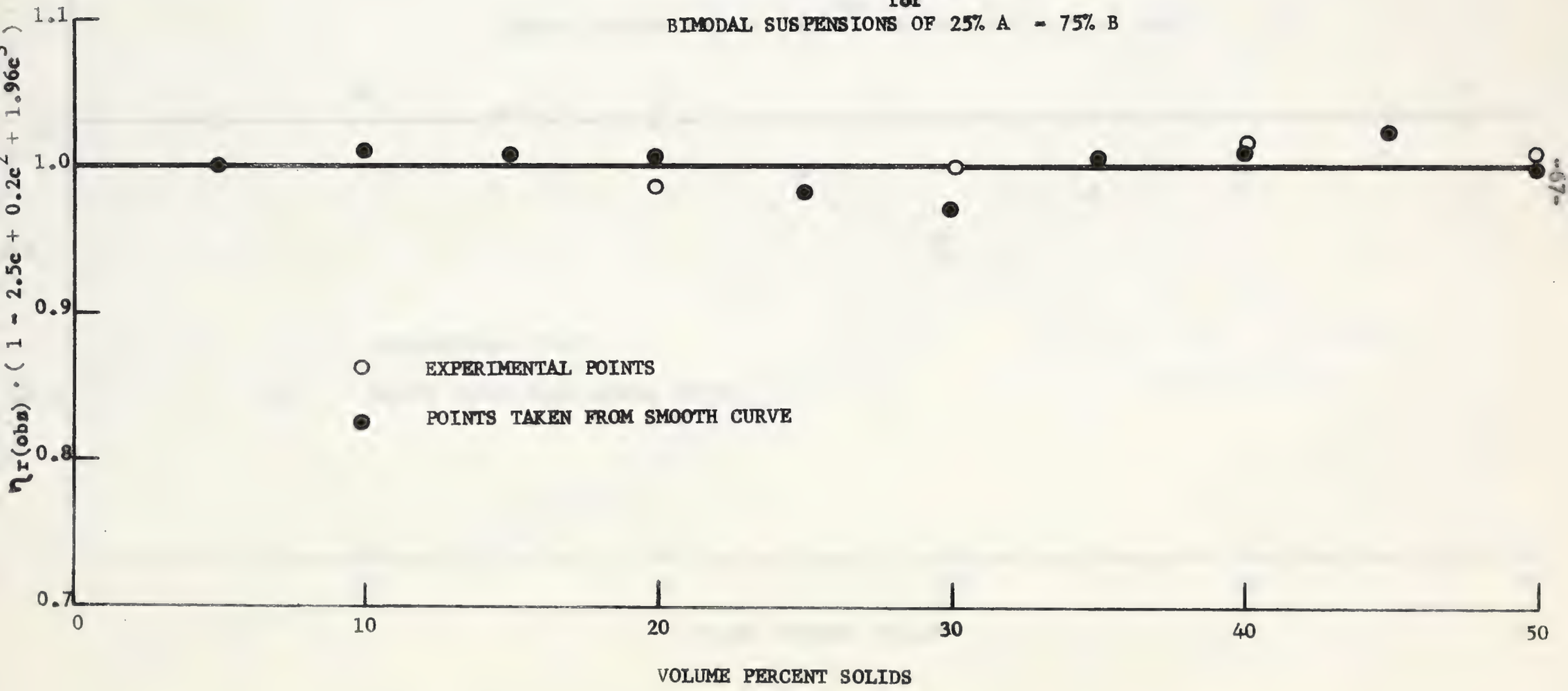

FIGURE 14

TEST OF FITTED EQUATION
for
BIMODAL SUSPENSIONS OF 50% A - 50% B and 75% A - 25% B

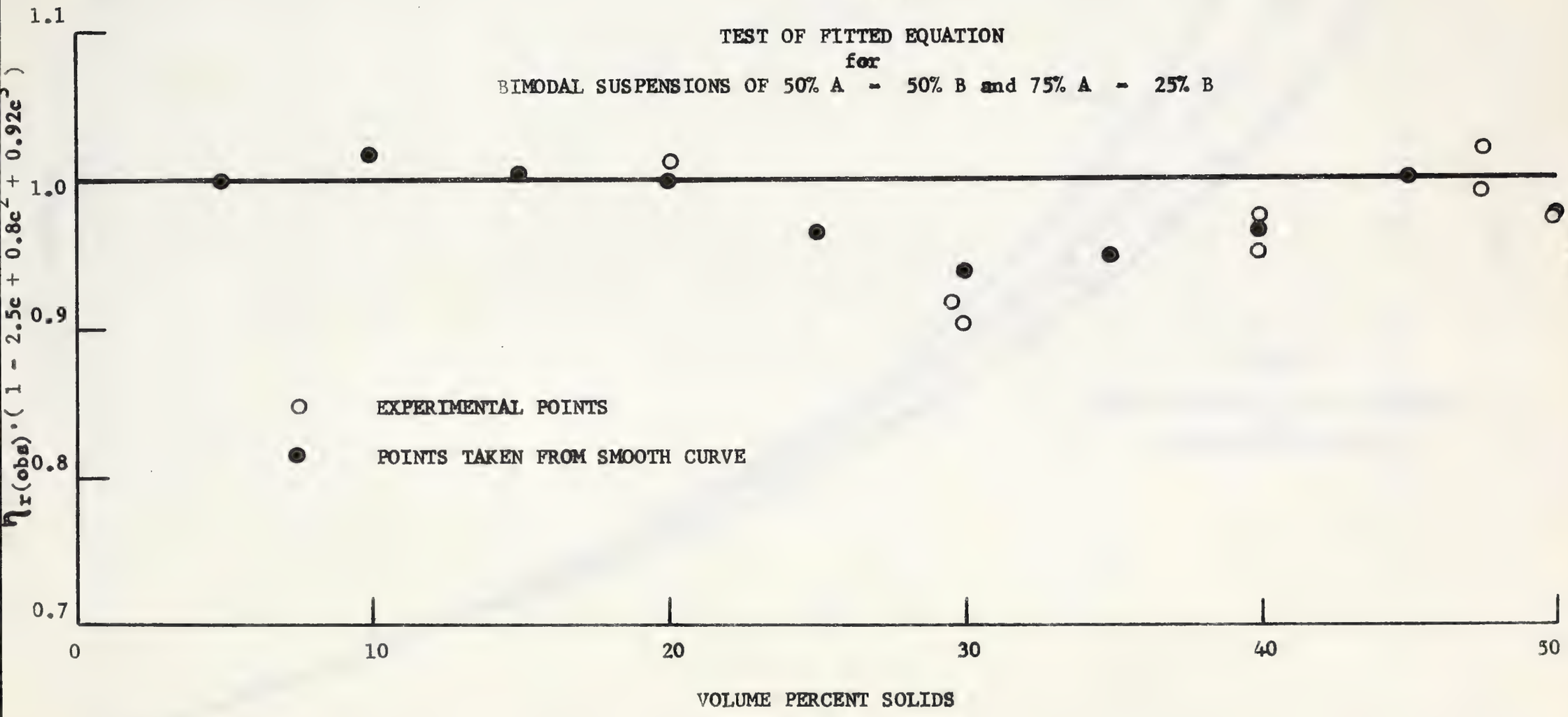

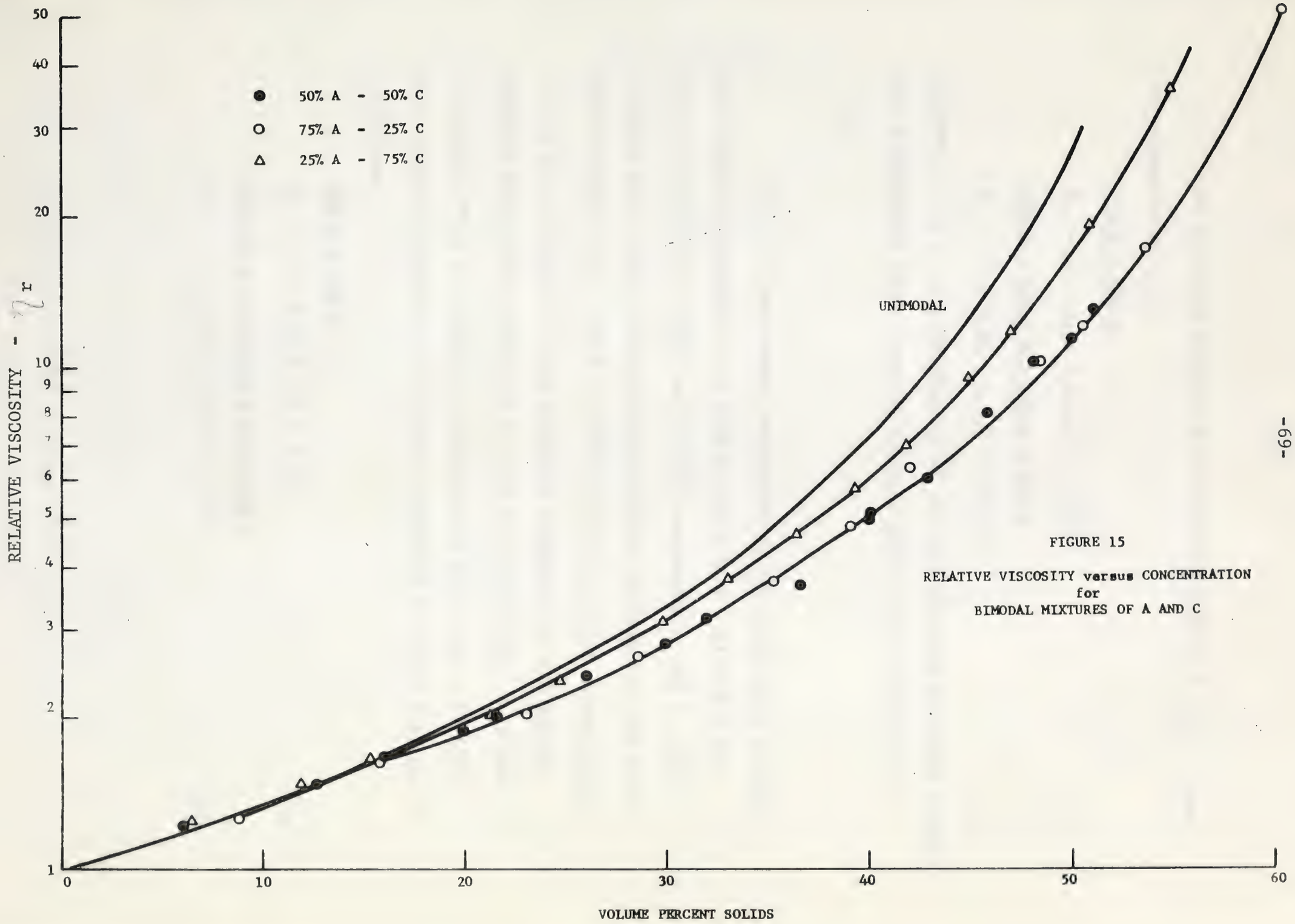

FIGURE 15

RELATIVE VISCOSITY versus CONCENTRATION
for
BIMODAL MIXTURES OF A AND C

The equations obtained by fitting the data to a power series in concentration are:

25% A - 75% C

$$\phi_r = 1 - 2.5c + 0.10c^2 + 2.26c^3 \quad (29)$$

50% A - 50% C and 75% A - 25% C

$$\phi_r = 1 - 2.5c + 0.9c^2 + 0.915c^3 \quad (30)$$

Figures 16 and 17 show the results of the test of these equations against the experimental data. Most of the data points are within $\pm$ 5% of unity.

Data for the bimodal suspension of 50% B and 50% C and for the trimodal suspension of 33 1/3% A - 33 1/3% B - 33 1/3% C are given in Figure 18. Since the data for suspension of 50% B - 50% C differed only slightly from that for unimodal suspensions, the other combinations, 25% B - 75% C and 75% B - 25% C were not investigated. It may be said that the three component suspension is not really trimodal since the diameters of B and C are very close. Thus this suspension would be expected to behave as 33 1/3% large - 66 2/3% small particle suspension. The fitted equations for these data are as follows:

50% B - 50% C

$$\phi_r = 1 - 2.5c + 0c^2 + 2.4c^3 \quad (31)$$

33 1/3% A - 33 1/3% B - 33 1/3% C

$$\phi_r = 1 - 2.5c + 0.5c^2 + 1.6c^3 \quad (32)$$

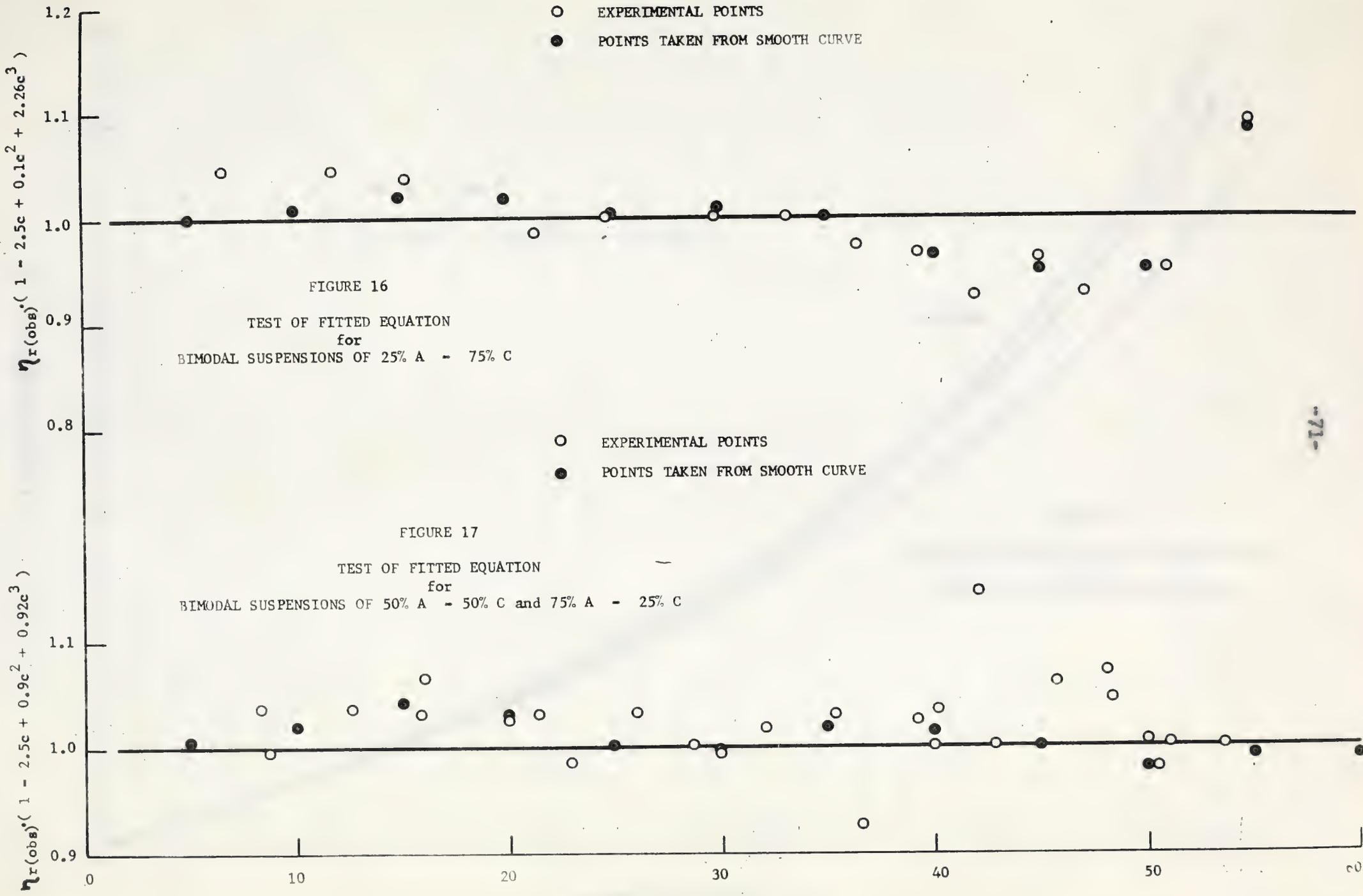

FIGURE 16

TEST OF FITTED EQUATION
for
BIMODAL SUSPENSIONS OF 25% A - 75% C

FIGURE 17

TEST OF FITTED EQUATION
for
BIMODAL SUSPENSIONS OF 50% A - 50% C and 75% A - 25% C

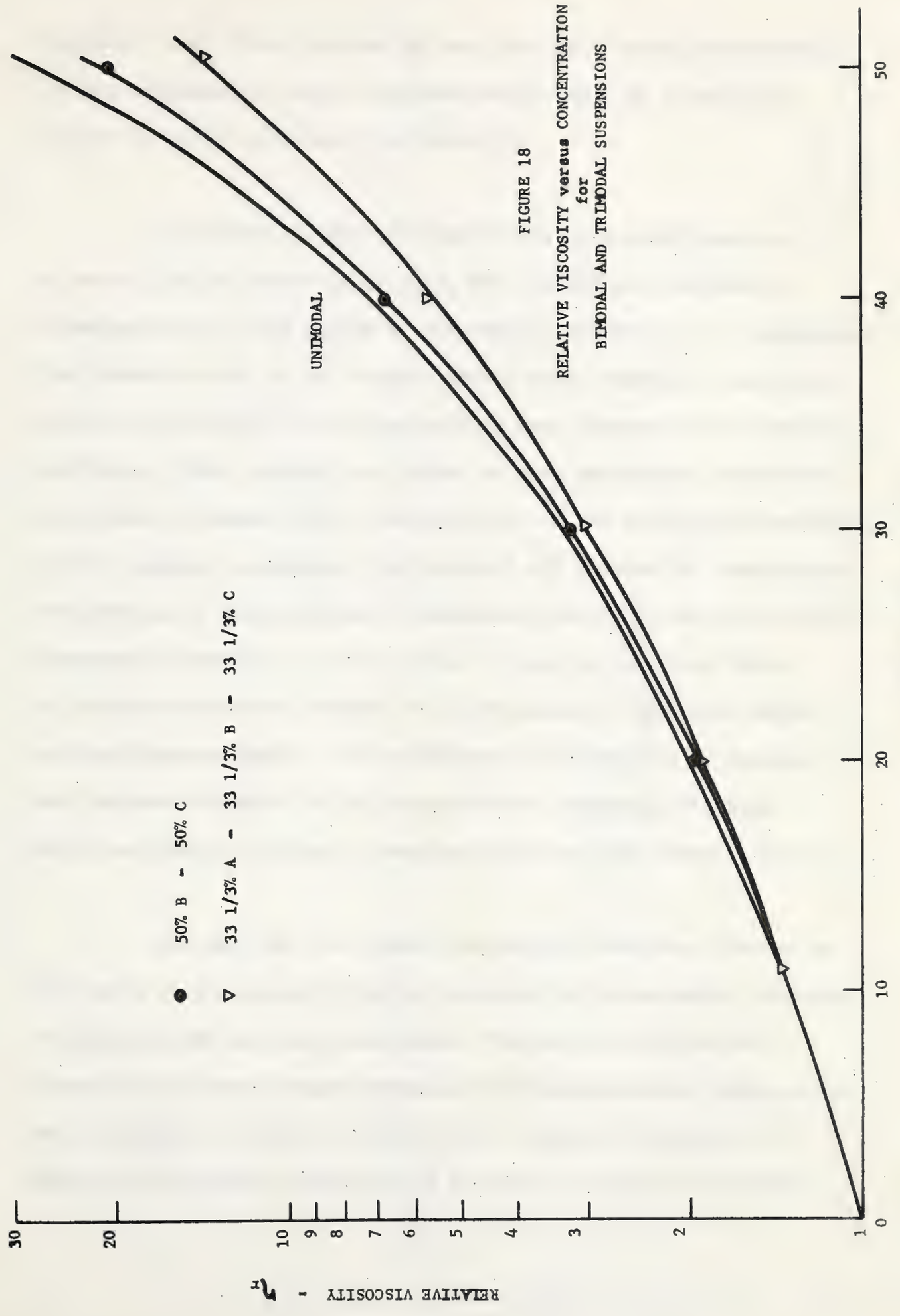

FIGURE 18

RELATIVE VISCOSITY versus CONCENTRATION
for
BIMODAL AND TRIMODAL SUSPENSIONS

Figures 19 and 20 are plotted to test the fit of these expressions to the experimental data. The data points are $\pm$ 3% of unity in Figure 19 and $\pm$ 5% of unity in Figure 20.

In Figures 21 and 22 respectively, the coefficients of c^2 and c^3 in the power series in ϕ_r are plotted as a function of diameter ratio of the larger to the smaller spheres in the suspension. The diameter ratio is the volume-surface mean diameter of the larger particles divided by the volume-surface mean diameter of the smaller particles. This diameter was chosen to make the results consistent with those of Sweeny (46). The point for the 33 1/3% larger particles is the trimodal suspension, the value of d/D obtained by considering the average of the diameters of Materials B and C as one size and the diameter of Material A as the other. It can be seen that there is a fair correlation between the coefficients of the power series and the diameter ratio. The coefficient of c^2 appears to increase and the coefficient of c^3 to decrease with increasing diameter ratio and seem to approach a constant value at high diameter ratios.

The data for the bimodal suspensions have been plotted as the ratio of the bimodal relative viscosity to the unimodal relative viscosity under the same conditions. The ratio is plotted as a function of percent larger particles with volume percent total solids as a parameter in Figures 23,24 and 25. Figure 23 contains the results for bimodal suspensions of B and C, for which the diameter

FIGURE 19

TEST OF FITTED EQUATION
for
BIMODAL SUSPENSIONS OF 50% B - 50% C

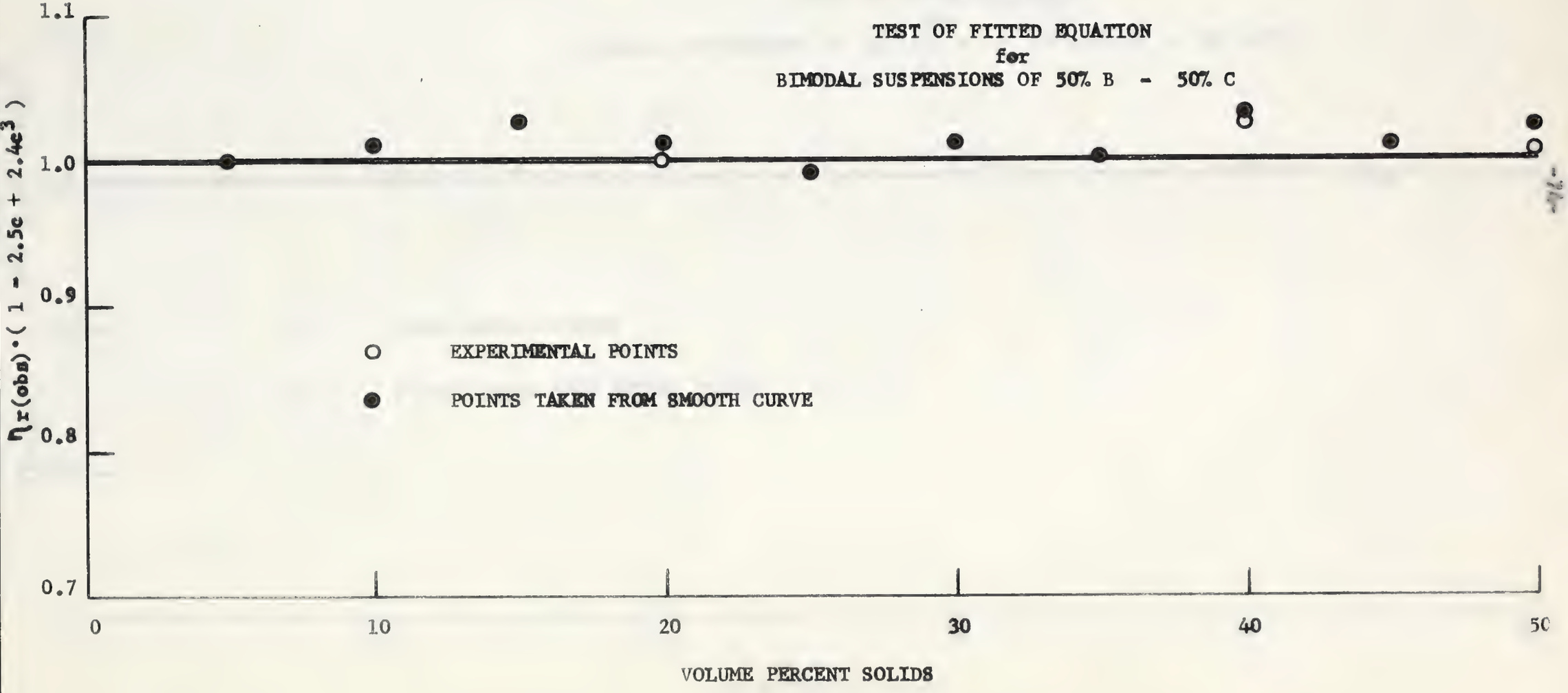

FIGURE 20

TEST OF FITTED EQUATION
for
TRIMODAL SUSPENSIONS OF 33 1/3% A - 33 1/3% B - 33 1/3% C

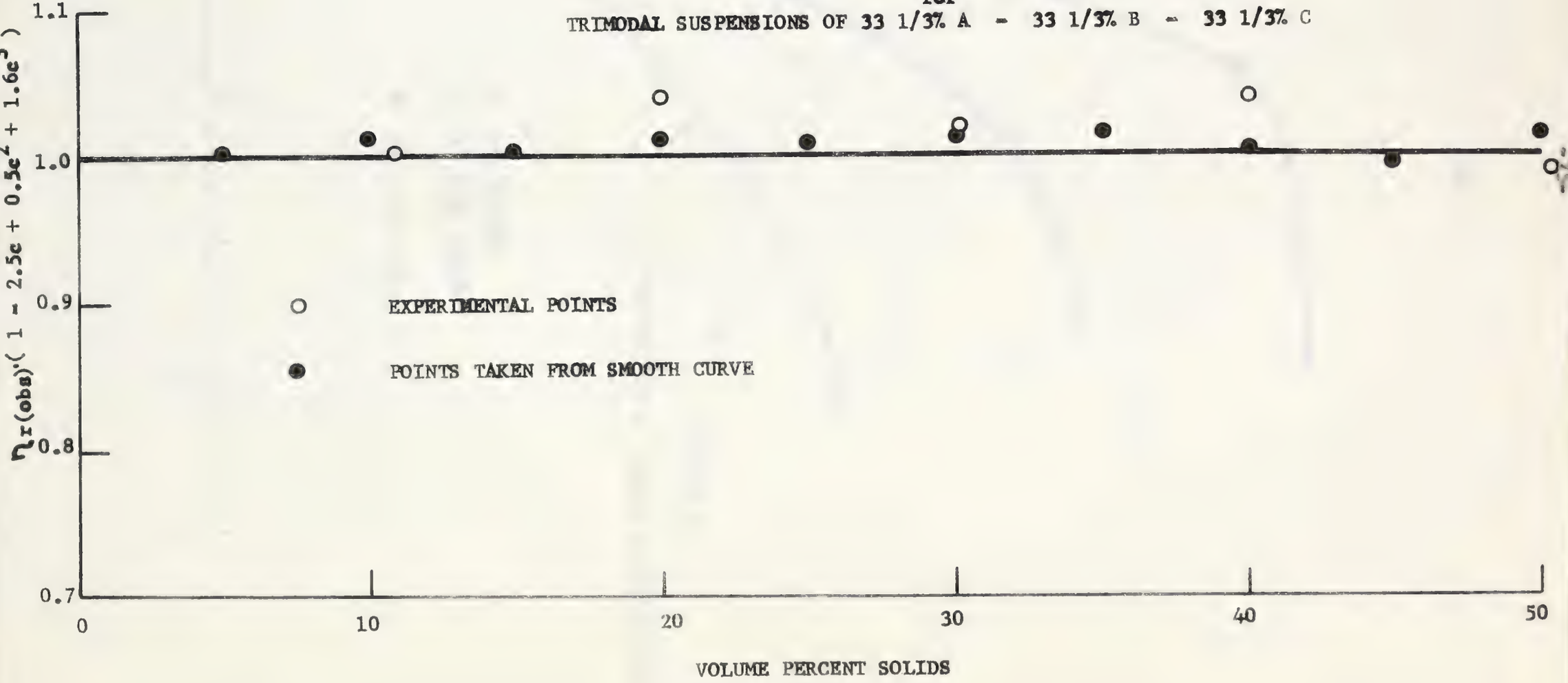

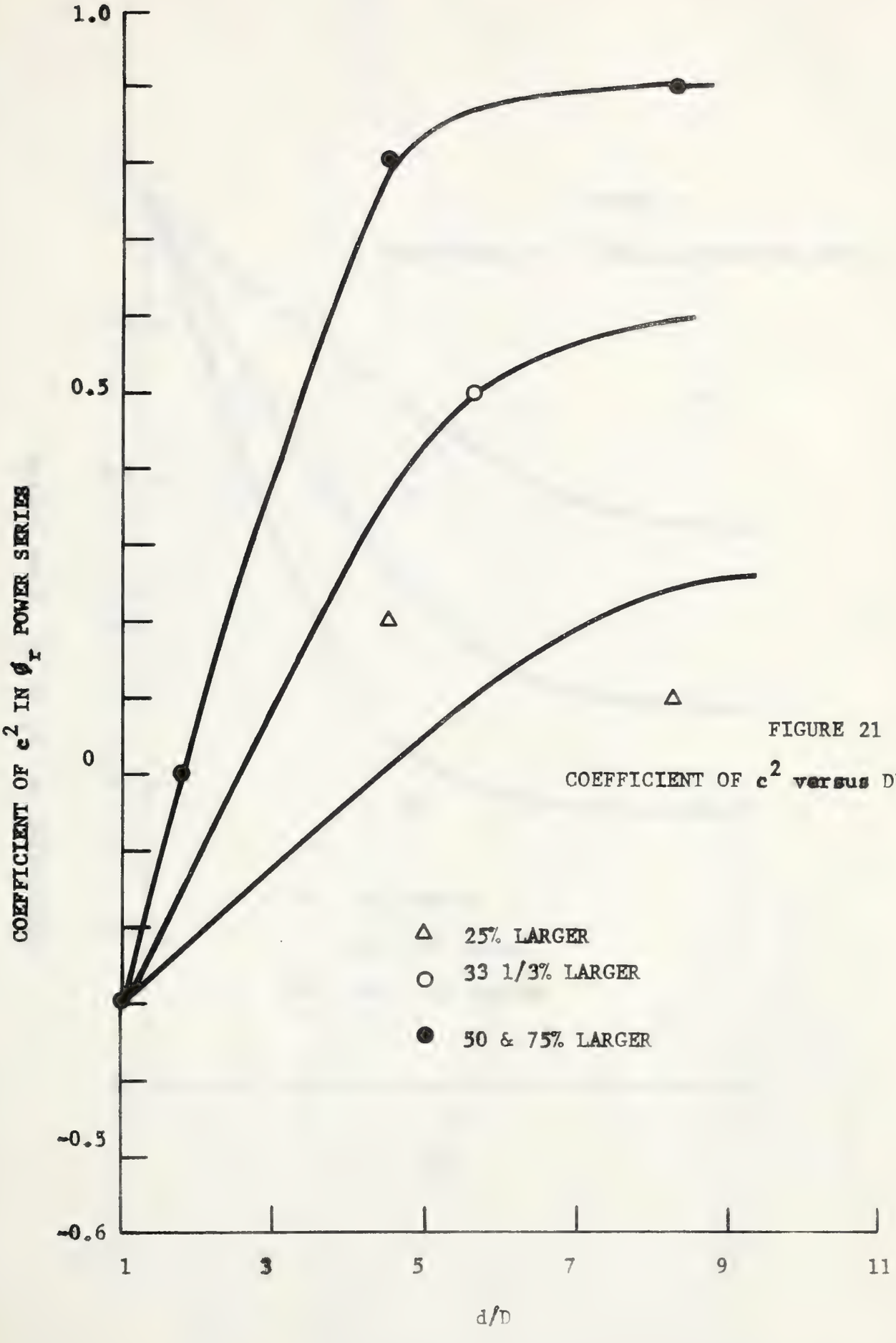

FIGURE 21

COEFFICIENT OF c^2 versus DIAMETER RATIO

FIGURE 22

COEFFICIENT OF e^3 versus DIAMETER RATIO

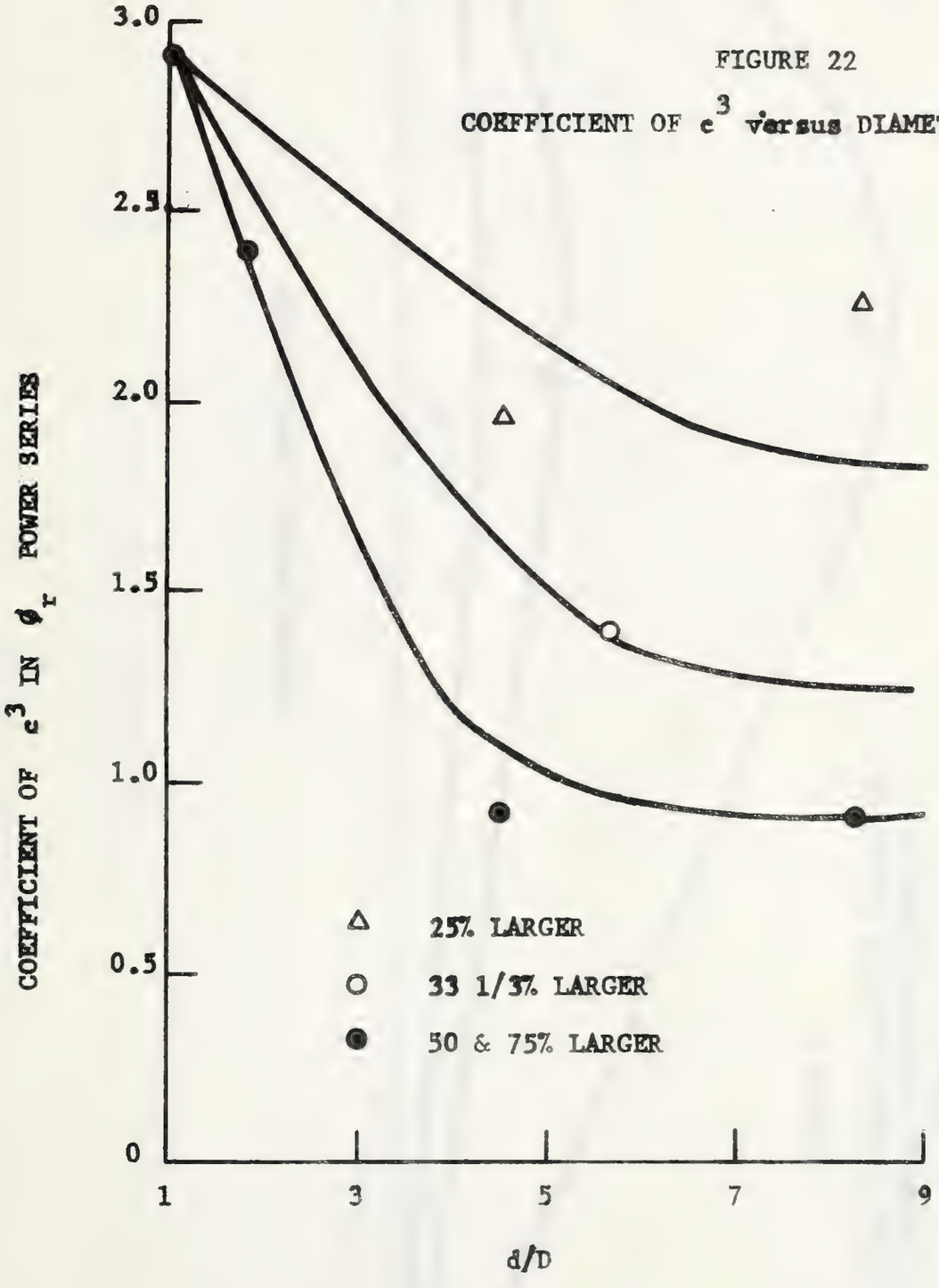

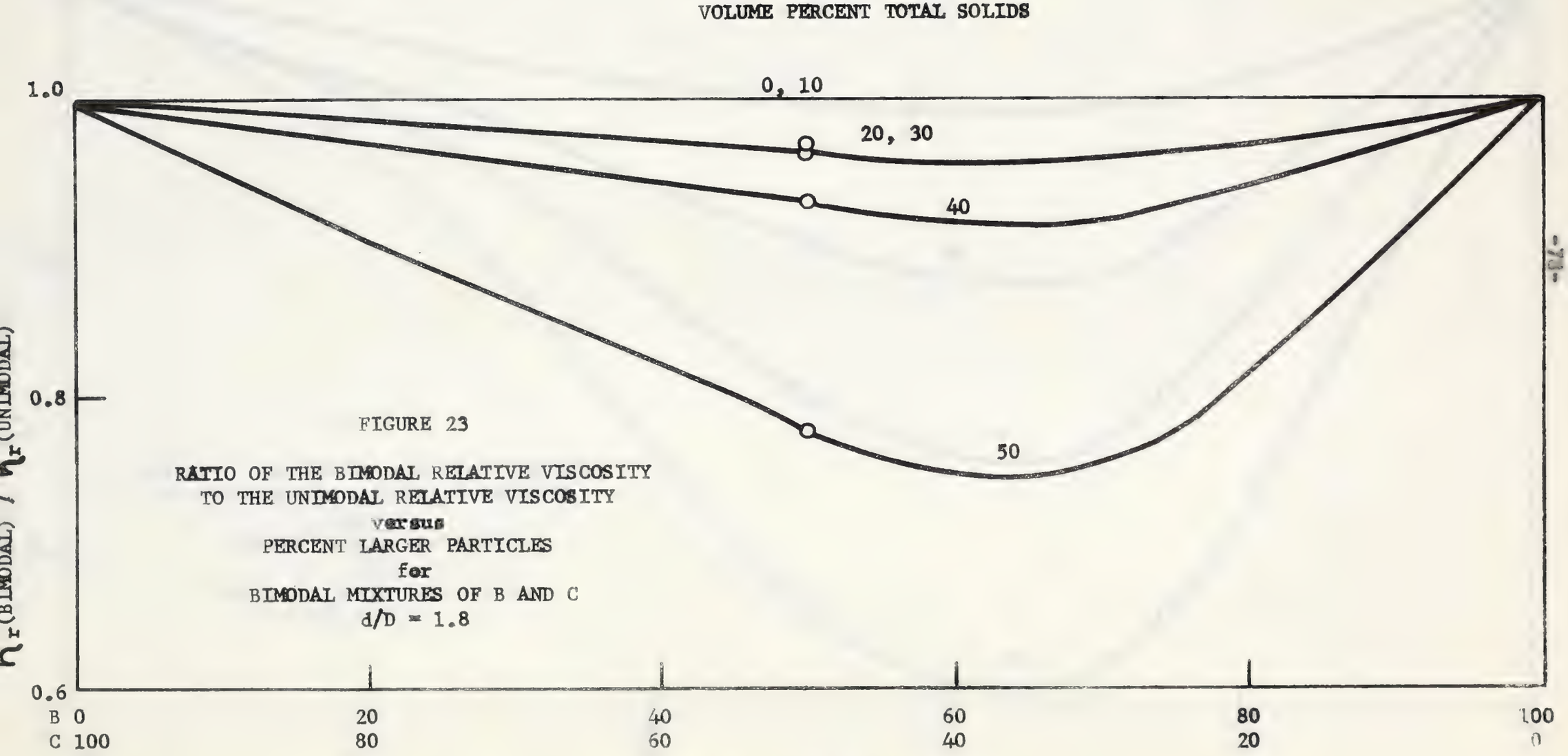

FIGURE 23

RATIO OF THE BIMODAL RELATIVE VISCOSITY
TO THE UNIMODAL RELATIVE VISCOSITY
versus
PERCENT LARGER PARTICLES
for
BIMODAL MIXTURES OF B AND C
d/D = 1.8

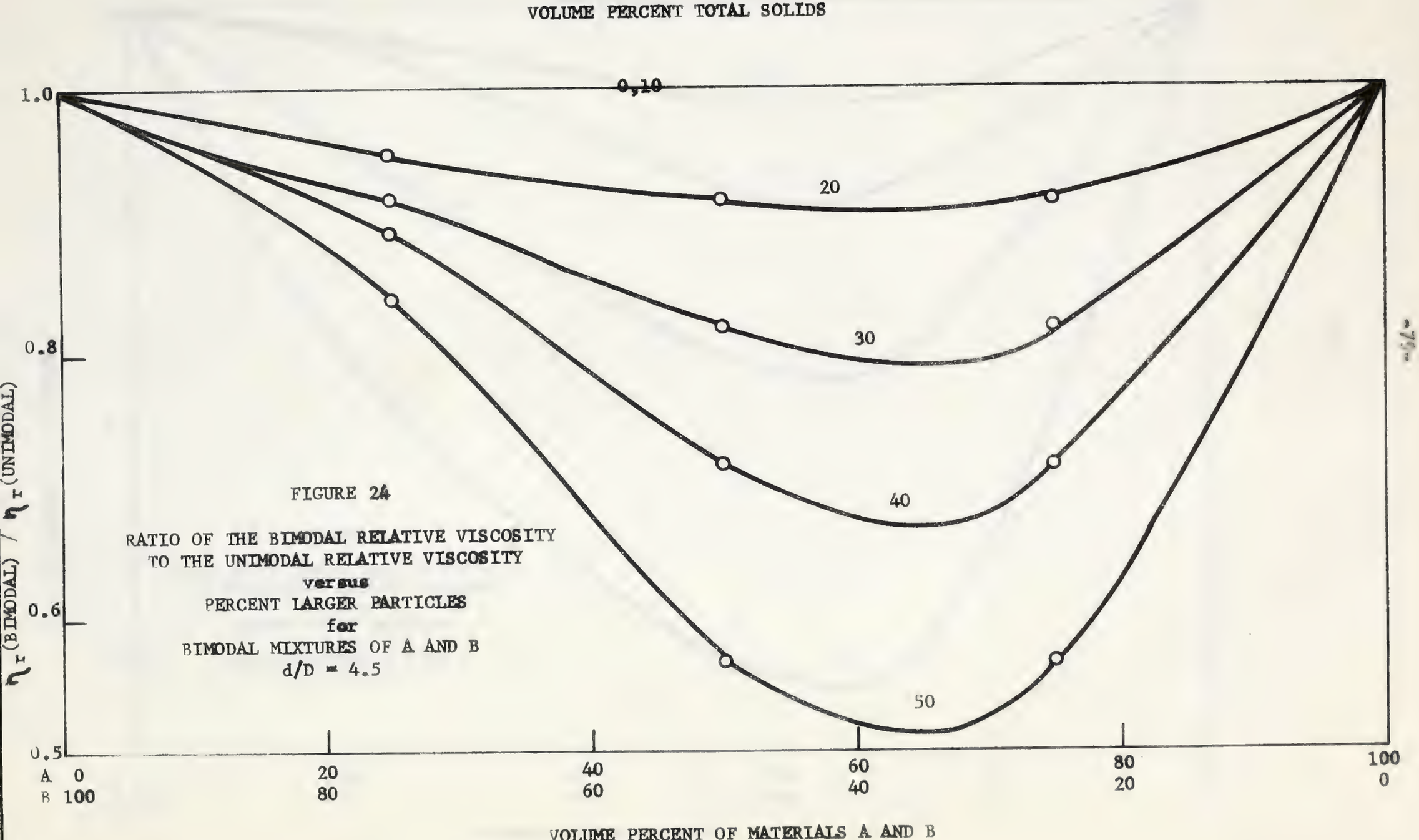

FIGURE 24

RATIO OF THE BIMODAL RELATIVE VISCOSITY
TO THE UNIMODAL RELATIVE VISCOSITY
versus
PERCENT LARGER PARTICLES
for
BIMODAL MIXTURES OF A AND B
d/D = 4.5

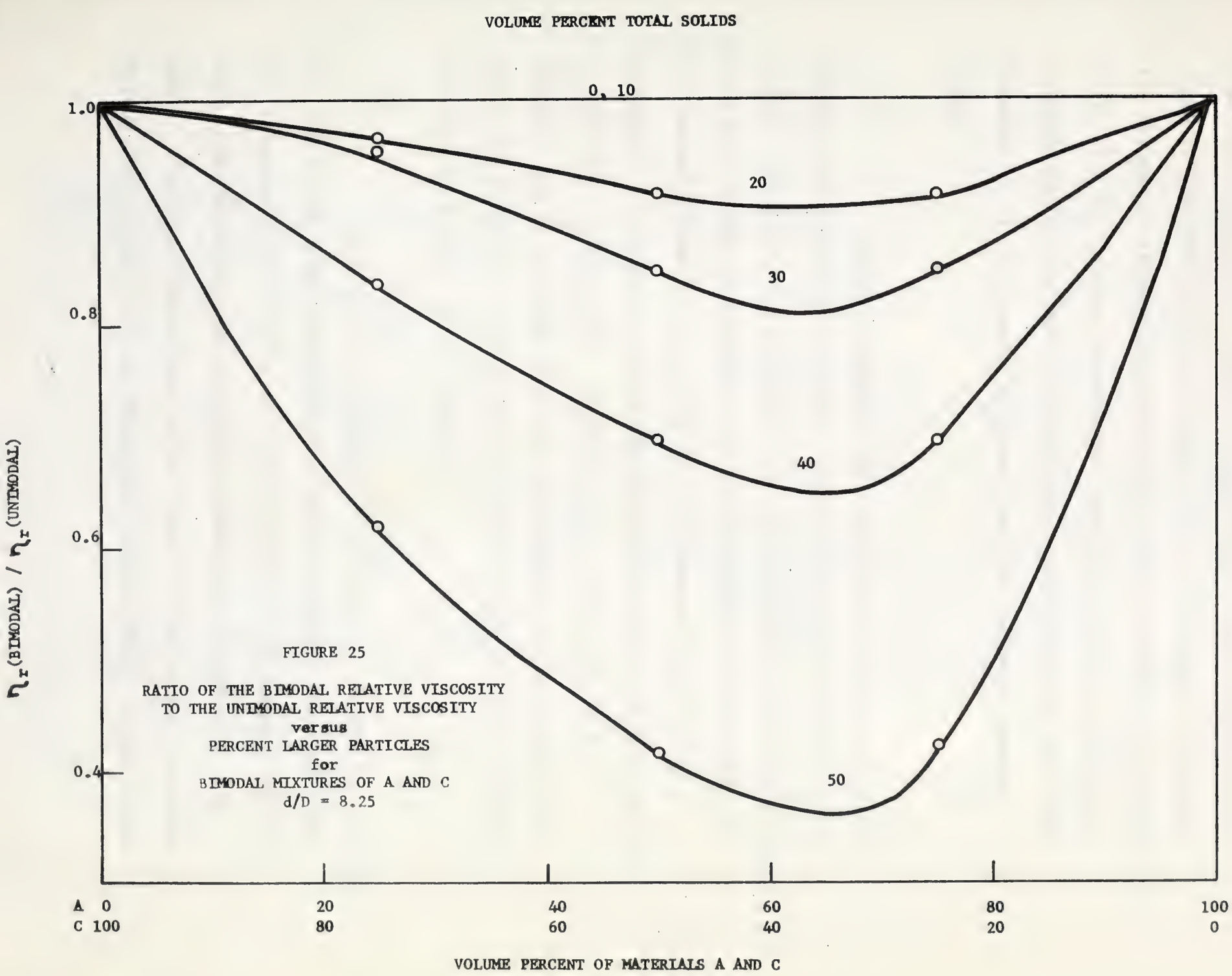

FIGURE 25

RATIO OF THE BIMODAL RELATIVE VISCOSITY
TO THE UNIMODAL RELATIVE VISCOSITY
versus
PERCENT LARGER PARTICLES
for
BIMODAL MIXTURES OF A AND C
d/D = 8.25

ratio, the ratio of the average diameter of B to that of C, is 1.8. Similarly, Figure 24 presents the results of bimodal suspensions of A and B, for which the diameter ratio is 4.5 and Figure 25 presents the results of bimodal suspensions of A and C, for which the diameter ratio is 8.25. It can be seen that there is a pronounced effect of diameter ratio, the ratio of the relative viscosities for the large diameter ratio being much lower than that for the small diameter ratio.

Figure 26 compares the present work with the results of Sweeny (46) at 40 volume percent, the only value at which Sweeny has results which are also available from the experimental data. The figure is a plot of the ratio of the relative viscosities as a function of the volume percent larger particles with diameter ratio d/D as a parameter. In general, the agreement between Sweeny's results and the present work is very good. Sweeny's results for a d/D of 7.3, however, lie in the same region as experimental data from this work for a d/D of 8.25. In this work all references to Sweeny's data are to viscosities at zero rate of shear.

Cross plots of Figures 23, 24 and 25 were made at 25%, 50% and 75% of the larger particles in a bimodal mixture. The ratio of the relative viscosities is plotted as a function of diameter ratio with total volume percent solids as a parameter in Figures 27, 28 and 29. On these figures are plotted data of other workers including Eveson (15), Sweeny (46) and Sweeny and Geckler (45). It can be seen

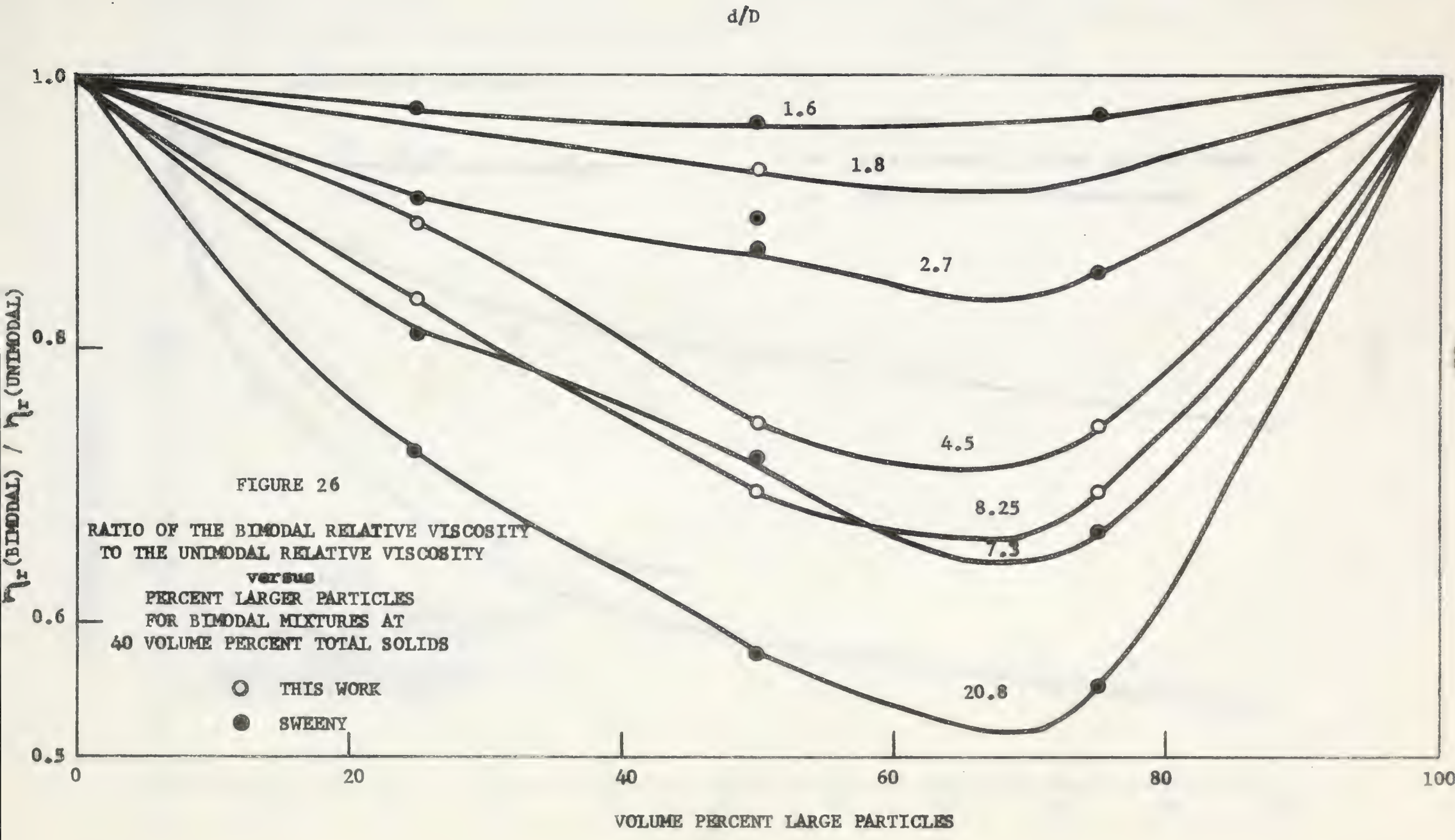
d/D
1.0
0.8
0.6
0.5
η_r (BIMODAL) / η_r (UNIMODAL)
1.6
1.8
2.7
4.5
8.25
7.3
20.8
0
20
40
60
80
100
VOLUME PERCENT LARGE PARTICLES
FIGURE 26
RATIO OF THE BIMODAL RELATIVE VISCOSITY
TO THE UNIMODAL RELATIVE VISCOSITY
versus
PERCENT LARGER PARTICLES
FOR BIMODAL MIXTURES AT
40 VOLUME PERCENT TOTAL SOLIDS
THIS WORK
SWEENY

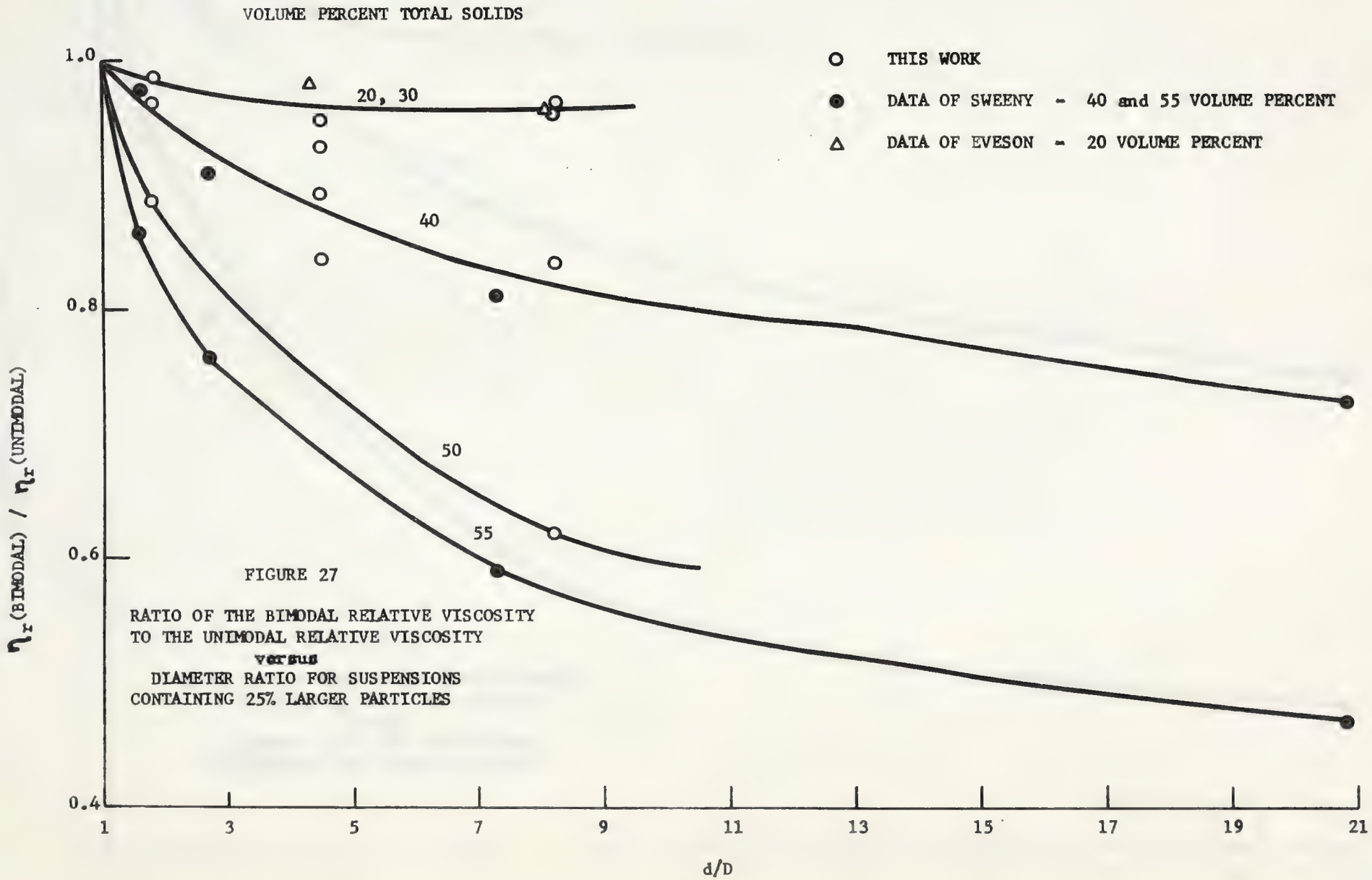

FIGURE 27

RATIO OF THE BIMODAL RELATIVE VISCOSITY
TO THE UNIMODAL RELATIVE VISCOSITY
versus
DIAMETER RATIO FOR SUSPENSIONS
CONTAINING 25% LARGER PARTICLES

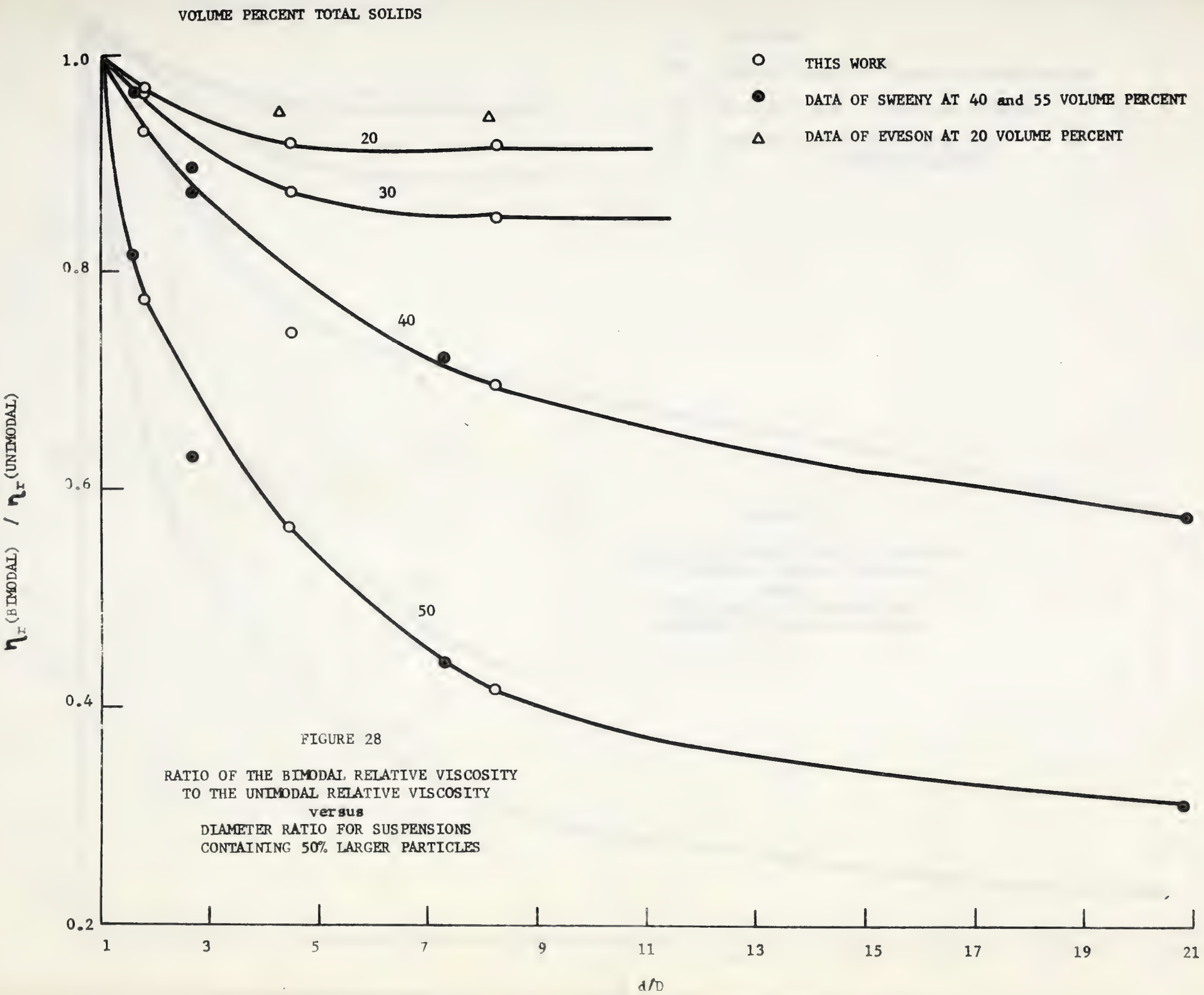

FIGURE 28

RATIO OF THE BIMODAL RELATIVE VISCOSITY
TO THE UNIMODAL RELATIVE VISCOSITY
versus
DIAMETER RATIO FOR SUSPENSIONS
CONTAINING 50% LARGER PARTICLES

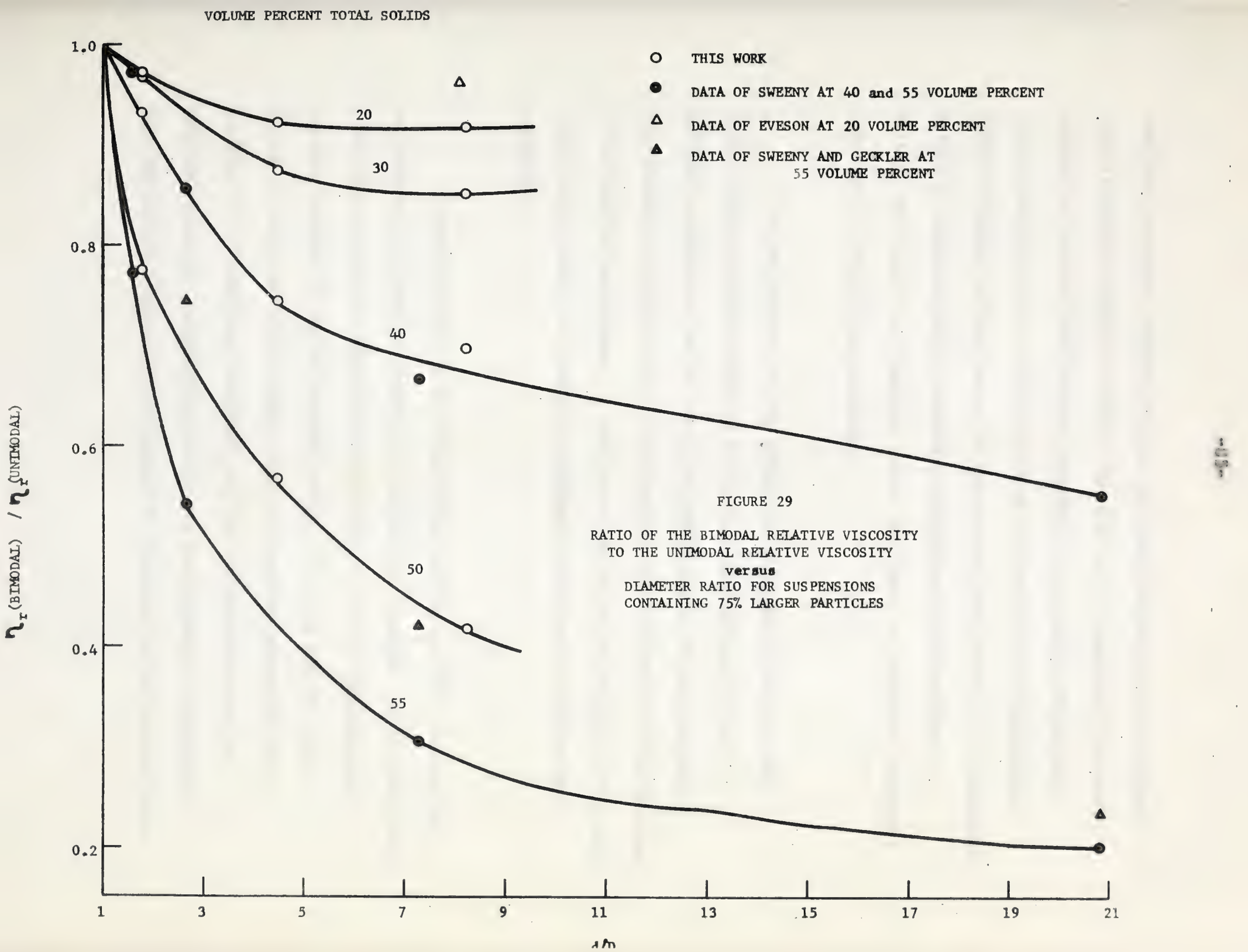

FIGURE 29

RATIO OF THE BIMODAL RELATIVE VISCOSITY
TO THE UNIMODAL RELATIVE VISCOSITY
versus
DIAMETER RATIO FOR SUSPENSIONS
CONTAINING 75% LARGER PARTICLES

that the agreement between the data of other workers and the present work is generally good, although the results of Sweeny at 55 volume percent solids and with bimodal suspensions containing 50% of the larger particles lie on the same curve as data for 50 volume percent solids obtained in this work. It can be seen that there is a pronounced effect of diameter ratio, especially at higher concentrations of solids, the higher the diameter ratio, the lower the relative viscosity compared to unimodal suspensions.

An explanation of the effect of diameter ratio upon the ratio of the relative viscosity of bimodal suspensions to the unimodal suspensions may be found in consideration of the packing of the spheres in a suspension. The viscosity of a suspension is a function of the spatial arrangement of the particles in the suspension. Thus anything that affects the spatial arrangement would tend to affect the viscosity.

Numerous workers including White and Walton (56), Hudson (25), and Furnas (20) have considered the packing of spheres. It is found that a bed of m spheres of equal diameter d in the closest (rhombohedral) packing contains 74 volume percent solids. In this bed are interstices of two kinds - the "square hole" (a reversed spherical cube bounded by six spherical surfaces) and the "triangular hole" (a reversed spherical tetrahedron bounded by four spherical surfaces). Into the square interstices, m spheres of diameter 0.414d can be fitted

raising the solid content to about 79 volume percent. Into the triangular interstices 2m spheres of diameter 0.225d can be placed at which time the solid content is 81 volume percent. This process can be continued indefinitely but it can be seen to obtain an arrangement of spheres having a high solids content, it is necessary to add spheres of different sizes in definite quantities.

The reduction in the viscosity of suspensions upon the addition of fine particles to large particles is then a result of the packing of the small particles into the interstices between the large particles, which although it increases the volume concentration, does not reduce the volume of "free" liquid which determines the flow behavior of the suspension. Thus a bimodal suspension in which the smaller spheres pack into the interstices between the larger spheres would be expected to have a lower viscosity at the same solid content or conversely, would have the same viscosity at a higher total solids content. For this reason, it is to be expected that unimodal suspensions would tend to have a fairly constant viscosity - concentration relationship. Unless it had an extremely wide size distribution, a unimodal suspension would have only a few small particles to fit into the interstices between the larger particles. There would be some effect, most noticeable at high concentrations, but suspensions consisting of spheres possessing a bimodal or trimodal discontinuous size-distribution curve would be more likely to show a large reduction in viscosity compared to a unimodal suspension.

These results may have practical significance in the transport of solids in conduits if similar results are found for suspensions of materials commonly transported in slurry form. It can be seen from Figure 24 that for a bimodal suspension with a diameter ratio of 8.25, the viscosity at 40 volume percent is only 65% of the unimodal viscosity and at 50 volume percent it is only 36% of the unimodal viscosity for the optimum percent of large and small materials. If similar results are obtained for practical suspensions, it might be possible to prepare the solid phase by segregation of the feed to a slurry pipeline to obtain the lowest possible consistency. This will reduce the power requirement since the pressure drop is directly proportional to the viscosity in the laminar flow region in which a slurry transport line might operate. The beneficial effect of reduced viscosity would not be as important in the turbulent region because of the reduced dependence of the pressure drop upon the viscosity.

Evidence that this method is being used in industry is given in the paper by Dekker and Zimmerman (5), who reveal that in the production of solid rocket fuel, mixtures of various sizes of oxidizers are used to lower the consistency of the fuel before casting. It is found that the maximum amount of oxidizer is desirable for best performance. However, the final mixture must be castable into the varied shapes required for rocket motors. It is probable that the work of Sweeny and Geckler (45) and Sweeny (46) was done to investigate the possiblility of increasing the amount of solid in the slurry while still retaining a low

enough consistency so that casting into molds was possible. Dekker and Zimmerman show that a mixture of fine and coarse oxidizer in propellant in the ratio of 70% coarse and 30% fine particles produces a minimum apparent viscosity at the shear rate at which the suspensions were tested.

V. CONCLUSIONS AND RECOMMENDATIONS

From this study on the rheology of suspensions of spherical particles, it can be stated that:

i) Over the range of concentration (0 to 50 volume percent) and shear rate (0 to 1019 sec^{-1}) studied the suspensions behaved as Newtonian fluids.

ii) Over the size range studied (47 to 390 microns diameter) there is no effect of particle size upon the viscosity of the suspension, provided the particles in the suspension are of approximately the same size.

iii) The viscosity of a suspension of spheres is strongly dependent upon the size distribution of the particles. For bimodal mixtures, the minimum viscosity occurs when 70% by volume of the total solid phase is composed of large particles.

iv) Increasing the diameter ratio (the disparity between the diameters of the two sizes of spheres in the bimodal mixture) decreases the viscosity at concentrations above 15 volume percent. The decrease in viscosity is more pronounced the higher the volume concentration of solids.

v) The effect of the size distribution upon the viscosity of the suspension can be explained in terms of the packing of the

smaller spheres into the interstices between the larger spheres. An even greater reduction in viscosity is possible with a selected trimodal size distribution of spheres.

vi) The coefficients in a power series in concentration of relative fluidity give a fair correlation with diameter ratio at any given percentage of large particles in the suspension.

vii) The results of this work agree well with those of Sweeny (46) who studied the effect of bimodal size distribution at volume concentrations of 40 and 55 volume percent solids.

As an outcome of this work, the following recommendations can be made:

i) A rotational viscometer suitable for the study of the rheology of various suspensions should be constructed. A design similar to that of the viscometer used by Dudgeon and Michie (9) in their work on the rheology of uranium oxide suspensions would probably be satisfactory for most suspensions of interest.

ii) With such a viscometer, a study could be made of the effect of size distribution upon the rheology of more practical suspensions than spheres. The effect of particle shape and density difference between the solid and the suspending solution upon the rheological behavior could also be studied.

iii) Investigation of the effect of interparticle forces upon the rheological properties of suspensions should be made. Since it is known that non-Newtonian behavior in suspensions is the result of such forces, the measurement of the zeta potential by such a technique as the streaming potential and the correlation of this factor as a function of the flow behavior of the suspension might yield an insight into the mechanism of flow in particle suspensions.

NOMENCLATURE

a	Coefficient in power series
A	Designation of 40/60 mesh spheres
b	Coefficient in power series
B	Designation of 100/200 mesh spheres
c	Concentration, volume fraction solids
C	Designation of 200/400 mesh spheres
d	Diameter of large spheres in suspension
du/dr	Shear rate (polar coordinates)
$(du/dr)_{R_i}$	Shear rate at inner cylinder (bob)
du/dx	Shear rate (cartesian coordinates)
D	Diameter of small spheres in suspension
D_{avg}	Arithmetic average diameter
D_i	Diameter of the ith sphere
D_s	Mean surface diameter
D_v	Mean volume diameter
D_{vs}	Mean volume-surface diameter
e	Coefficient in power series
h	Height of cylinder immersed in sample
k	Self-crowding factor in Equation (21)
k_1 and k_2	Instrument constants in Equation (10) for calculation of shear rates from speed and dimensions of a viscometer
K	Fluid consistency index, defined by Equation (3)
K_1	Shearing stress constant, $\tau = K_1\theta$

K_2	Rate of shear constant for Newtonian fluid, $du/dr = K_2N$
K_s	Spring constant of viscometer torsion spring
m	Constant
M	Torque exerted on the inner cylinder of a concentric cylinder viscometer
n	Flow behavior index, defined by Equation (3)
n"	Slope of a logarithmic plot of M versus N
N	Rotational speed
r	Radial distance
R_i	Radius of inner cylinder of a concentric cylinder viscometer
R_o	Radius of outer cylinder of a concentric cylinder viscometer
s	Radius ratio, R_o/R_i
t	Gap between cylinders of a concentric cylinder viscometer
U	Linear velocity of outer cylinder of a concentric cylinder viscometer
x_i	Mass fraction of material of diameter D_i
η	Viscosity of Newtonian fluid
η_o	Viscosity at zero rate of shear
η_r	Relative viscosity = η_s/η
η_s	Viscosity of suspension
η_∞	Viscosity at infinite rate of shear

θ	Dial deflection of bob of a concentric cylinder viscometer
λ_{ji}	Crowding factor in Equation (20)
μ_R	Coefficient of rigidity of a Bingham plastic fluid
ν	Kinematic viscosity
π	3.1415 . . .
τ	Shearing stress
τ_i	Shearing stress at bob
τ_o	Shearing stress at cup
$f(\tau)$	Shear rate = du/dr
$\tau(r)$	Shearing stress at radius r
τ_{Ri}	Shearing stress at bob
τ_y	Yield value of a Bingham plastic fluid
ϕ_r	Relative fluidity = $1/\eta_r$
ω	Angular velocity at radius r
Ω	Angular velocity of outer cylinder of concentric cylinder viscometer

REFERENCES

1. Alcorn, A., M.Sc. Thesis, University of Alberta, 1961.
2. Chandrasekhar, S., "Hydrodynamic and Hydromagnetic Stability", Chapter VII, pp. 272 - 341, Oxford Univ. Press, 1961.
3. Chandrasekhar, S., Mathematika, 1, 5 - 13, 1954.
4. Couette, M., Ann. chim. (phys.), 21, 433 - 510, 1890.
5. Dekker, A.O. and G.A. Zimmerman, I&EC Product Research and Development, 1, 23 - 27, 1962.
6. Di Prima, R.C., Quart. Appl. Math., 13, 55 - 62, 1955.
7. Donnelly, R.J., Proc. Roy. Soc. (London), A246, 312 - 25, 1958.
8. Donnelly, R.J. and D. Fultz, Ibid., A258, 101 - 23, 1960.
9. Dudgeon, E.H. and W.C. Michie, National Research Council of Canada Report No. MT-34, January 16, 1957.
10. Einstein, A., Ann. Physik, 19, 289 - 306, 1906.
11. Eirich, F., M. Bunzl and H. Margaretha, Kolloid - Z., 74, 276 - 85, 1936.
12. Eirich, F. and O. Goldschmid, Kolloid - Z., 81, 7 - 18, 1937.
13. Eveson, G.F., Ph.D. Thesis, University of Birmingham, 1950.
14. Eveson, G.F., R.L. Whitmore and S.G. Ward, Nature (London), 166, 1074, 1950.
15. Eveson, G.F. in "Rheology of Disperse Systems", 61 - 83, ed. by C.C. Mill, Pergamon Press, London, 1959.
16. Eveson, G.F., J. Oil & Colour Chem. Assoc., 41, 150 - 55, 1958.
17. Freundlich, H. and H.L. Röder, Trans. Farad. Soc., 34, 308 - 16, 1938.
18. Freundlich, H. and F. Juliusberger, Trans. Farad. Soc., 31, 920 - 1, 1935.

19. Frisch, H.L. and R. Simha in "Rheology", Volume 1, ed. by F. Eirich, Chapter 14, 525 - 613, Academic Press, New York, 1956.

20. Furnas, C.C., U.S. Bur. Mines, Rept. Investigations No. 2894, 1928.

21. Guth, E. and R. Simha, Kolloid - Z., 74, 266 - 75, 1936.

22. Guth E. and O. Gold, Phys. Rev., 53, 322, 1938.

23. Hatschek, E., "The Viscosity of Liquids", p. 52, G. Bell and Sons, Ltd., London, 1928.

24. Higginbotham, G.H., D.R. Oliver and S.G. Ward, Brit. J. Appl. Phys., 9, 372 - 7, 1958.

25. Hudson, D.R., J. Appl. Phys., 20, 154 - 62, 1949.

26. Johnson, P.H. and R.H. Kelsey, Rubber World, 138, 877 - 82, 1958.

27. Kelsey, R.H. and P.H. Johnson, Rubber World, 139, 227 - 31, 1958.

28. Krieger, I.M. and H. Elrod, J. Appl. Phys., 24, 134 - 6, 1953.

29. Lewis, J.W., Proc. Roy. Soc. (London), A117, 388 - 407, 1928.

30. Lindley, W.G.G., M.Sc. Thesis, University of Alberta, 1958.

31. Manley, R.St.J. and S.G. Mason, J. Colloid Sci., 7, 354 - 69, 1952.

32. Manley, R.St.J. and S.G. Mason, Can. J. Chem., 32, 763 - 7, 1954.

33. Maron, S.H. and B.P. Madow, J. Colloid Sci., 8, 300 - 8, 1953.

34. Meksyn, D., Proc. Roy. Soc. (London), A187, 115 - 28, 1946.

35. Mooney, M., J. Colloid Sci., 6, 162 - 70, 1951.

36. Newton, I., "Principia", F. Cajori, ed., "Sir Isaac Newton's Mathematical Principles of Natural Philosophy and His System of the World", 385 - 7, Cambridge University Press, 1934.

37. Ostwald, W., Kolloid - Z., 36, 99 - 117, 1925.

38. Pawlowski, J., Kolloid - Z., 130, 129 - 31, 1953.

39. Reiner, M., "Deformation, Strain and Flow", 2nd ed., 243 - 55, Interscience Publishers, Inc., New York, 1960.

40. Reynolds, O., Phil. Mag., 20, 469 - 81, 1885.

41. Roscoe, R. in "Flow Properties of Disperse Systems", ed. by J.J. Hermans, Chapter I, 1 - 37, North - Holland, Amsterdam, 1953.

42. Savins, J.G. and W.F. Roper, API, Drilling and Production Practice, 7 - 22, 1954.

43. Schlichting, H., "Boundary Layer Theory", 4th ed., p. 420, McGraw - Hill, 1960.

44. Shangraw, R., W. Grim and A.M. Mattocks, Trans. Soc. Rheol., 5, 247 - 60, 1961.

45. Sweeny, K.H. and R.D. Geckler, J. Appl. Phys., 25, 1135 - 44, 1954.

46. Sweeny, K.H., Paper presented at West Coast Region Meeting, Society of Rheology, February 1 - 2, 1962, at California Institute of Technology, Pasadena, California.

47. Terada, R. and K. Hattori, Rep. Aero. Res. Inst. Tokyo, 2, 287 - 326, 1926.

48. Taylor, G.I., Phil. Trans. Roy. Soc. (London), A223, 289 - 343, 1923.

49. Taylor, G.I., Proc. Roy. Soc. (London), A 157, 546 - 64, 1936.

50. Vand, V., J. Phys. & Colloid Chem., 52, 277 - 99, 1948.

51. Vand, V., Ibid., 300 - 14, 1948.

52. Ward, S.G. and R.L. Whitmore, Brit. J. Appl. Phys., 1, 286 - 90, 1950.

53. Ward, S.G., J. Oil & Colour Chem. Assoc., 38, 9 - 31, 1955.

54. Weltmann, R.N., J. Appl. Phys., 18, 933 - 40, 1947.

55. Wendt, F., Ingen. Arch., 4, 577 - 95, 1933.

56. White, H.E. and S.F. Walton, J. Am. Ceram. Soc., 20, 155 - 66, 1937.

57. Yannas, J.B. and R.N. Gonzalez, Nature (London), 191, 1384 - 5, 1961.

APPENDIX A

CALIBRATION OF THE VISCOMETER

Three different cups and three different springs were used in this work.

Bob diameter = $2R_i$ = 1.357 inches

Cup diameter = $2R_o$

No. 1 = 1.449 inches

No. 2 = 1.507 inches

No. 3 = 1.650 inches

$s = R_o/R_i$

No. 1 = 1.068

No. 2 = 1.1105

No. 3 = 1.216

Spring Constant = K_s

No. 1 = 387 dyne-cm/degree

No. 2 = 193.5 dyne-cm/degree

No. 3 = 77.4 dyne-cm/degree

For a Newtonian fluid the rate of shear at the bob is:

$$(du/dr)_{R_i} = \frac{4\pi N}{1 - 1/s^2} = K_2 N$$

The values of K_2 are: No. 1 = 101.9

No. 2 = 66.5

No. 3 = 38.8

The shear stress at the bob is given by:

$$\tau_{R_i} = \frac{K_s\theta}{2\pi R_i^2 h} = K_1\theta$$

By lumping all the values except θ into K_1, the end effect is absorbed and the value of K_1 can be determined using standard oils.

Since for a Newtonian fluid,

$$\tau_{R_i} = \eta\,(du/dr)_{R_i}$$

Therefore,

$$K_1\theta = \eta K_2 N$$

$$K_1 = \eta K_2 N/\theta$$

Values of K_1 determined with four standard oils are given in the following table. There appears to be an effect of viscosity and gap between cup and bob upon the end effect. The calibration data obtained with the standard oils follow the calculated values of K_1.

CALIBRATION VALUES OF K_1

$$\tau = K_1 \theta$$

τ = shear stress, dynes/cm^2

θ = dial deflection, degrees

SPRING NUMBER	CUP NUMBER	OIL VISCOSITY 19.1 cp	56.7 cp	93.6 cp	147.9 cp	Average K_1
		K_1				
One	Cup No. 1	-	5.22	5.22	5.35	5.25
	Cup No. 2	-	-	5.18	5.22	5.20
	Cup No. 3	-	-	4.98	4.95	4.97
Two	Cup No. 1	2.62	2.62	2.66	2.68	2.64
	Cup No. 2	2.53	2.57	2.59	2.65	2.57
	Cup No. 3	2.48	2.45	2.48	2.48	2.47
Three	Cup No. 1	1.025	1.035	1.055	-	1.035
	Cup No. 2	0.99	1.005	1.02	-	1.00
	Cup No. 3	0.985	0.985	0.985	-	0.985

CALIBRATION OF SPRINGS

SPRING NUMBER	OIL cp.	N Speed	θ Deflection		
			Cup No. 1	Cup No. 2	Cup No. 3
One	56.7	10.0	111	-	-
		5.0	55.5	-	-
		3.33	37	-	-
		1.67	18.5	-	-
	93.6	10.0	183	120	73
		5.0	91.5	60	37
		3.33	61	40	24.5
		1.67	30.5	20	12
	147.9	10.0	282	188	116
		5.0	141	94	58
		3.33	94	63	39
		1.67	46.5	31.5	19.5
Two	19.1	10.0	74	50	30
		5.0	37	25	15
		3.33	24.5	16.5	10
		1.67	12	8	5
	56.7	10.0	221	146	90
		5.0	110.5	73	45
		3.33	74	49	30
		1.67	37	24	15
	93.6	10.0	-	240	148
		5.0	180	120	74
		3.33	120	80	49
		1.67	60	40	24.5
	147.9	10.0	-	-	232
		5.0	-	185	116
		3.33	187.5	124	78
		1.67	94	62	39

CALIBRATION OF SPRINGS (cont.)

SPRING NUMBER	OIL cp.	N Speed	θ Deflection Cup No. 1	Cup No. 2	Cup No. 3
Three	19.1	10.0	190	128	75.5
		5.0	95.5	64	38
		3.33	63	42.5	25
		1.67	31	20.5	12.5
	56.7	10.0	-	-	224
		5.0	279	187	112
		3.33	187.5	125.5	74.5
		1.67	93.5	63	37.5
	93.6	10.0	-	-	-
		5.0	-	-	185
		3.33	-	202.5	123
		1.67	151	101.5	61.5
		1.11	100	68	41
		0.55	50	34	20.5

APPENDIX B

CRITERIA FOR LAMINAR FLOW IN THE ANNULUS OF THE VISCOMETER

I. Correlation of G.I. Taylor

CUP NO.	R_o	t	t/R_o	$\log_{10} t/R_o$	$\log_{10}\left(\frac{Ut}{\nu}\right)_{crit}$	$\left(\frac{Ut}{\nu}\right)_{crit}$	N_{crit}
1	0.06038	0.0038	0.0635	$\bar{2}.8028$	3.50	3160	$23.4\nu'$
2	0.06278	0.0063	0.0995	$\bar{2}.9978$	3.86	7250	$31.7\nu'$
3	0.06875	0.0122	0.1776	$\bar{1}.2495$	4.25	17800	$26.3\nu'$

R_o = radius of outer cylinder, feet

t = annular gap, feet

ν' = kinematic viscosity, centistokes

ν = kinematic viscosity, $feet^2/second$

$U = 2\pi NR_o$ = linear velocity, feet/second

N = revolutions/second

II. Correlation of H. Schlichting

CUP NO.	t/R_o	$\left(\frac{UR_o}{\nu}\right)_{crit}$	N_{crit}
1	0.0635	5×10^4	$23.6\nu'$
2	0.0995	7×10^4	$30.5\nu'$
3	0.1776	10×10^4	$36.3\nu'$

These correlations are plotted in Figure 30.

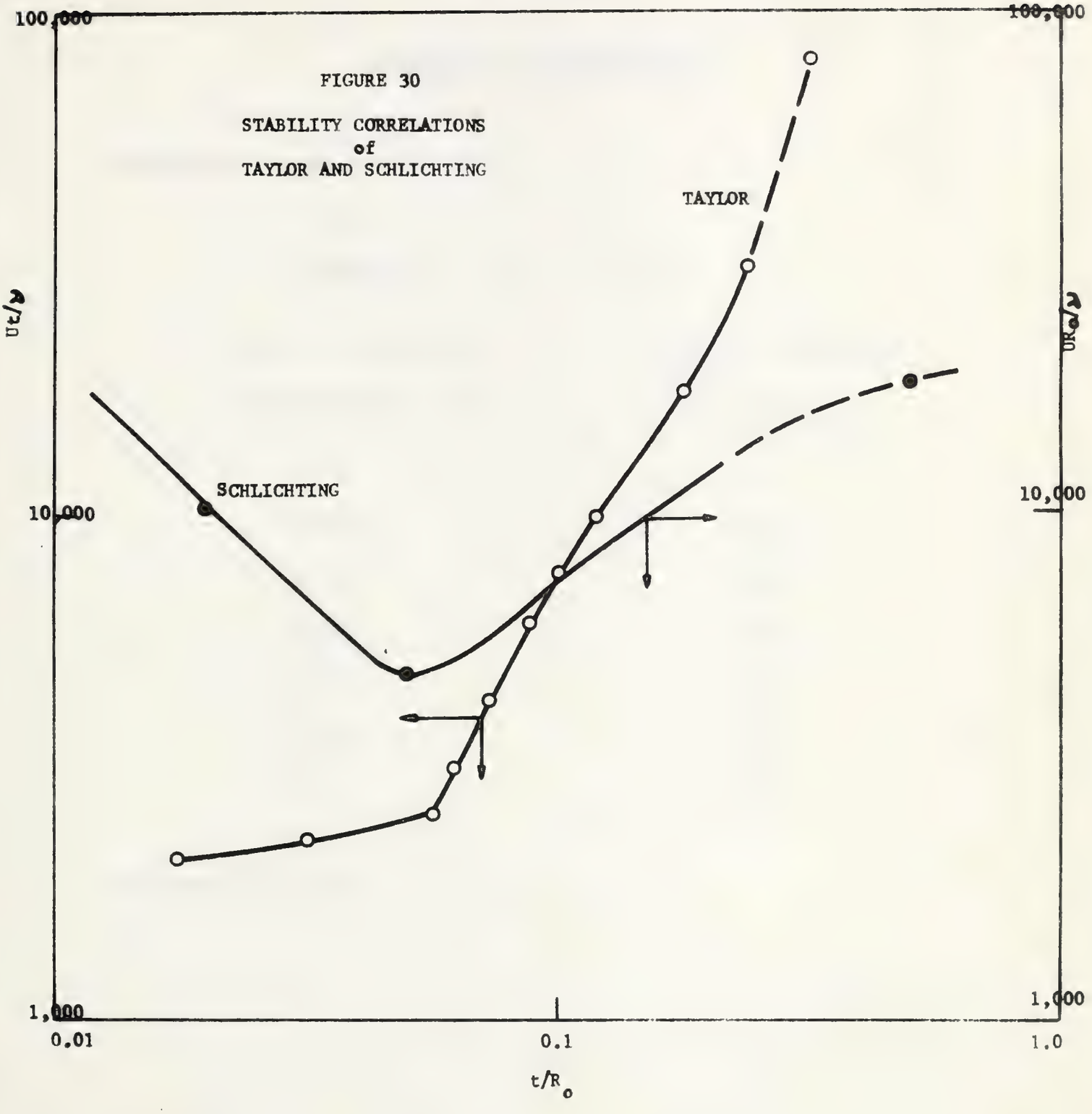

FIGURE 30

STABILITY CORRELATIONS
of
TAYLOR AND SCHLICHTING

Consistent units - ordinates and abscissa dimensionless.

APPENDIX C

CALIBRATION OF THERMOMETER

Thermometer - Mercury-in-Glass No. 249

Range: - 1° to + 51° C

Immersion: 76 mm (Vertical)

Observed Temperature Thermometer No. 249	Standard Resistance Thermometer
°C	°C
20.00	19.897
21.00	20.906
22.00	21.930
23.03	22.940
24.00	23.856
25.11	25.005

These data are plotted on Figure 31.

FIGURE 31

CALIBRATION OF MERCURY-IN-GLASS
THERMOMETER NO. 249

RANGE: - 1°C to + 51°C
IMMERSION: 76 mm (VERTICAL)
NITROGEN FILLED

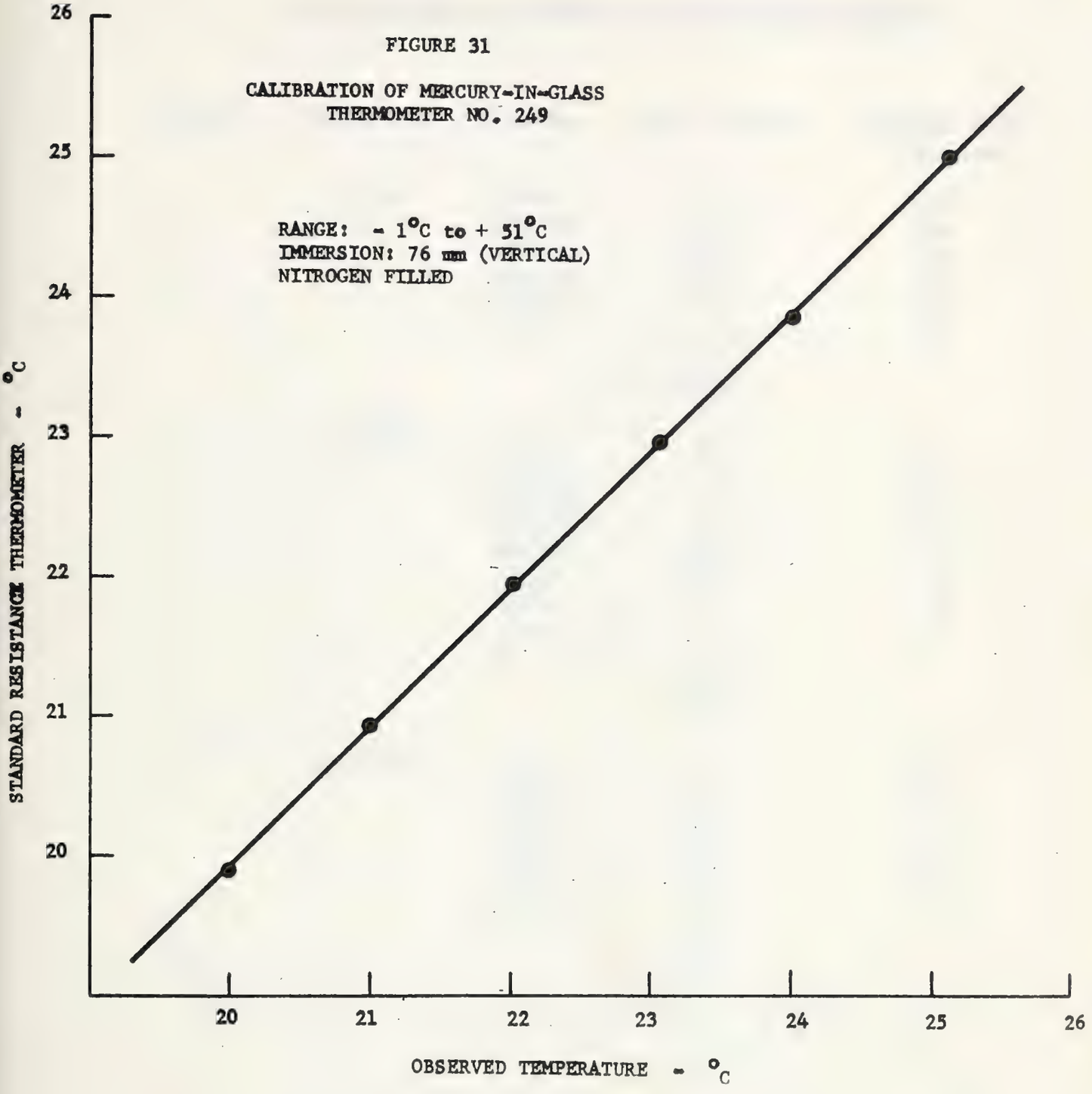

APPENDIX D

SIZE ANALYSES OF STYRENE-DIVINYLBENZENE POWDERS

Material	Mesh Size	Microns	Mass Percent	Average Size Microns
A	40/60	500+	13.4	545
		420/500	34.3	460
		350/420	20.2	385
		297/350	22.2	324
		250/297	9.5	274
		-250	0.4	230
			100.0	
B	100/200	177+	1.7	193
		149/177	5.5	163
		125/149	6.5	137
		105/125	8.1	115
		88/105	33.6	96
		74/88	21.0	81
		62/74	14.3	68
		53/62	4.1	58
		-62	5.2	-
			100.0	
C	200/400	88+	1.2	96
		74/88	11.3	81
		62/74	15.3	68
		53/62	18.6	58
		44/53	25.4	48
		37/44	5.5	40.5
		-37	22.7	-
			100.0	

AVERAGE DIAMETERS OF POWDERS

1. Arithmetic Average Diameter

$$D_{avg} = \frac{\sum N_i D_i}{\sum N_i} = \frac{\sum (x_i/D_i^2)}{\sum (x_i/D_i^3)}$$

where x_i = mass fraction of material of diameter D_i

N_i = number of particles of diameter D_i

2. Mean Surface Diameter

$$D_s = \sqrt{\frac{\sum N_i D_i^2}{\sum N_i}} = \sqrt{\frac{\sum (x_i/D_i)}{\sum (x_i/D_i^3)}}$$

3. Mean Volume Diameter

$$D_v = \sqrt[3]{\frac{\sum N_i D_i^3}{\sum N_i}} = \sqrt[3]{\frac{\sum x_i}{\sum (x_i/D_i^3)}}$$

4. Volume-Surface Diameter

$$D_{vs} = \frac{\sum N_i D_i^3}{\sum N_i D_i^2} = \frac{\sum (x_i)}{\sum (x_i/D_i)}$$

Using these formulae, the average diameters of the three powders were calculated.

Material	Mesh Size	D_{avg}	D_s	D_v	D_{vs}
			Microns		
A	40/60	356	364	371	390
B	100/200	73.5	76.5	79.8	86.5
C	200/400	38.0	40.1	42.2	47.2

APPENDIX E

EXPERIMENTAL DATA

The experimental data are presented in the following table. The tests are numbered in order, with the letter designating the suspension material used. For example,

A - 40/60 mesh material

B - 100/200 mesh material

C - 200/400 mesh material

BW - 100/200 mesh material after Isopropanol Wash

Combinations of these designations have been used for the bimodal suspensions. As well, the percentages of each material are indicated before each series for the bimodal suspensions. In the last two series of tests, Numbers 23 and 24, the suspending solution Number 2 was used. All other tests were conducted with suspending solution Number 1.

(1)	(2)	(3)	(4)	(5)	(6)	(7)	(8)
TEST NUMBER	VOLUME PERCENT SOLIDS	DEFLECTION* degrees	CUP SPEED rps	RATE OF SHEAR sec^{-1}	SHEAR STRESS $dynes/cm^2$	APPARENT VISCOSITY centipoise	SPRING-CUP COMBINATION
1-1B	0	24	5.0	194	23.6	12.2	3-3
		16	3.33	129	15.8	12.2	
		8	1.67	64.8	7.9	12.15	
1-2B	3.38	26.5	5.0	194	26.1	13.45	3-3
		17.5	3.33	129	17.3	13.35	
		9	1.67	64.8	8.9	13.7	
1-3B	5.8	29.5	5.0	194	29.1	15.0	3-3
		19.5	3.33	129	19.2	14.9	
		9.75	1.67	64.8	9.6	14.8	
1-4B	8.9	32.0	5.0	194	31.5	16.25	3-3
		21.4	3.33	129	21.1	16.35	
		10.75	1.67	64.8	10.6	16.4	
1-5B	11.3	35.5	5.0	194	35.0	18.0	3-3
		23.5	3.33	129	23.2	18.0	
		11.75	1.67	64.8	11.6	17.9	
1-6B	14.2	39	5.0	194	38.4	19.8	3-3
		26	3.33	129	25.6	19.85	
		13	1.67	64.8	12.8	19.75	
1-7B	18.9	46.25	5.0	194	45.5	23.5	3-3
		31	3.33	129	30.5	23.6	
		15.5	1.67	64.8	15.25	23.6	
1-8B	25.0	62	5.0	194	61.0	31.4	3-3
		41.25	3.33	129	40.6	31.5	
		20.75	1.67	64.8	30.4	31.5	

* Smoothed values of the dial deflection

(1)	(2)	(3)	(4)	(5)	(6)	(7)	(8)
2-1B	0	82	10.0	665	82	12.3	3-2
		41	5.0	333	41	12.3	
		27	3.33	222	27	12.15	
		13.5	1.67	111	13.5	12.15	
2-2B	7.6	103	10.0	665	103	15.5	3-2
		51.5	5.0	333	51.5	15.45	
		34.1	3.33	222	34.1	15.35	
		17	1.67	111	17	15.3	
2-3B	10.9	57.5	5.0	333	57.5	17.3	3-2
		38.1	3.33	222	38.1	17.15	
		19.1	1.67	111	19.1	17.2	
2-4B	14.8	133	10.0	665	133	20.0	3-2
		66	5.0	333	66	19.8	
		44	3.33	222	44	19.8	
		22	1.67	111	22	19.8	
2-5B	18.8	158	10.0	665	158	23.8	3-2
		79	5.0	333	79	23.7	
		53	3.33	222	53	23.9	
		26.5	1.67	111	26.5	23.9	
2-6B	22.1	184	10.0	665	184	27.7	3-2
		92	5.0	333	92	27.6	
		61	3.33	222	61	27.5	
		30.5	1.67	111	30.5	27.5	
2-7B	26.9	235	10.0	665	235	35.3	3-2
		117.5	5.0	333	117.5	35.3	
		78	3.33	222	78	35.1	
		39	1.67	111	39	35.2	
2-8B	30.5	150	5.0	333	150	45.0	3-2
		100	3.33	222	100	45.0	
		50	1.67	111	50	45.0	

(1)	(2)	(3)	(4)	(5)	(6)	(7)	(8)
2-9B	30.5	120	10.0	665	309	46.5	2-2
		60	5.0	333	154	46.4	
		40	3.33	222	102.5	46.2	
		20	1.67	111	51.5	46.4	
2-10B	34.1	159	10.0	665	409	61.5	2-2
		79.5	5.0	333	204	61.4	
		53	3.33	222	136	61.4	
		26.5	1.67	111	68	61.3	
2-11B	36.4	200	10.0	665	515	77.5	2-2
		100	5.0	333	257	77.2	
		67	3.33	222	172.5	77.7	
		33.5	1.67	111	86	77.5	
2-12B	38.5	121	5.0	333	311	93.5	2-2
		81	3.33	222	208	93.6	
		40.5	1.67	111	104	93.6	
2-13B	40.5	150	5.0	333	385	115.5	2-2
		100	3.33	222	257	116	
		50	1.67	111	128.5	116	
3-1C	0	65.5	5.0	510	67.8	13.3	3-1
		43.6	3.33	339	45.1	13.3	
		21.8	1.67	169.5	22.6	13.35	
3-2C	5.0	75	5.0	510	77.6	15.2	3-1
		50	3.33	339	51.7	15.25	
		25	1.67	169.5	25.9	15.25	
3-3C	8.7	84	5.0	510	87	17.1	3-1
		56	3.33	339	58	17.1	
		28	1.67	169.5	29	17.1	

(1)	(2)	(3)	(4)	(5)	(6)	(7)	(8)
3-4C	11.3	91.5	5.0	510	94.6	18.55	3-1
		61	3.33	339	63.1	18.6	
		30.5	1.67	169.5	31.6	18.6	
4-1C	0	125.5	10.0	1019	129.8	12.75	3-1
		62.5	5.0	510	64.6	12.70	
		42	3.33	339	43.5	12.85	
		21	1.67	169.5	21.7	12.8	
4-2C	4.06	142	10.0	1019	147	14.45	3-1
		71	5.0	510	73.5	14.45	
		47	3.33	339	48.6	14.35	
		23.5	1.67	169.5	24.3	14.35	
4-3C	6.3	152	10.0	1019	157	15.4	3-1
		75.5	5.0	510	78.1	15.3	
		50.5	3.33	339	52.2	15.4	
		25.5	1.67	169.5	26.4	15.5	
4-4C	10.2	172.5	10.0	1019	178.5	17.5	3-1
		86	5.0	510	89	17.45	
		57	3.33	339	59	17.4	
		28.5	1.67	169.5	29.5	17.4	
4-5C	13.4	193.5	10.0	1019	200	19.7	3-1
		97	5.0	510	100.5	19.7	
		65	3.33	339	67.3	19.85	
		32.5	1.67	169.5	33.6	19.8	
4-6C	16.5	108	5.0	510	112	21.9	3-1
		72	3.33	339	74.5	22.0	
		36	1.67	169.5	37.3	22.0	
4-7C	19.7	122.5	5.0	510	127	24.9	3-1
		81.5	3.33	339	84.5	24.9	
		41	1.67	169.5	42.5	25.1	

(1)	(2)	(3)	(4)	(5)	(6)	(7)	(8)
4-8C	21.7	137.5	5.0	510	142.5	28.0	3-1
		92	3.33	339	95.4	28.1	
		46	1.67	169.5	47.6	28.1	
4-9C	25.6	164	5.0	510	170	33.4	3-1
		110	3.33	339	114	33.6	
		55	1.67	169.5	57	33.6	
4-10C	27.2	136.5	10.0	1019	360	35.4	2-1
		68	5.0	510	179.5	35.2	
		45.5	3.33	339	120	35.4	
		22.5	1.67	169.5	59.5	35.1	
4-11C	29.5	156	10.0	1019	412	40.5	2-1
		78	5.0	510	206	40.5	
		52	3.33	339	137	40.5	
		26	1.67	169.5	68.6	40.5	
4-12C	33.4	200	10.0	1019	529	52.0	2-1
		100	5.0	510	264	51.8	
		66.5	3.33	339	175.5	51.8	
		33.5	1.67	169.5	88.5	52.1	
4-13C	36.0	120	5.0	510	317	62.1	2-1
		80	3.33	339	211	62.2	
		40	1.67	169.5	105.5	62.2	
4-14C	38.8	153.5	5.0	510	405	79.5	2-1
		102.5	3.33	339	271	80.0	
		51.5	1.67	169.5	136	80.2	
4-15C	40.9	185	5.0	510	489	95.9	2-1
		124	3.33	339	328	96.8	
		62	1.67	169.5	163.5	96.5	
4-16C	43.1	150	3.33	339	397	117	2-1
		75	1.67	169.5	198	117	

(1)	(2)	(3)	(4)	(5)	(6)	(7)	(8)
4-17C	44.5	183	3.33	339	484	142.5	2-1
		91	1.67	169.5	240	141.5	
4-18C	46.6	217	3.33	339	574	169	2-1
		108	1.67	169.5	285	168	
5-1A	0	24	5.0	194	23.6	12.2	3-3
		16	3.33	129	15.75	12.2	
		8	1.67	64.8	7.9	12.17	
5-2A	8.3	29.5	5.0	194	29	14.95	3-3
		19.5	3.33	129	19.2	14.9	
		10	1.67	64.8	9.85	15.2	
5-3A	10.8	33	5.0	194	32.5	16.75	3-3
		22	3.33	129	21.7	16.8	
		11	1.67	64.8	10.85	16.75	
5-4A	15.2	39	5.0	194	38.4	19.8	3-3
		26	3.33	129	25.6	19.85	
		13	1.67	64.8	12.8	19.75	
5-5A	20.2	48	5.0	194	47.3	24.4	3-3
		32	3.33	129	31.5	24.4	
		16	1.67	64.8	15.75	24.3	
5-6A	25.7	63.5	5.0	194	62.5	32.2	3-3
		42	3.33	129	41.5	32.1	
		21	1.67	64.8	20.7	31.9	
5-7A	29.8	82	5.0	194	80.7	41.6	3-3
		54	3.33	129	53.2	41.2	
		27	1.67	64.8	26.6	41.1	

(1)	(2)	(3)	(4)	(5)	(6)	(7)	(8)
5-8A	33.1	99	5.0	194	97.5	50.3	3-3
		66	3.33	129	65	50.4	
		33	1.67	64.8	32.5	50.2	
5-9A	37.5	136	5.0	194	134	69.1	3-3
		90	3.33	129	88.6	68.7	
		45	1.67	64.8	44.3	68.5	
5-10A	39.8	170	5.0	194	167.5	86.5	3-3
		113.5	3.33	129	111.8	86.6	
		56.5	1.67	64.8	55.6	86.0	
6-1C	0	126	10.0	1019	131	12.85	3-1
		63	5.0	510	65.5	12.85	
		42	3.33	339	43.6	12.9	
		21	1.67	169.5	21.8	12.85	
6-2C	4.96	70	5.0	510	72.5	14.2	3-1
		47	3.33	339	48.6	14.35	
		23.5	1.67	169.5	24.3	14.35	
6-3C	8.3	156	10.0	1019	161.5	15.85	3-1
		78	5.0	510	80.7	15.85	
		52	3.33	339	53.8	15.85	
		26	1.67	169.5	26.9	15.85	
6-4C	12.5	180	10.0	1019	186.3	18.3	3-1
		90	5.0	510	93.1	18.25	
		60	3.33	339	62.1	18.35	
		30	1.67	169.5	31.0	18.3	
6-5C	14.55	99	5.0	510	102.5	20.1	3-1
		66	3.33	339	68.4	20.15	
		33	1.67	169.5	34.2	20.2	

(1)	(2)	(3)	(4)	(5)	(6)	(7)	(8)
6-6C	18.15	113	5.0	510	117	22.95	3-1
		75	3.33	339	77.6	22.9	
		37.5	1.67	169.5	38.8	22.9	
6-7C	22.1	137	5.0	510	142	27.9	3-1
		91.5	3.33	339	94.7	27.9	
		46	1.67	169.5	47.5	28.0	
7-1A	0	23	5.0	194	22.7	11.7	3-3
		15	3.33	129	14.75	11.45	
		7.5	1.67	64.8	7.4	11.4	
7-2A	7.65	29	5.0	194	28.6	14.75	3-3
		19	3.33	129	18.7	14.5	
		9.5	1.67	64.8	9.35	14.45	
7-3A	14.50	36	5.0	194	35.4	18.25	3-3
		24	3.33	129	23.6	18.3	
		12	1.67	64.8	11.8	18.2	
7-4A	19.2	45	5.0	194	44.3	22.8	3-3
		30	3.33	129	29.6	22.9	
		15	1.67	64.8	14.8	22.9	
7-5A	23.8	54.5	5.0	194	53.7	27.7	3-3
		36.5	3.33	129	35.9	27.8	
		18.25	1.67	64.8	18.0	27.8	
7-6A	28.5	68.5	5.0	194	67.5	34.8	3-3
		45.5	3.33	129	44.8	34.7	
		22.5	1.67	64.8	22.2	34.3	
7-7A	32.4	89.5	5.0	194	88.1	45.5	3-3
		59.5	3.33	129	58.6	45.5	
		30	1.67	64.8	29.5	45.5	

(1)	(2)	(3)	(4)	(5)	(6)	(7)	(8)
7-8A	36.4	122	5.0	194	120	61.9	3-3
		81.5	3.33	129	80.3	62.2	
		40.5	1.67	64.8	39.9	61.6	
7-9A	40.1	165	5.0	194	162.5	83.8	3-3
		108	3.33	129	106.5	82.5	
		54	1.67	64.8	53.2	82.1	
8-1B	0	41	5.0	333	41	12.3	3-2
		27.5	3.33	222	27.5	12.35	
		13.5	1.67	111	13.5	12.15	
8-2B	5.1	47.5	5.0	333	47.5	14.25	3-2
		31.5	3.33	222	31.5	14.2	
		16	1.67	111	16	14.4	
8-3B	8.8	53.5	5.0	333	53.5	16.05	3-2
		36	3.33	222	36	16.2	
		18	1.67	111	18	16.2	
8-4B	14.1	65.5	5.0	333	65.5	19.7	3-2
		43.5	3.33	222	43.5	19.6	
		22	1.67	111	22	19.8	
8-5B	17.55	74.5	5.0	333	74.5	22.4	3-2
		49.5	3.33	222	49.5	22.3	
		24.5	1.67	111	24.5	22.1	
8-6B	23.8	100	5.0	333	100	30.0	3-2
		66.5	3.33	222	66.5	30.0	
		33.5	1.67	111	33.5	30.1	
8-7B	26.0	112	5.0	333	112	33.7	3-2
		74.5	3.33	222	74.5	33.6	
		37.5	1.67	111	37.5	33.8	

(1)	(2)	(3)	(4)	(5)	(6)	(7)	(8)
8-8B	30.0	150	5.0	333	150	45.0	3-2
		100	3.33	222	100	45.0	
		50	1.67	111	50	45.0	
8-9B	32.8	180.5	5.0	333	180.5	54.2	3-2
		120	3.33	222	120	54.0	
		60	1.67	111	60	54.0	
		40	1.11	74	40	54.1	
8-10B	36.1	170	3.33	222	170	76.5	3-2
		85	1.67	111	85	76.6	
		56.5	1.11	74	56.5	76.4	
		28	0.55	37	28	75.8	
8-11B	40.6	156	5.0	333	401	120.5	2-2
		104	3.33	222	267	120	
		52	1.67	111	134	120.5	
		34.5	1.11	74	88.6	120	
		17.75	0.55	37	44.4	120	
8-12B	43.5	238	5.0	333	613	184	2-2
		158.5	3.33	222	408	183.5	
		79	1.67	111	203	183	
		52.5	1.11	74	135	183	
		26.25	0.55	37	67.5	182.5	
8-13B	46.1	178.5	5.0	333	930	279	1-2
		118	3.33	222	615	277	
		59.5	1.67	111	310	280	
		39.5	1.11	74	205	277	
		20	0.55	37	104	281	
9-1C	0	60.5	5.0	510	62.5	12.25	3-1
		40	3.33	339	41.5	12.2	
		20	1.67	169.5	20.7	12.2	

(1)	(2)	(3)	(4)	(5)	(6)	(7)	(8)
9-2C	6.14	71	5.0	510	73.5	14.4	3-1
		47.5	3.33	339	49.1	14.5	
		23.5	1.67	169.5	24.3	14.35	
9-3C	10.6	82	5.0	510	84.9	16.65	3-1
		54.5	3.33	339	56.5	16.65	
		27	1.67	169.5	28	16.5	
9-4C	15.15	97	5.0	510	100.5	19.7	3-1
		64.5	3.33	339	66.8	19.7	
		32	1.67	169.5	33.2	19.6	
9-5C	18.7	113	5.0	510	117	23.0	3-1
		75	3.33	339	77.6	22.9	
		37.5	1.67	169.5	38.8	22.9	
9-6C	23.3	139	5.0	510	144	28.3	3-1
		92.5	3.33	339	95.7	28.2	
		46	1.67	169.5	47.5	28.0	
		30.5	1.11	113	31.6	28.0	
9-7C	28.8	188	5.0	510	194.5	38.1	3-1
		125	3.33	339	129.5	38.2	
		62.5	1.67	169.5	64.7	38.2	
		41.5	1.11	113	43.0	38.0	
		20.5	0.55	56	21.2	37.9	
9-8C	32.8	234	5.0	510	242	47.5	3-1
		156	3.33	339	161.5	47.6	
		78	1.67	169.5	80.7	47.6	
		51.5	1.11	113	53.3	47.1	
		26	0.55	56	26.9	48.0	
9-9C	35.4	190	3.33	339	196.5	58.0	3-1
		95	1.67	169.5	98.4	58.0	
		63	1.11	113	65.2	57.7	
		31	0.55	56	32.1	57.4	

(1)	(2)	(3)	(4)	(5)	(6)	(7)	(8)
9-10C	38.5	146	5.0	510	385	75.5	2-1
		97.5	3.33	339	258	76.1	
		49	1.67	169.5	129.5	76.5	
		32.5	1.11	113	86	76.1	
		16.25	0.55	56	43	76.8	
9-11C	41.5	197	5.0	510	520	102	2-1
		131	3.33	339	346	102	
		65.5	1.67	169.5	173	102	
		43	1.11	113	113.5	100.5	
		22	0.55	56	58.1	103.5	
9-12C	44.5	187	3.33	339	494	145.5	2-1
		93	1.67	169.5	246	145	
		62	1.11	113	163.5	145	
		31	0.55	56	82	146.5	
9-13C	49.6	189	3.33	339	994	293	1-1
		94.5	1.67	169.5	496	293	
		63	1.11	113	331	293	
		31.5	0.55	56	165.5	296	
				50% A - 50% C			
10-1AC	0	23	5.0	194	22.6	11.65	3-3
		15	3.33	129	14.75	11.45	
		7.5	1.67	64.8	7.4	11.4	
10-2AC	6.16	28	5.0	194	27.6	14.25	3-3
		18.5	3.33	129	18.2	14.1	
		9.25	1.67	64.8	9.1	14.05	
10-3AC	12.65	34	5.0	194	33.5	17.25	3-3
		22.5	3.33	129	22.2	17.2	
		11	1.67	64.8	10.8	16.75	

(1)	(2)	(3)	(4)	(5)	(6)	(7)	(8)
10-4AC	16.0	39	5.0	194	38.4	19.8	3-3
		26	3.33	129	25.6	19.85	
		13	1.67	64.8	12.8	19.75	
10-5AC	21.5	46.5	5.0	194	45.8	23.6	3-3
		31	3.33	129	30.5	23.7	
		15.5	1.67	64.8	15.25	23.5	
10-6AC	26.0	56	5.0	194	58.1	28.4	3-3
		37.5	3.33	129	36.9	28.6	
		18.5	1.67	64.8	18.2	28.1	
		12.5	1.11	43.1	12.3	28.6	
10-7AC	32.1	74	5.0	194	72.9	37.6	3-3
		49	3.33	129	48.3	37.4	
		24.5	1.67	64.8	24.1	37.2	
		16	1.11	43.1	15.75	36.6	
10-8AC	36.6	86	5.0	194	84.7	43.6	3-3
		57	3.33	129	56.1	43.5	
		28.5	1.67	64.8	28.0	43.2	
		18.5	1.11	43.1	18.2	42.2	
10-9AC	40.1	121	5.0	194	119	61.5	3-3
		80.5	3.33	129	79.3	61.5	
		40	1.67	64.8	39.5	60.8	
		26.5	1.11	43.1	26.1	60.6	
		13	0.55	21.4	12.8	59.9	
10-10AC	42.8	141	5.0	194	139	71.6	3-3
		94	3.33	129	92.5	71.7	
		47	1.67	64.8	46.3	71.5	
		31	1.11	43.1	30.5	70.8	
		15.5	0.55	21.4	15.25	71.5	

(1)	(2)	(3)	(4)	(5)	(6)	(7)	(8)
10-11AC	45.8	191	5.0	194	188	97	3-3
		127	3.33	129	125	97	
		63.5	1.67	64.8	62.5	96.5	
		42	1.11	43.1	41.4	96	
		21	0.55	21.4	20.7	96.8	
		14	0.37	14.35	13.8	96.4	
10-12AC	48.2	240	5.0	194	236	121.6	3-3
		160	3.33	129	157.5	122	
		80	1.67	64.8	78.8	121.6	
		53	1.11	43.1	52.2	121	
		26.5	0.55	21.4	26.1	122	
		18	0.37	14.35	17.75	123.5	
10-13AC	51.1	204	3.33	129	201	156	3-3
		102	1.67	64.8	100.5	155	
		67.5	1.11	43.1	66.5	154.5	
		33.5	0.55	21.4	33.0	154.5	
		22.5	0.37	14.35	22.2	155	
				25% A - 75% C			
11-1AC	0	23	5.0	194	22.7	11.7	3-3
		15	3.33	129	14.8	11.45	
		7.5	1.67	64.8	7.4	11.40	
11-2AC	6.6	28.5	5.0	194	28.0	14.45	3-3
		19	3.33	129	18.7	14.5	
		9.5	1.67	64.8	9.35	14.4	
11-3AC	11.9	33.5	5.0	194	33	17.0	3-3
		22.5	3.33	129	22.2	17.2	
		11	1.67	64.8	11.3	17.5	

(1)	(2)	(3)	(4)	(5)	(6)	(7)	(8)
11-4AC	15.3	38	5.0	194	37.4	19.3	3-3
		25.5	3.33	129	25.1	19.45	
		13	1.67	64.8	12.8	19.8	
11-5AC	21.3	46.5	5.0	194	45.8	23.6	3-3
		31	3.33	129	30.5	23.6	
		15.5	1.67	64.8	15.25	23.5	
11-6AC	24.8	55.5	5.0	194	54.6	28.2	3-3
		37	3.33	129	36.5	28.3	
		18.25	1.67	64.8	18.0	27.8	
		12	1.11	43.1	11.8	27.4	
11-7AC	29.8	73	5.0	194	72	37.1	3-3
		48.5	3.33	129	47.7	37.0	
		24	1.67	64.8	23.6	36.5	
		15.75	1.11	43.1	15.5	36.0	
11-8AC	33.2	88	5.0	194	86.6	44.6	3-3
		59	3.33	129	58.1	45.0	
		29.5	1.67	64.8	29.1	44.9	
		19.25	1.11	43.1	18.95	44.0	
		9.75	0.55	21.4	9.6	44.9	
11-9AC	36.5	110	5.0	194	108.3	55.9	3-3
		73	3.33	129	72	55.8	
		36	1.67	64.8	35.5	54.9	
		24	1.11	43.1	23.6	54.9	
		12	0.55	21.4	11.8	55.2	
11-10AC	39.4	135.5	5.0	194	133.5	68.9	3-3
		90	3.33	129	88.6	68.6	
		45	1.67	64.8	44.3	68.5	
		30	1.11	43.1	29.6	68.8	
		15	0.55	21.4	14.75	69.0	

(1)	(2)	(3)	(4)	(5)	(6)	(7)	(8)
11-11AC	42.0	164.5	5.0	194	162	83.5	3-3
		109.5	3.33	129	108	83.8	
		54.5	1.67	64.8	53.6	82.9	
		36	1.11	43.1	35.5	82.5	
		18	0.55	21.4	17.7	82.8	
11-12AC	45.0	234.5	5.0	194	231	119	3-3
		149.5	3.33	129	147	114	
		75	1.67	64.8	74	116	
		49.5	1.11	43.1	48.8	113	
		24.5	0.55	21.4	24.15	113	
11-13AC	47.1	183	3.33	129	180	139.5	3-3
		91.5	1.67	64.8	90	139	
		61	1.11	43.1	60	139.5	
		30.5	0.55	21.4	30	140	
11-14AC	51.0	180	5.0	194	445	229.5	2-3
		120	3.33	129	297	230	
		60	1.67	64.8	148	229	
		40	1.11	43.1	99	230	
		20	0.55	21.4	49.5	231	
11-15AC	55.0	224	3.33	129	555	430	2-3
		112	1.67	64.8	277	427	
		74	1.11	43.1	183	425	
		37	0.55	21.4	91.5	428	
				75% A - 25% C			
12-1AC	0	24	5.0	194	23.6	12.15	3-3
		16	3.33	129	15.75	12.2	
		8	1.67	64.8	7.88	12.15	
12-2AC	8.8	30	5.0	194	29.6	15.25	3-3
		20	3.33	129	19.7	15.25	
		10	1.67	64.8	9.85	15.2	

(1)	(2)	(3)	(4)	(5)	(6)	(7)	(8)
12-3AC	15.9	26	3.33	129	25.6	19.85	3-3
		13	1.67	64.8	12.8	19.75	
12-4AC	23.0	48.5	5.0	194	47.8	24.6	3-3
		32.25	3.33	129	31.8	24.6	
		16	1.67	64.8	15.75	24.3	
12-5AC	28.7	63	5.0	194	62	32.0	3-3
		42	3.33	129	41.4	32.0	
		21	1.67	64.8	20.7	32.0	
12-6AC	35.3	90	5.0	194	88.6	45.7	3-3
		60	3.33	129	59.1	45.8	
		30	1.67	64.8	29.5	45.6	
12-7AC	39.2	113	5.0	194	111.5	57.5	3-3
		75.5	3.33	129	74.4	57.5	
		37.5	1.67	64.8	36.9	57.0	
		25	1.11	43.1	24.6	57.1	
		12.5	0.55	21.4	12.3	57.5	
12-8AC	42.1	150	5.0	194	147.5	76.0	3-3
		100	3.33	129	98.5	76.3	
		50	1.67	64.8	49.25	76.0	
		33	1.11	43.1	32.5	75.5	
		16.5	0.55	21.4	16.25	76.0	
12-9AC	48.4	243	5.0	194	239	123	3-3
		161	3.33	129	158.5	123	
		81	1.67	64.8	79.7	123	
		54	1.11	43.1	53.1	123	
		27	0.55	21.4	26.6	124	
12-10AC	50.5	114	5.0	194	282	145.5	2-3
		76	3.33	129	187.5	145.5	
		38	1.67	64.8	93.9	145.	
		25	1.11	43.1	61.8	143	
		12.5	0.55	21.4	30.9	144.5	

(1)	(2)	(3)	(4)	(5)	(6)	(7)	(8)
12-11AC	53.6	164	5.0	194	405	209	2-3
		109	3.33	129	269	209	
		54.5	1.67	64.8	134.5	208	
		36	1.11	43.1	89	207	
		18	0.55	21.4	44.5	208	
12-12AC	60.5	242	5.0	194	1205	621	1-3
		161	3.33	129	801	620	
		80.5	1.67	64.8	400	618	
		53.5	1.11	43.1	266	618	
		26.75	0.55	21.4	133	622	
13-1BW	0	40.5	5.0	333	40.5	12.16	3-2
		27	3.33	222	27	12.16	
		13.5	1.67	111	13.5	12.16	
13-2BW	7.3	50.5	5.0	333	50.5	15.15	3-2
		33.5	3.33	222	33.5	15.1	
		16.75	1.67	111	16.75	15.1	
13-3BW	11.9	59	5.0	333	59	17.75	3-2
		39	3.33	222	39	17.55	
		19.5	1.67	111	19.5	17.55	
13-4BW	16.5	72	5.0	333	72	21.6	3-2
		48	3.33	222	48	21.6	
		24	1.67	111	24	21.6	
13-5BW	22.1	91	5.0	333	91	27.3	3-2
		60.5	3.33	222	60.5	27.2	
		30.25	1.67	111	30.25	27.3	
		20	1.11	74	20	27.1	
		10	0.55	37	10	27.1	

(1)	(2)	(3)	(4)	(5)	(6)	(7)	(8)
13-6BW	29.8	140	5.0	333	140	42.0	3-2
		93	3.33	222	93	42.0	
		46.5	1.67	111	46.5	42.0	
		31	1.11	74	31	42.0	
		15.5	0.55	37	15.5	42.0	
13-7BW	37.1	221	5.0	333	221	66.5	3-2
		147	3.33	222	147	66.2	
		73.5	1.67	111	73.5	66.2	
		48.75	1.11	74	48.75	66.0	
		24.4	0.55	37	24.4	66.0	
13-8BW	42.1	246	3.33	222	246	111	3-2
		123	1.67	111	123	111	
		82	1.11	74	82	111	
		41	0.55	37	41	111	
		27	0.37	24.6	27	110	
		13.5	0.185	12.3	13.5	110	
14-1BW	40.1	121.5	5.0	333	312.5	94.0	2-2
		81	3.33	222	208	93.8	
		40.5	1.67	111	104	93.8	
		27	1.11	74	69.5	93.9	
		13.5	0.55	37	34.7	93.8	
15-1A	41.0	210	5.0	194	207	107	3-3
		140	3.33	129	138	107	
		70	1.67	64.8	69	106.5	
		46.5	1.11	43.1	45.8	106.5	
		23.25	0.55	21.4	22.9	107	
15-2A	50.0	177	3.33	129	437.5	339	2-3
		88.5	1.67	64.8	219	338	
		59	1.11	43.1	146	339	
		29.5	0.55	21.4	73	341	

(1)	(2)	(3)	(4)	(5)	(6)	(7)	(8)
16-1C	42.5	210	5.0	510	555	109	2-1
		140	3.33	339	370	109	
		70	1.67	169.5	185	109	
		46.5	1.11	113	122.5	108.5	
		23.25	0.55	56	61.5	110	
17-1BW	50.1	144	1.67	111	370	334	2-2
		96	1.11	74	241	334	
		48	0.55	37	123.5	333	
17-2BW	50.1	216	5.0	333	1120	337	1-2
		144	3.33	222	749	338	
		72	1.67	111	374	337	
		48	1.11	74	249.5	337	
		24	0.55	37	125	337	
				50% A - 50% B			
18-1AB	20.2	45	5.0	194	44.4	22.9	3-3
		30	3.33	129	29.6	22.9	
		15	1.67	64.8	14.75	22.9	
18-2AB	29.6	62	5.0	194	61.1	31.5	3-3
		41	3.33	129	40.5	31.3	
		20.5	1.67	64.8	20.2	31.2	
18-3AB	40.0	121.5	5.0	194	119.5	61.6	3-3
		81	3.33	129	79.8	61.9	
		40.5	1.67	64.8	39.9	61.5	
		27	1.11	43.1	26.6	61.8	
		13.5	0.55	21.4	13.3	62.1	

(1)	(2)	(3)	(4)	(5)	(6)	(7)	(8)
18-4AB	47.6	180	3.33	129	177.5	137.5	3-3
		90	1.67	64.8	88.6	137	
		60	1.11	43.1	59.1	137	
		30	0.55	21.4	29.6	138	
18-5AB	47.6	210	10.0	388	519	134	2-3
		105	5.0	194	259	133.5	
		70	3.33	129	172.5	133.5	
		35	1.67	64.8	86.5	133.5	
		23	1.11	43.1	56.8	131.5	
		11.5	0.55	21.4	28.4	133.5	
				75% A - 25% B			
19-1AB	20.1	45	5.0	194	44.4	22.8	3-3
		30	3.33	129	29.6	22.9	
		15	1.67	64.8	14.8	22.9	
19-2AB	30.0	64.5	5.0	194	63.5	32.7	3-3
		43	3.33	129	42.5	32.9	
		21.5	1.67	64.8	21.2	32.7	
19-3AB	40.0	124	5.0	194	122	63.0	3-3
		82	3.33	129	80.8	62.6	
		41	1.67	64.8	40.5	62.5	
		28	1.11	43.1	27.6	64.1	
		14	0.55	21.4	13.8	64.5	
19-4AB	50.0	142.5	5.0	194	352	181.5	2-3
		94.5	3.33	129	234	181	
		47.5	1.67	64.8	117.5	181.5	
		31.5	1.11	43.1	78	181	
		16	0.55	21.4	39.5	184.5	

(1)	(2)	(3)	(4)	(5)	(6)	(7)	(8)
			25% A - 75% B				
20-1AB	20.0	45	5.0	194	44.4	22.8	3-3
		30	3.33	129	29.6	22.9	
		15	1.67	64.8	14.8	22.9	
20-2AB	30.2	74	5.0	194	73	37.6	3-3
		49	3.33	129	48.3	37.4	
		24.5	1.67	64.8	24.1	37.3	
20-3AB	40.1	157.5	5.0	194	155	80.0	3-3
		105	3.33	129	103.5	80.2	
		52.5	1.67	64.8	51.7	80.0	
		35	1.11	43.1	34.5	80.1	
		17.5	0.55	21.4	17.25	80.5	
20-4AB	50.0	214.5	5.0	194	530	273	2-3
		143	3.33	129	353	274	
		71.5	1.67	64.8	176.5	273	
		47.5	1.11	43.1	117.5	272	
		23.75	0.55	21.4	58.6	274	
			50% A - 50% C				
21-1AC	20.0	45	5.0	194	44.4	22.8	3-3
		30	3.33	129	29.6	22.9	
		15	1.67	64.8	14.8	22.9	
21-2AC	30.0	66.5	5.0	194	65.5	33.7	3-3
		44.5	3.33	129	43.9	34.0	
		22.25	1.67	64.8	21.9	33.9	
21-3AC	40.1	118.5	5.0	194	117	60.3	3-3
		79	3.33	129	77.9	60.4	
		39.5	1.67	64.8	39	60.3	
		26.25	1.11	43.1	25.9	60.1	
		13	0.55	21.4	12.8	60.0	

(1)	(2)	(3)	(4)	(5)	(6)	(7)	(8)
21-4AC	50.0	107.5	5.0	194	266	137	2-3
		71.5	3.33	129	177	137.5	
		36	1.67	64.8	89	137.5	
		24	1.11	43.1	59.4	137.5	
		12	0.55	21.4	29.7	139	
				50% B - 50% C			
22-1BC	0	115	10.0	665	115	17.3	3-2
		57.5	5.0	333	57.5	17.3	
		38	3.33	222	38	17.15	
		19	1.67	111	19	17.15	
22-2BC	19.95	111	5.0	333	111	33.3	3-2
		74	3.33	222	74	33.3	
		37	1.67	111	37	33.3	
22-3BC	30.0	184.5	5.0	333	184.5	55.5	3-2
		123	3.33	222	123	55.5	
		61.5	1.67	111	61.5	55.4	
		41	1.11	74	41	55.4	
		20.5	0.55	37	20.5	55.4	
22-4BC	40.0	258	3.33	222	258	116	3-2
		129	1.67	111	129	116	
		86	1.11	74	86	116	
		43	0.55	37	43	116	
22-5BC	40.0	150	5.0	333	386	116	2-2
		100	3.33	222	257	115.5	
		50	1.67	111	128.5	115.5	
		32.5	1.11	74	83.5	113	
		16.5	0.55	37	42.5	115	

(1)	(2)	(3)	(4)	(5)	(6)	(7)	(8)
22-6BC	50.0	300	3.33	222	773	348	2-2
		150	1.67	111	386	348	
		100	1.11	74	257	347	
		50	0.55	37	128.5	347	
		33	0.37	24.6	84.9	345	
		16.5	0.185	12.3	42.5	346	
				33 1/3% A - 33 1/3% B - 33 1/3% C			
23-1ABC	0	34	5.0	194	33.5	17.25	3-3
		22.5	3.33	129	22.2	17.2	
		11.25	1.67	64.8	11.1	17.2	
23-2ABC	10.9	46.5	5.0	194	45.8	23.6	3-3
		31	3.33	129	30.55	23.7	
		15.5	1.67	64.8	15.25	23.6	
23-3ABC	20.0	63.5	5.0	194	62.5	32.2	3-3
		42.5	3.33	129	41.9	32.5	
		21.25	1.67	64.8	20.95	32.4	
23-4ABC	30.2	103	5.0	194	101.5	52.5	3-3
		69	3.33	129	68	52.6	
		34.5	1.67	64.8	34	52.5	
		23	1.11	43.1	22.65	52.6	
		11.5	0.55	21.4	11.3	52.8	
23-5ABC	40.0	193.5	5.0	194	190.5	98.2	3-3
		129	3.33	129	127	98.5	
		64.5	1.67	64.8	63.5	98.1	
		43	1.11	43.1	42.4	98.1	
		21.5	0.55	21.4	21.2	99.0	
23-6ABC	50.5	187.5	5.0	194	464	239	2-3
		125	3.33	129	309	239	
		62.5	1.67	64.8	154.5	239	
		41.5	1.11	43.1	102.5	238	
		20.75	0.55	21.4	51.3	240	

APPENDIX F

CALCULATED DATA

The viscosity data of Appendix E are given here as relative viscosity and relative fluidity. These were obtained by division of the observed viscosity by the viscosity of the suspending solution and by division of the viscosity of the suspending solution by the observed viscosity respectively.

Column (4) contains the corrected viscosity. It was noted that the observed viscosity of the suspending solution was sometimes different from that obtained in the capillary viscometer. Since this error was probably due to instrument errors, the observed viscosity of all tests in the series was corrected by the addition or subtraction of the amount necessary to make the zero percent solids value equal to that obtained in the capillary viscometer.

(1) TEST NUMBER	(2) VOLUME PERCENT SOLIDS	(3) VISCOSITY centipoise	(4) CORRECTED VISCOSITY centipoise	(5) RELATIVE VISCOSITY η_r	(6) RELATIVE FLUIDITY ϕ_r
1-1B	0	12.2	-	-	-
1-2B	3.38	13.4	-	1.105	0.906
1-3B	5.8	14.9	-	1.23	0.815
1-4B	8.9	16.3	-	1.34	0.745
1-5B	11.3	18.0	-	1.48	0.675
1-6B	14.2	19.8	-	1.63	0.615
1-7B	18.9	23.6	-	1.94	0.515
1-8B	25.0	31.5	-	2.60	0.385
2-1B	0	12.25	-	-	-
2-2B	7.6	15.4	-	1.27	0.790
2-3B	10.9	17.2	-	1.415	0.706
2-4B	14.8	19.8	-	1.63	0.614
2-5B	18.8	23.9	-	1.97	0.509
2-6B	22.1	27.5	-	2.26	0.442
2-7B	26.9	35.3	-	2.90	0.344
2-8B	30.5	45.0	-	3.71	0.270
2-9B	30.5	46.4	-	3.82	0.262
2-10B	34.1	61.4	-	5.05	0.198
2-11B	36.4	77.5	-	6.38	0.157
2-12B	38.5	93.6	-	7.71	0.130
2-13B	40.5	116	-	9.56	0.1045
3-1C	0	13.3	12.2	-	-
3-2C	5.0	15.25	14.15	1.165	0.858
3-3C	8.7	17.1	16.0	1.32	0.759
3-4C	11.3	18.6	17.5	1.44	0.694
4-1C	0	12.8	12.2	-	-
4-2C	4.06	14.4	13.8	1.135	0.880
4-3C	6.3	15.4	14.8	1.22	0.820
4-4C	10.2	17.45	16.85	1.39	0.721
4-5C	13.4	19.75	19.15	1.575	0.635
4-6C	16.5	22.0	21.4	1.76	0.568
4-7C	19.7	24.9	24.3	2.00	0.500
4-8C	21.7	28.1	27.5	2.26	0.442
4-9C	25.6	33.5	32.9	2.71	0.369
4-10C	27.2	35.4	34.8	2.87	0.349
4-11C	29.5	40.5	39.9	3.29	0.304
4-12C	33.4	51.9	51.3	4.22	0.237
4-13C	36.0	62.2	61.6	5.09	0.197
4-14C	38.8	80.0	79.4	6.54	0.153
4-15C	40.9	96.5	95.9	7.9	0.127

(1)	(2)	(3)	(4)	(5)	(6)
4-16C	43.1	117	116.4	9.6	0.104
4-17C	44.5	142	141.4	11.6	0.086
4-18C	46.6	168.5	167.9	13.8	0.072
5-1A	0	12.2	-	-	-
5-2A	8.3	15.0	-	1.235	0.810
5-3A	10.8	16.75	-	1.38	0.725
5-4A	15.2	19.8	-	1.63	0.614
5-5A	20.2	24.4	-	2.01	0.498
5-6A	25.7	32.1	-	2.64	0.378
5-7A	29.8	41.3	-	3.40	0.294
5-8A	33.1	50.3	-	4.15	0.242
5-9A	37.5	68.8	-	5.66	0.177
5-10A	39.8	86.5	-	7.13	0.141
6-1C	0	12.85	12.2	-	-
6-2C	4.96	14.3	13.65	1.123	0.890
6-3C	8.3	15.85	15.2	1.25	0.799
6-4C	12.5	18.3	17.65	1.453	0.689
6-5C	14.55	20.15	19.5	1.605	0.624
6-6C	18.15	22.9	22.25	1.83	0.545
6-7C	22.1	27.9	27.25	2.24	0.446
7-1A	0	11.5	12.2	-	-
7-2A	7.65	14.6	15.3	1.26	0.794
7-3A	14.50	18.25	18.95	1.56	0.641
7-4A	19.2	22.9	23.6	1.945	0.515
7-5A	23.8	27.8	28.5	2.345	0.426
7-6A	28.5	34.75	35.45	2.92	0.343
7-7A	32.4	45.5	46.2	3.80	0.263
7-8A	36.4	61.9	62.6	5.15	0.194
7-9A	40.1	82.6	83.3	6.86	0.146
8-1B	0	12.3	-	-	-
8-2B	5.1	14.25	-	1.17	0.854
8-3B	8.8	16.1	-	1.325	0.755
8-4B	14.1	19.6	-	1.61	0.620
8-5B	17.55	22.3	-	1.835	0.545
8-6B	23.8	30.0	-	2.47	0.405
8-7B	26.0	33.7	-	2.77	0.361
8-8B	30.0	45.0	-	3.71	0.270
8-9B	32.8	54.1	-	4.45	0.224
8-10B	36.1	76.6	-	6.31	0.1585
8-11B	40.6	120	-	9.9	0.101
8-12B	43.5	183	-	15.1	0.066
8-13B	46.1	280	-	23.1	0.043

(1)	(2)	(3)	(4)	(5)	(6)
9-1C	0	12.2	-	-	-
9-2C	6.14	14.4	-	1.185	0.845
9-3C	10.6	16.65	-	1.37	0.730
9-4C	15.15	19.7	-	1.625	0.616
9-5C	18.7	23.0	-	1.895	0.529
9-6C	23.3	28.2	-	2.32	0.431
9-7C	28.8	38.1	-	3.14	0.319
9-8C	32.8	47.5	-	3.91	0.256
9-9C	35.4	58.0	-	4.78	0.210
9-10C	38.5	76.1	-	6.26	0.160
9-11C	41.5	102	-	8.41	0.119
9-12C	44.5	145	-	11.95	0.084
9-13C	49.6	293	-	24.1	0.042
		50% A - 50% C			
10-1AC	0	11.5	12.2	-	-
10-2AC	6.16	14.15	14.85	1.22	0.819
10-3AC	12.65	17.2	17.9	1.47	0.679
10-4AC	16.0	19.8	20.5	1.69	0.593
10-5AC	21.5	23.6	24.3	2.00	0.500
10-6AC	26.0	28.5	29.2	2.40	0.416
10-7AC	32.1	37.5	38.2	3.15	0.318
10-8AC	36.6	43.5	44.2	3.64	0.275
10-9AC	40.1	61.5	62.2	5.12	0.195
10-10AC	42.8	71.6	72.3	5.95	0.168
10-11AC	45.8	97	97.7	8.05	0.124
10-12AC	48.2	121.6	122.3	10.06	0.099
10-13AC	51.1	155	155.7	12.8	0.078
		25% A - 75% C			
11-1AC	0	11.5	12.2	-	-
11-2AC	6.6	14.45	15.15	1.25	0.801
11-3AC	11.9	17.2	17.9	1.475	0.679
11-4AC	15.3	19.4	20.1	1.655	0.605
11-5AC	21.3	23.6	24.3	2.00	0.500
11-6AC	24.8	28.2	28.9	2.38	0.420
11-7AC	29.8	37.0	37.7	3.10	0.322
11-8AC	33.2	45.0	45.7	3.76	0.266
11-9AC	36.5	55.2	55.9	4.60	0.218
11-10AC	39.4	68.7	69.4	5.71	0.175
11-11AC	42.0	83.2	83.9	6.9	0.145
11-12AC	45.0	115	115.7	9.5	0.105
11-13AC	47.1	139.5	140.2	11.6	0.086
11-14AC	51.0	230	230.7	19	0.052
11-15AC	55.0	427	427.7	35.2	0.028

(1)	(2)	(3)	(4)	(5)	(6)
		75% A - 25% C			
12-1AC	0	12.15	-	-	-
12-2AC	8.8	15.25	-	1.255	0.796
12-3AC	15.9	19.8	-	1.63	0.614
12-4AC	23.0	24.6	-	2.03	0.494
12-5AC	28.7	32.0	-	2.64	0.380
12-6AC	35.3	45.7	-	3.77	0.266
12-7AC	39.2	57.5	-	4.75	0.211
12-8AC	42.1	76.0	-	6.26	0.160
12-9AC	48.4	123	-	10.12	0.099
12-10AC	50.5	145	-	11.95	0.084
12-11AC	53.6	209	-	17.2	0.058
12-12AC	60.5	620	-	51	0.020
13-1BW	0	12.16	-	-	-
13-2BW	7.3	15.1	-	1.245	0.805
13-3BW	11.9	17.6	-	1.45	0.690
13-4BW	16.5	21.6	-	1.78	0.563
13-5BW	22.1	27.2	-	2.24	0.446
13-6BW	29.8	42.0	-	3.46	0.289
13-7BW	37.1	66.2	-	5.45	0.184
13-8BW	42.1	111	-	9.15	0.109
14-1BW	40.1	93.8	-	7.72	0.1295
15-1A	41.0	107	-	8.82	0.1135
15-2A	50.0	339	-	27.9	0.036
16-1C	42.5	109	-	8.99	0.1115
17-1BW	50.1	334	-	27.5	0.036
17-2BW	50.1	337	-	27.7	0.036
		50% A - 50% B			
18-1AB	20.2	22.9	-	1.885	0.530
18-2AB	29.6	31.3	-	2.58	0.388
18-3AB	40.0	61.7	-	5.08	0.197
18-4AB	47.6	137.5	-	11.3	0.088
18-5AB	47.6	133.5	-	11.0	0.091
		75% A - 25% B			
19-1AB	20.1	22.9	-	1.885	0.530
19-2AB	30.0	32.7	-	2.59	0.371
19-3AB	40.0	63.0	-	5.20	0.193
19-4AB	50.0	181.5	-	14.95	0.067

(1)	(2)	(3)	(4)	(5)	(6)
		25% A - 75% B			
20-1AB	20.0	22.9	-	1.885	0.530
20-2AB	30.2	37.5	-	3.09	0.324
20-3AB	40.1	80.1	-	6.6	0.1515
20-4AB	50.0	273	-	22.4	0.0445
		50% A - 50% C			
21-1AC	20.0	22.9	-	1.885	0.530
21-2AC	30.0	33.9	-	2.79	0.358
21-3AC	40.1	60.3	-	4.95	0.201
21-4AC	50.0	137.5	-	11.3	0.088
		50% B - 50% C			
22-1BC	0	17.2	-	-	-
22-2BC	19.95	33.3	-	1.93	0.520
22-3BC	30.0	55.4	-	3.20	0.312
22-4BC	40.0	116	-	6.71	0.149
22-5BC	40.0	115.5	-	6.69	0.1495
22-6BC	50.0	347	-	20.1	0.050
		33 1/3% A - 33 1/3% B - 33 1/3% C			
23-1ABC	0	17.25	-	-	-
23-2ABC	10.9	23.6	-	1.365	0.733
23-3ABC	20.0	32.4	-	1.885	0.535
23-4ABC	30.2	52.6	-	3.05	0.329
23-5ABC	40.0	98.3	-	5.7	0.176
23-6ABC	50.5	239	-	13.8	0.0745

APPENDIX G

DERIVATION OF EQUATION FOR CONCENTRIC CYLINDER VISCOMETER

Consider a time-independent fluid of arbitrary behavior $f(\tau) = (du/dr)$ to be contained in the annulus. Since there is no slip at the wall, the liquid in contact with the outer rotating cylinder has an angular velocity Ω, while that in contact with the inner cylinder will be stationary. If the angular velocity is ω at any intermediate radius, the angular velocity gradient is $d\omega/dr$ and the linear velocity gradient across a small element of the fluid at the circumference of this circle of radius r is $rd\omega/dr$.

Then $$rd\omega/dr = f(\tau)$$

But $$\tau(r) = M/(2\pi r^2 h)$$

$$rd\omega/dr = f\left(M/(2\pi r^2 h)\right)$$

At $r = R_i$, $\omega = 0$

$r = R_o$, $\omega = \Omega$

Integrating the above equation between the limits

$$\Omega = \int_{R_i}^{R_o} f(M/(2\pi r^2 h))\, dr/r$$

Substituting $\tau(r) = M/(2\pi r^2 h)$ and $dr/r = -d\tau/(2\tau)$

$$\Omega = \int_{\tau_o}^{\tau_i} \frac{f(\tau)\, d\tau}{2\tau}$$

APPENDIX H

POWER SERIES CORRELATION OF THE DATA

UNIMODAL SYSTEMS

(1)	(2)	(3)	(4)	(5)	(6)	(7)	(8)	(9)	(10)
c	$\eta_{r(obs)}$	ϕ_r	$1 - \phi_r$	$\frac{1 - \phi_r}{c^2}$	$\frac{2.5}{c}$	(5) - (6)	$\phi_{r(calc)}$	$\eta_{r(calc)}$	$\eta_{r(obs)}(\phi_r)_{(calc)}$
0.05	1.14	0.878	0.122	48.9	50.0	-1.1	0.874	1.142	0.996
0.10	1.34	0.746	0.254	25.4	25.0	+0.4	0.750	1.335	1.005
0.15	1.625	0.615	0.385	17.1	16.7	+0.4	0.628	1.595	1.020
0.20	2.02	0.495	0.505	12.6	12.5	+0.1	0.511	1.96	1.030
0.25	2.55	0.392	0.608	9.72	10.0	-0.28	0.404	2.48	1.030
0.30	3.30	0.303	0.697	7.76	8.35	-0.59	0.301	3.32	0.995
0.35	4.70	0.213	0.787	6.44	7.15	-0.71	0.211	4.74	0.993
0.40	7.2	0.139	0.861	5.4	6.25	-0.85	0.138	7.25	0.994
0.45	12.4	0.0806	0.9194	4.55	5.56	-1.01	0.078	12.8	0.967
0.50	26.5	0.038	0.962	3.85	5.0	-1.15	0.037	27.0	0.980

$$\phi_r = 1 - 2.5c - 0.3c^2 + 2.9c^3$$

The plot of $\frac{1 - \phi_r}{c^2} - \frac{2.5}{c}$ versus c in Figure 32 gives the coefficient of c^2 and c^3 in the power series.

FIGURE 32

POWER SERIES CORRELATION FOR UNIMODAL SUSPENSIONS

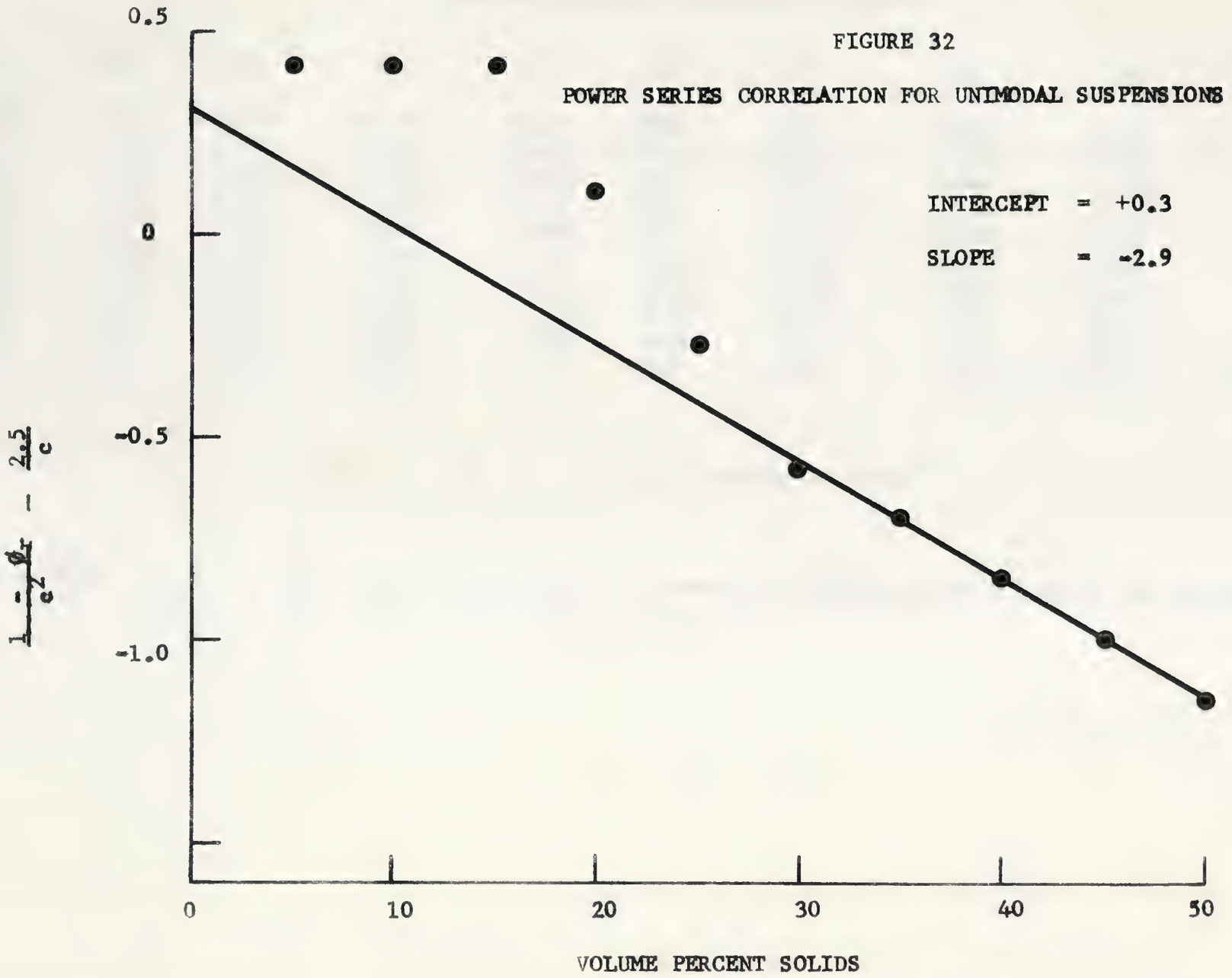

BIMODAL MIXTURES OF A AND B

50% A - 50% B and 75% A - 25% B

(1)	(2)	(3)	(4)	(5)	(6)	(7)	(8)	(9)	(10)
0.05	1.14	0.878	0.122	48.9	50.0	-1.1	0.877	1.14	1.000
0.10	1.34	0.746	0.254	25.4	25.0	+0.4	0.759	1.32	1.015
0.15	1.55	0.645	0.355	15.75	16.7	-0.95	0.646	1.546	1.001
0.20	1.85	0.541	0.459	11.5	12.5	-1.0	0.539	1.855	0.997
0.25	2.19	0.457	0.543	8.69	10.0	-1.31	0.439	2.28	0.965
0.30	2.70	0.370	0.630	7.0	8.35	-1.35	0.347	2.88	0.938
0.35	3.60	0.278	0.722	5.9	7.15	-1.25	0.263	3.80	0.948
0.40	5.15	0.194	0.806	5.04	6.25	-1.21	0.187	5.35	0.965
0.45	8.2	0.122	0.878	4.34	5.56	-1.22	0.122	8.2	1.000
0.50	15.0	0.067	0.933	3.74	5.0	-1.26	0.065	15.4	0.976

$$\phi_r = 1 - 2.5c + 0.8c^2 + 0.92c^3$$

The plot of $\frac{1 - \phi_r}{c^2} - \frac{2.5}{c}$ versus c in Figure 33 gives the coefficient of c^2 and c^3 in the power series.

FIGURE 33

POWER SERIES CORRELATION FOR BIMODAL SUSPENSIONS OF A AND B

50% A - 50% B
75% A - 25% B

INTERCEPT = -0.8
SLOPE = -0.92

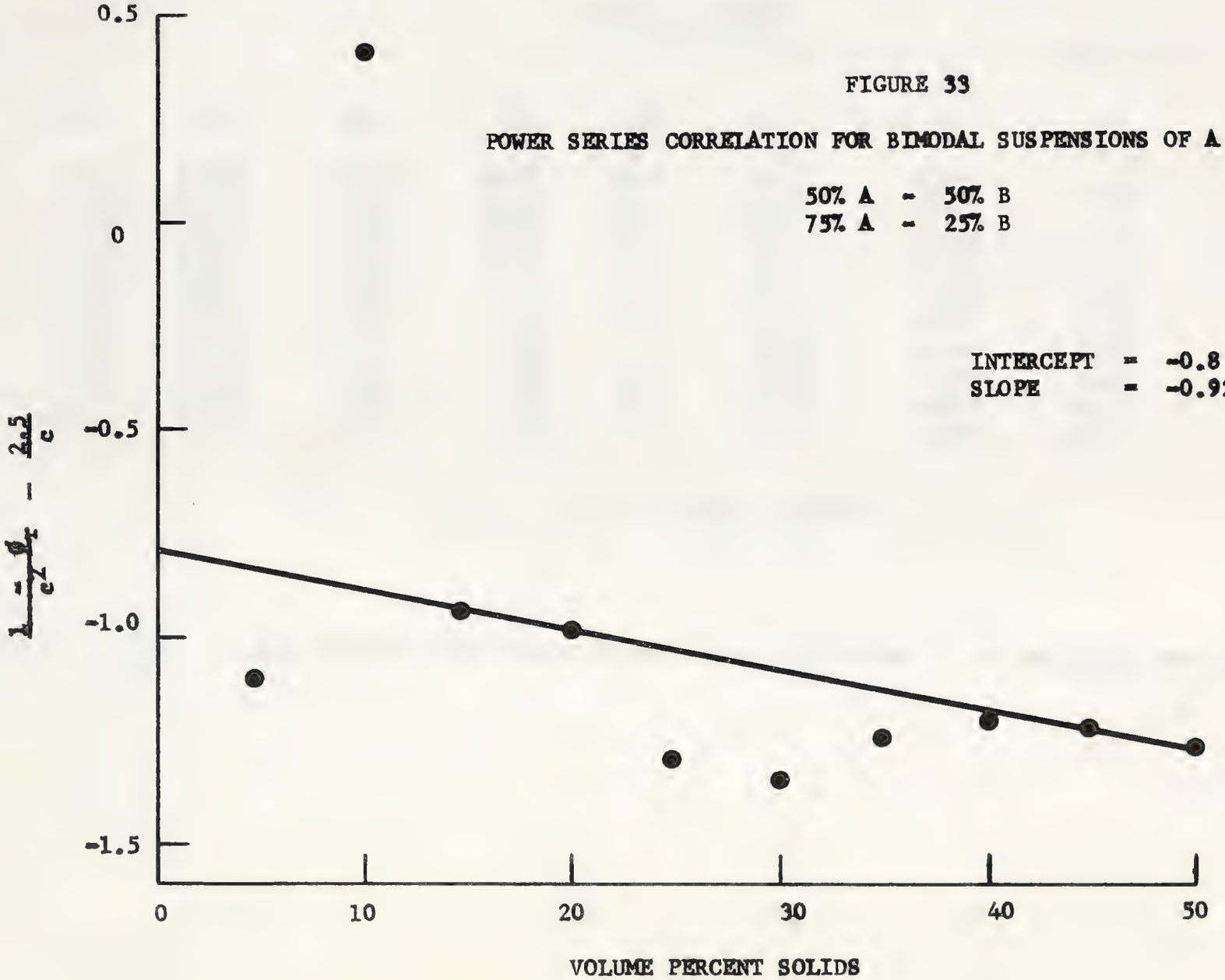

BIMODAL MIXTURES OF A AND B

25% A - 75% B

(1)	(2)	(3)	(4)	(5)	(6)	(7)	(8)	(9)	(10)
0.05	1.14	0.878	0.122	48.9	50.0	-1.1	0.876	1.14	1.000
0.10	1.34	0.746	0.254	25.4	25.0	+0.4	0.754	1.38	1.010
0.15	1.58	0.634	0.366	16.3	16.7	-0.4	0.637	1.57	1.007
0.20	1.92	0.521	0.479	12.0	12.5	-0.5	0.524	1.91	1.005
0.25	2.34	0.427	0.573	9.2	10.0	-0.8	0.418	2.39	0.980
0.30	3.02	0.331	0.669	7.45	8.35	-0.9	0.321	3.12	0.970
0.35	4.30	0.233	0.767	6.27	7.15	-0.88	0.234	4.28	1.005
0.40	6.40	0.156	0.844	5.28	6.25	-0.97	0.1575	6.25	1.009
0.45	10.9	0.092	0.908	4.49	5.56	-1.07	0.094	10.65	1.025
0.50	22.2	0.045	0.955	3.82	5.0	-1.18	0.045	22.2	1.000

$$\phi_r = 1 - 2.5c + 0.2c^2 + 1.96c^3$$

The plot of $\frac{1 - \phi_r}{c^2} - \frac{2.5}{c}$ versus c in Figure 34 gives the coefficient of c^2 and c^3 in the power series.

FIGURE 34

POWER SERIES CORRELATION FOR BIMODAL SUSPENSIONS A AND B

25% A - 75% B

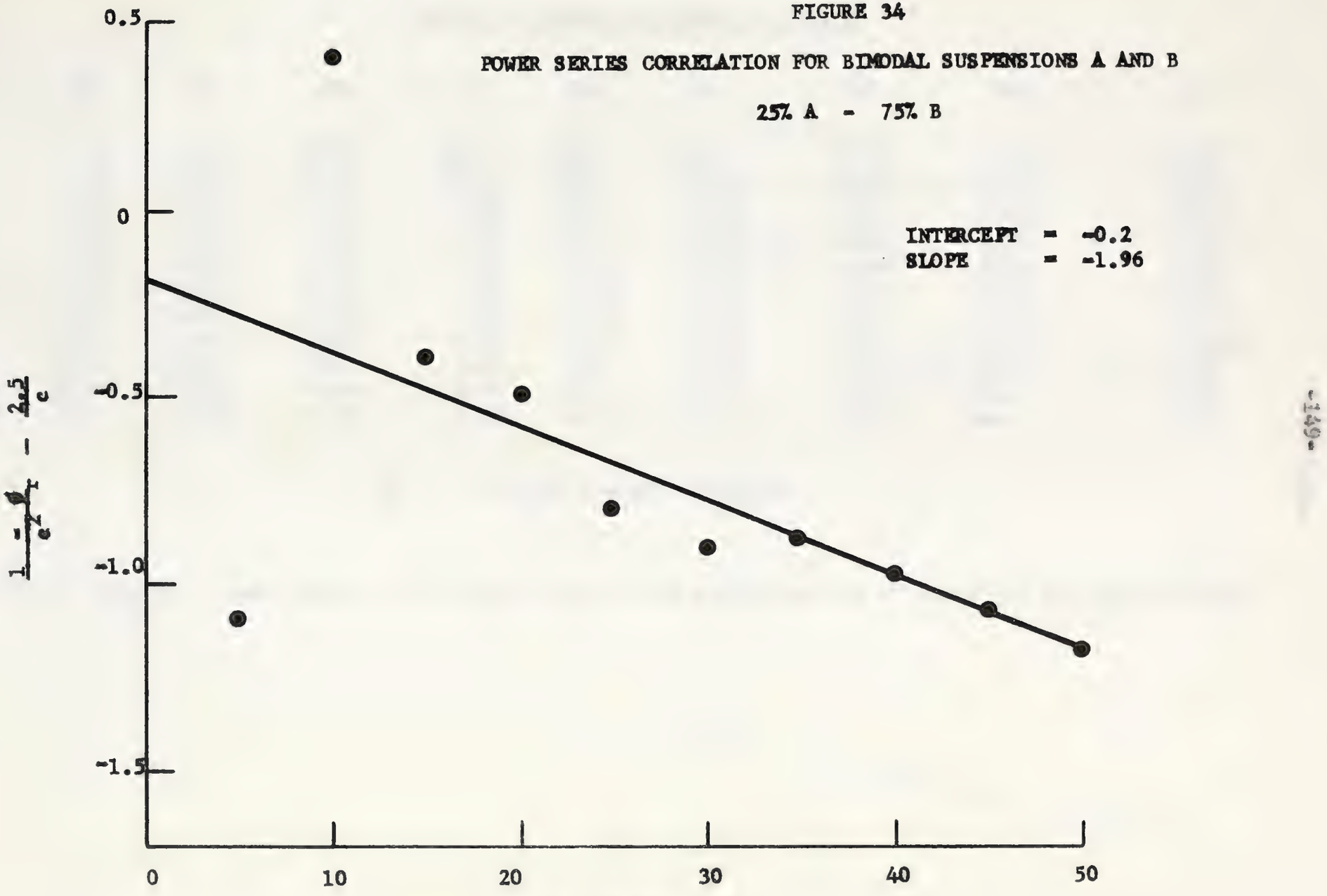

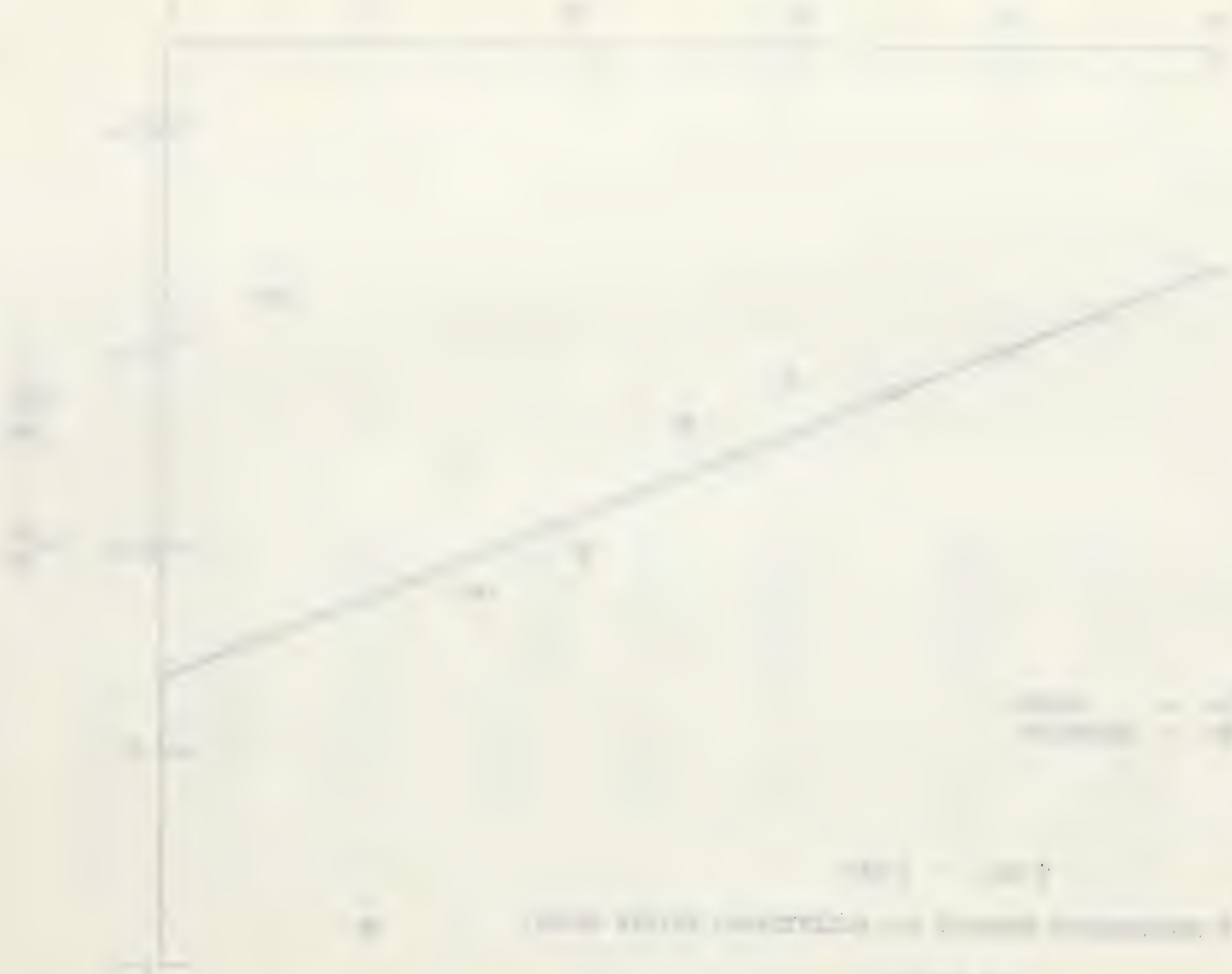

BIMODAL MIXTURES OF A AND C

50% A - 50% C and 75% A - 25% C

(1)	(2)	(3)	(4)	(5)	(6)	(7)	(8)	(9)	(10)
0.05	1.145	0.874	0.126	50.4	50.0	+0.4	0.877	1.14	1.005
0.10	1.34	0.746	0.254	25.4	25.0	+0.4	0.760	1.315	1.02
0.15	1.61	0.621	0.379	16.85	16.7	+0.15	0.648	1.54	1.042
0.20	1.90	0.526	0.474	11.85	12.5	-0.65	0.543	1.84	1.032
0.25	2.25	0.445	0.555	8.88	10.0	-1.12	0.445	2.25	1.000
0.30	2.80	0.357	0.643	7.15	8.35	-1.20	0.356	2.81	0.998
0.35	3.72	0.269	0.731	5.96	7.15	-1.19	0.274	3.65	1.020
0.40	5.0	0.200	0.800	5.00	6.25	-1.25	0.203	4.94	1.015
0.45	7.1	0.141	0.859	4.25	5.56	-1.31	0.141	7.1	1.000
0.50	11.0	0.091	0.909	3.64	5.0	-1.36	0.089	11.25	0.98
0.55	20.0	0.050	0.950	3.14	4.55	-1.41	0.0495	20.2	0.991
0.60	46	0.022	0.978	2.72	4.17	-1.45	0.0215	46.5	0.99

$$\phi_r = 1 - 2.5c + 0.9c^2 + 0.915c^3$$

The plot of $\frac{1 - \phi_r}{c^2} - \frac{2.5}{c}$ versus c in Figure 35 gives the coefficient of c^2 and c^3 in the power series.

FIGURE 35

POWER SERIES CORRELATION FOR BIMODAL SUSPENSIONS OF A AND C

50% A - 50% C
75% A - 25% C

INTERCEPT = -0.9
SLOPE = -0.915

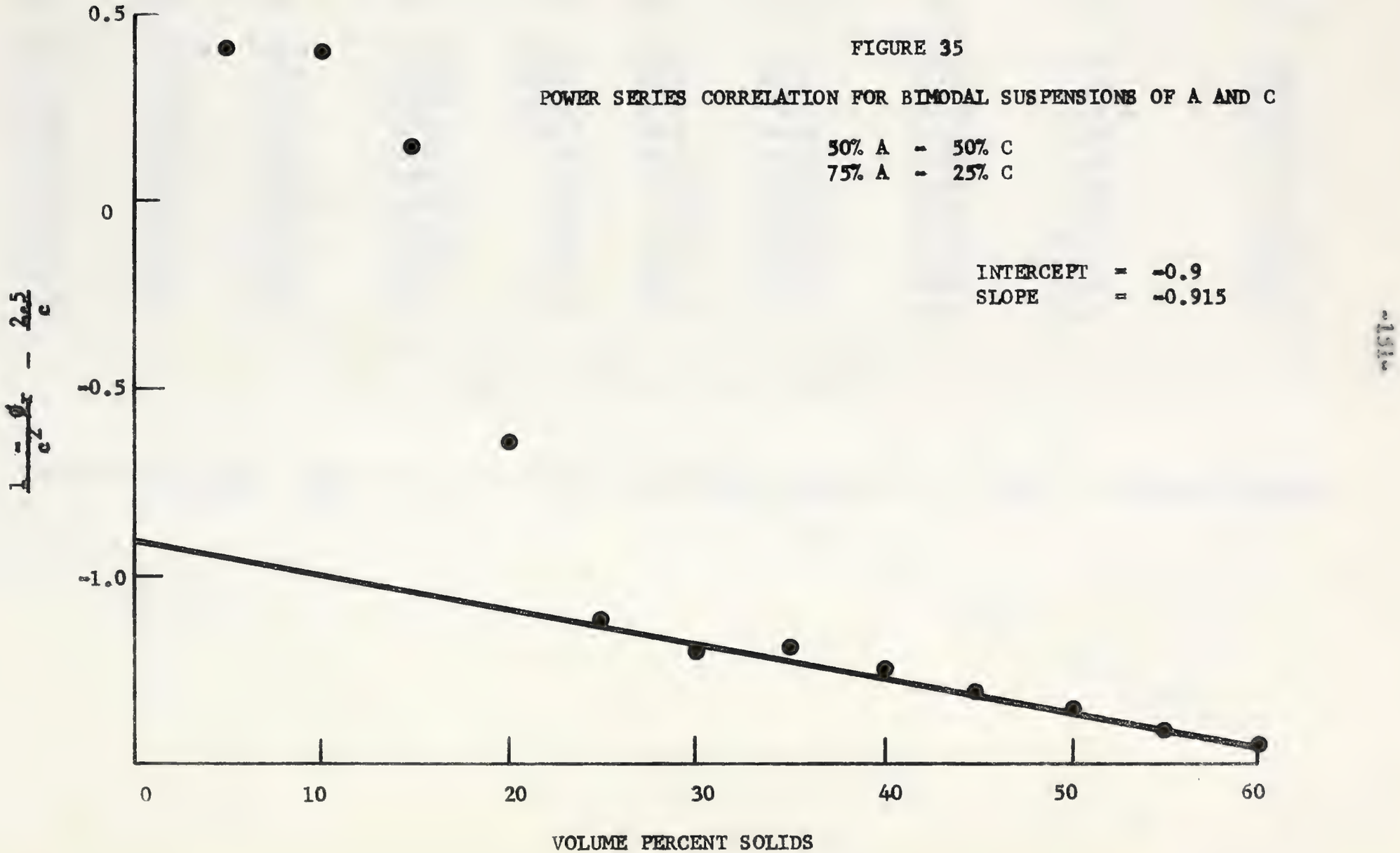

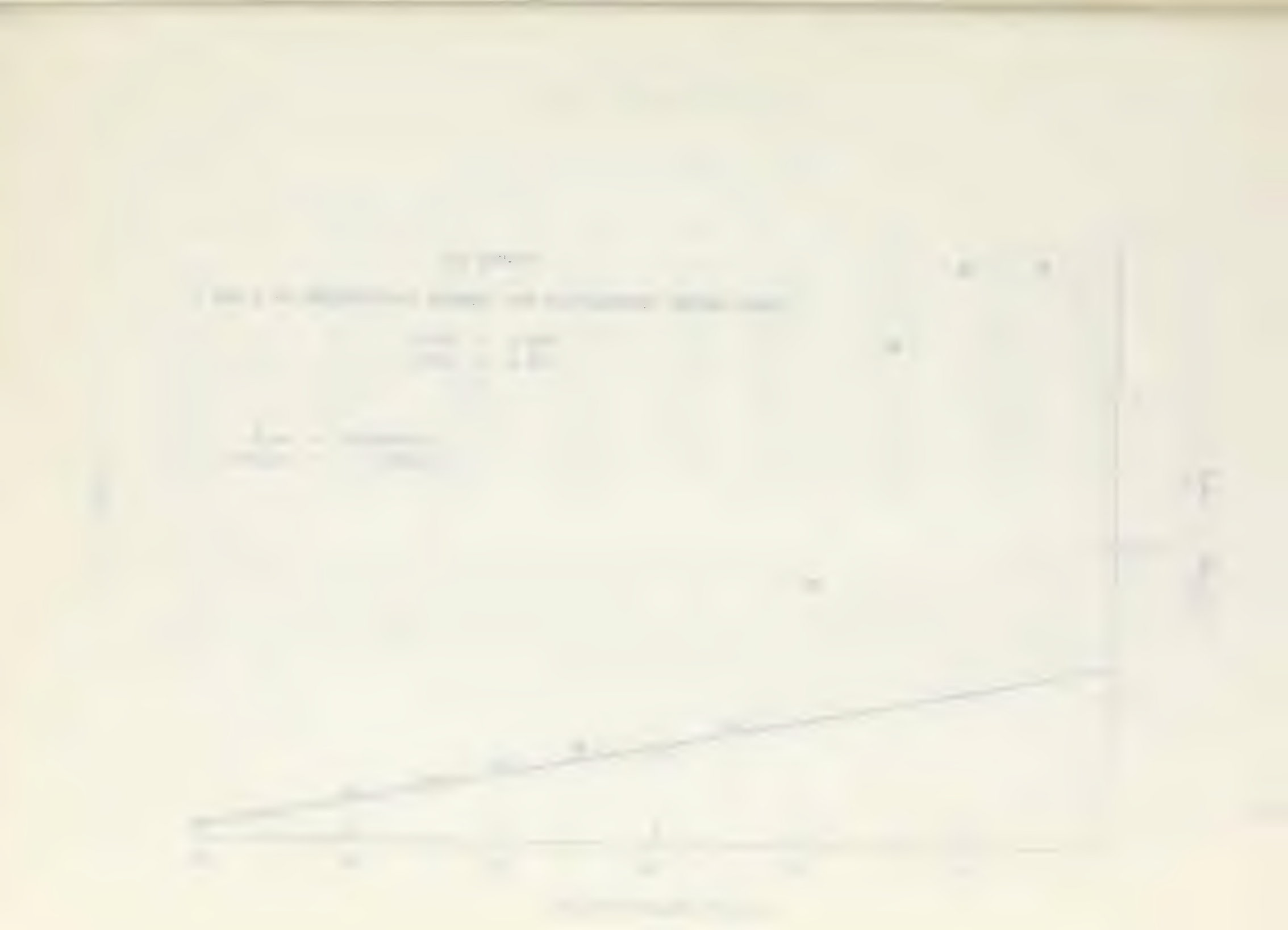

BIMODAL MIXTURES OF A AND C

25% A – 75% C

(1)	(2)	(3)	(4)	(5)	(6)	(7)	(8)	(9)	(10)
0.05	1.145	0.874	0.126	50.4	50.0	+0.4	0.875	1.14	1.00
0.10	1.34	0.746	0.254	25.4	25.0	+0.4	0.753	1.33	1.01
0.15	1.61	0.621	0.379	16.85	16.7	+0.15	0.635	1.575	1.02
0.20	1.95	0.514	0.486	12.17	12.5	-0.33	0.522	1.92	1.02
0.25	2.41	0.415	0.585	9.36	10.0	-0.64	0.416	2.40	1.004
0.30	3.15	0.318	0.682	7.59	8.35	-0.76	0.320	3.13	1.01
0.35	4.25	0.2355	0.7645	6.25	7.15	-0.90	0.235	4.25	1.00
0.40	6.0	0.167	0.833	5.21	6.25	-1.04	0.161	6.21	0.965
0.45	9.4	0.1065	0.8935	4.41	5.56	-1.15	0.101	9.9	0.95
0.50	16.4	0.061	0.939	3.76	5.0	-1.24	0.058	17.25	0.95
0.55	35	0.029	0.971	3.21	4.55	-1.34	0.031	32.3	1.085

$$\phi_r = 1 - 2.5c + 0.1c^2 + 2.26c^3$$

The plot of $\frac{1 - \phi_r}{c^2} - \frac{2.5}{c}$ versus c in Figure 36 gives the coefficient of c^2 and c^3 in the power series.

FIGURE 36

POWER SERIES CORRELATION FOR BIMODAL SUSPENSIONS OF A AND C

25% A - 75% C

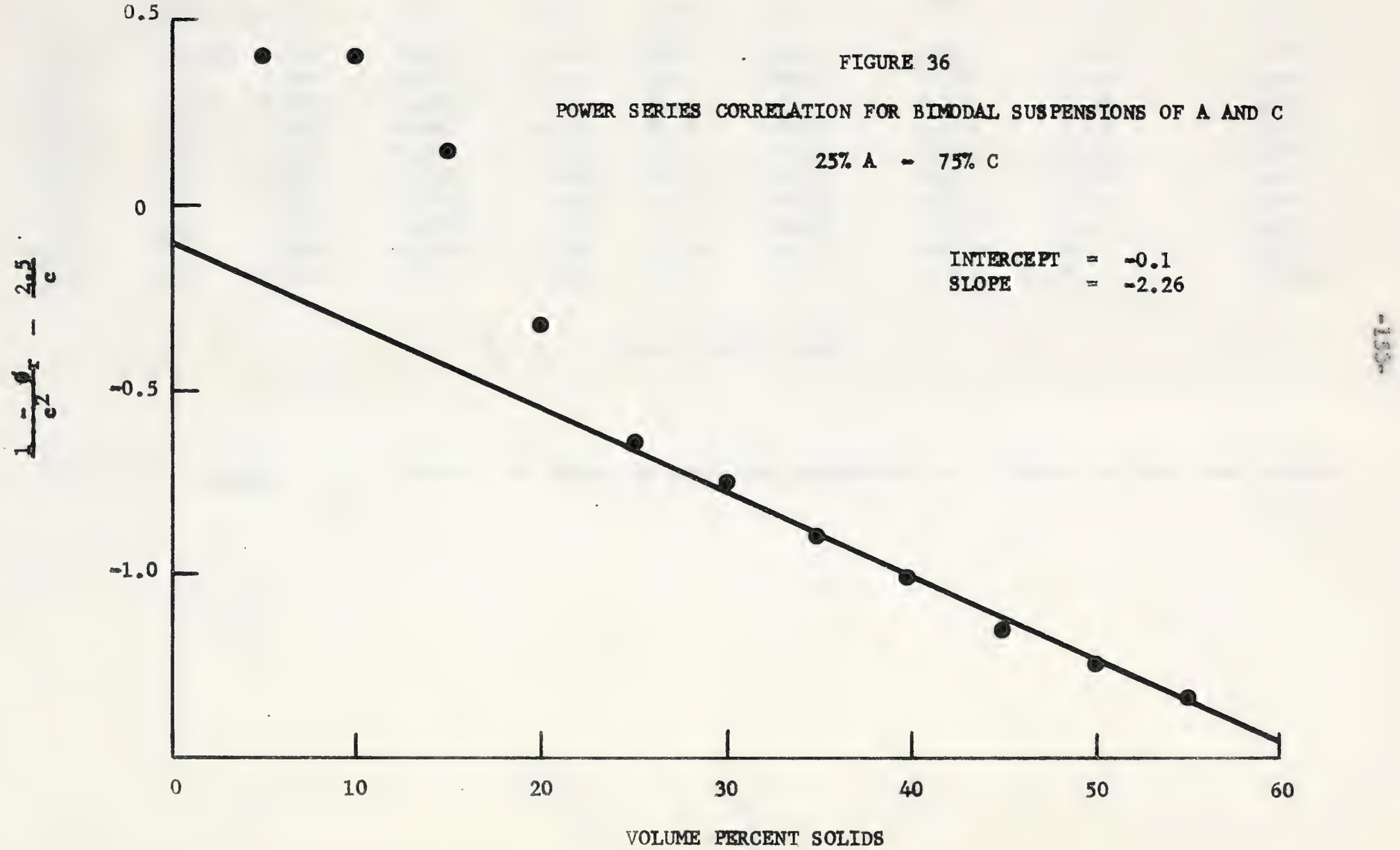

BIMODAL MIXTURE OF B AND C

50% B – 50% C

(1)	(2)	(3)	(4)	(5)	(6)	(7)	(8)	(9)	(10)
0.05	1.145	0.874	0.126	50.4	50.0	+0.4	0.875	1.143	1.000
0.10	1.34	0.746	0.254	25.4	25.0	+0.4	0.752	1.33	1.01
0.15	1.62	0.618	0.382	17.0	16.7	+0.3	0.633	1.58	1.025
0.20	1.95	0.513	0.487	12.16	12.5	-0.34	0.519	1.93	1.01
0.25	2.4	0.416	0.584	9.35	10.0	-0.65	0.413	2.42	0.99
0.30	3.2	0.313	0.686	7.64	8.35	-0.71	0.315	3.18	1.01
0.35	4.4	0.227	0.773	6.3	7.15	-0.85	0.228	4.39	1.002
0.40	6.7	0.1495	0.8505	5.32	6.25	-0.93	0.1535	6.5	1.03
0.45	10.8	0.0926	0.9074	4.49	5.56	-1.07	0.0935	10.7	1.01
0.50	20.5	0.049	0.951	3.80	5.0	-1.2	0.050	20	1.025

$$\phi_r = 1 - 2.5c - 0c^2 + 2.4c^3$$

The plot of $\frac{1-\phi_r}{c^2} - \frac{2.5}{c}$ versus c in Figure 37 gives the coefficient of c^2 and c^3 in the power series.

FIGURE 37

POWER SERIES CORRELATION FOR BIMODAL SUSPENSIONS OF B AND C

50% B - 50% C

INTERCEPT = 0.0
SLOPE = -2.4

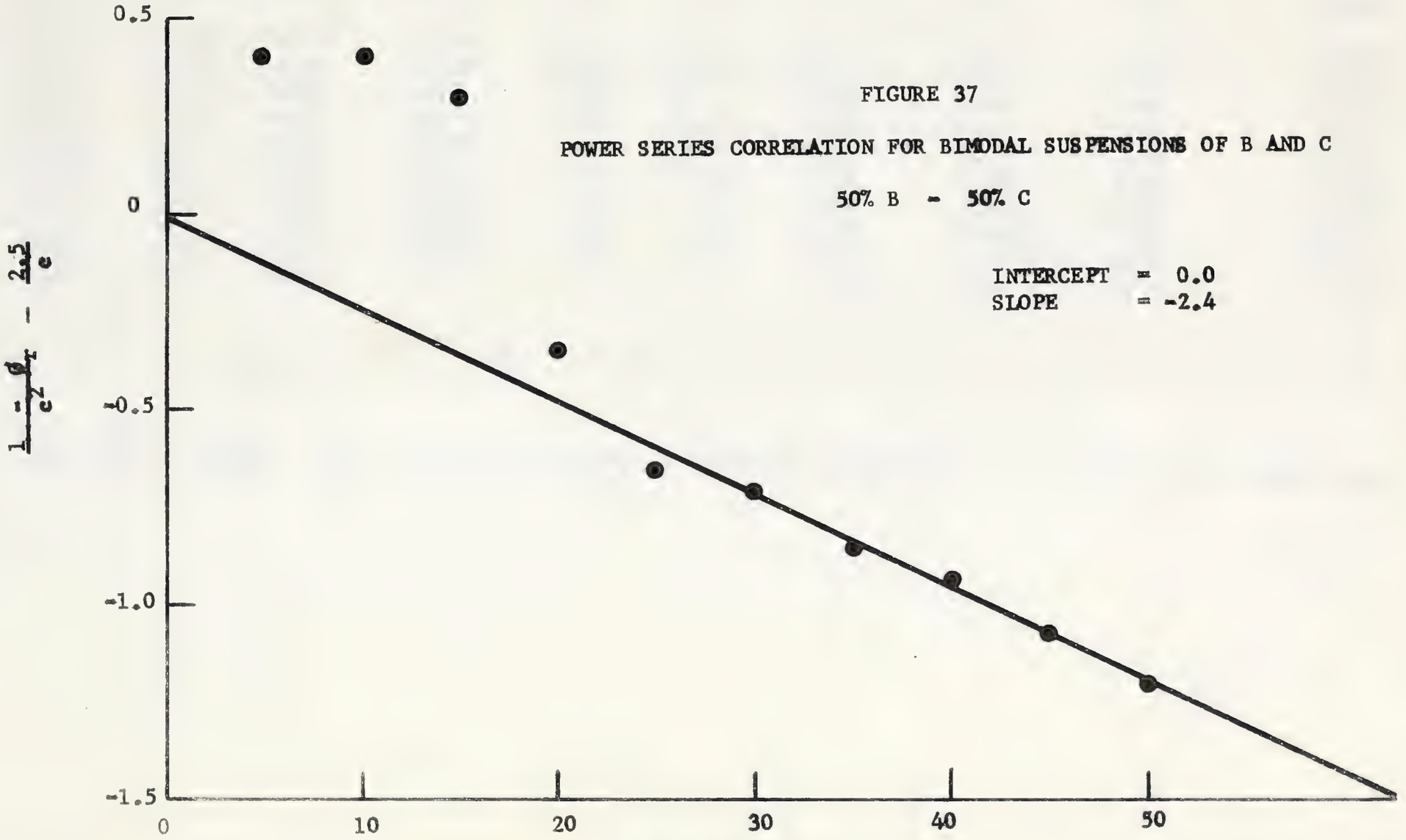

TRIMODAL MIXTURE OF A, B AND C

33 1/3% A – 33 1/3% B – 33 1/3% C

(1)	(2)	(3)	(4)	(5)	(6)	(7)	(8)	(9)	(10)
0.05	1.145	0.874	0.126	50.4	50.0	+0.4	0.876	1.14	1.002
0.10	1.34	0.746	0.254	25.4	25.0	+0.4	0.757	1.32	1.015
0.15	1.57	0.637	0.363	16.15	16.7	-0.55	0.641	1.56	1.006
0.20	1.90	0.526	0.474	11.85	12.5	-0.65	0.533	1.88	1.012
0.25	2.34	0.427	0.573	9.17	10.0	-0.83	0.431	2.32	1.010
0.30	3.0	0.333	0.667	7.41	8.35	-0.94	0.338	2.96	1.014
0.35	3.99	0.252	0.748	6.11	7.15	-1.04	0.255	3.92	1.018
0.40	5.5	0.182	0.818	5.11	6.25	-1.14	0.1825	5.48	1.004
0.45	8.2	0.122	0.878	4.34	5.56	-1.22	0.1215	8.23	0.997
0.50	13.5	0.074	0.926	3.71	5.0	-1.29	0.075	13.3	1.014

$$\phi_r = 1 - 2.5c + 0.5c^2 + 1.6c^3$$

The plot of $\frac{1 - \phi_r}{c^2} - \frac{2.5}{c}$ versus c in Figure 38 gives the coefficient of c^2 and c^3 in the power series.

FIGURE 38

POWER SERIES CORRELATION FOR TRIMODAL SUSPENSIONS

33 1/3% A - 33 1/3% B - 33 1/3% C

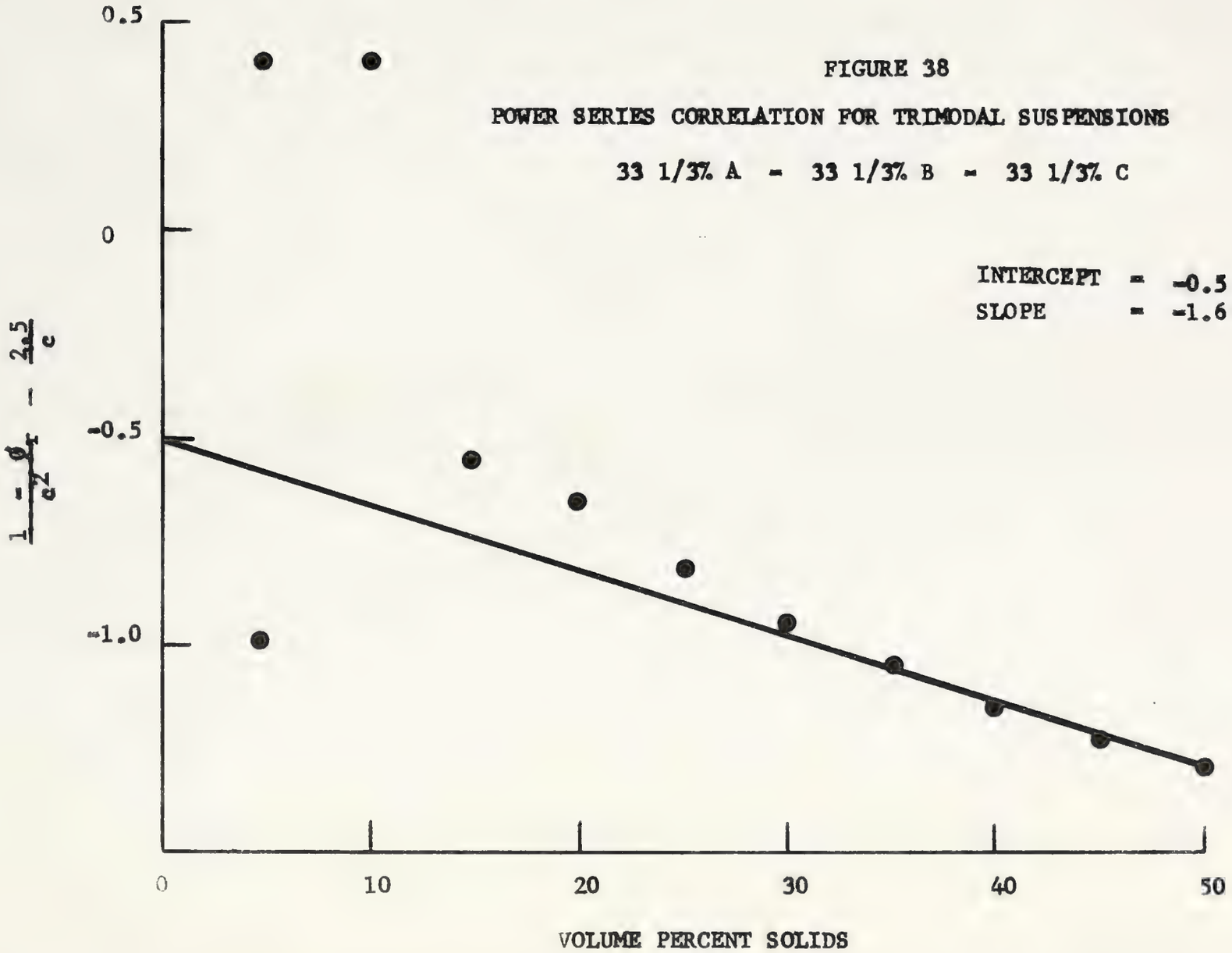

B29802